

University of Nottingham
UK | CHINA | MALAYSIA

System-Level Strategies for Heat Decarbonisation in Community Energy Systems: Utilising Renewable Energy, Thermal Energy Storage and Heat Pumps

Thesis submitted to the University of Nottingham for the degree of Doctor of Philosophy in Engineering

August 2025

Zaid Al-Atari

20365456

Supervisors: Prof Mark Gillott and Dr Rob Shipman

Faculty of Engineering

University of Nottingham

Published Work

Journal Article

Al-Atari, Z.; Shipman, R.; Gillott, M. Optimisation of Integrated Heat Pump and Thermal Energy Storage Systems in Active Buildings for Community Heat Decarbonisation. *Energies* 2024, *17*, 5310. https://doi.org/10.3390/en17215310

Conference Presentation

Al-Atari, Z.; Shipman, R.; Gillott, M. Utilisation of Digital Twins for Community Heat Decarbonisation. In Proceedings of the Sustainable Energy Technologies 2023 Conference Proceedings, Nottingham, UK, 15–17 August 2023; Volume 2, pp. 266–276.

Abstract

The immediate requirement to decarbonise residential heat to deliver net-zero targets creates considerable pressure on electrical distribution networks. Heat pumps (HPs) provide an efficient pathway route to decarbonisation, but widespread deployment threatens to challenge the capacity of low-voltage infrastructure at peak demand periods. This research examines the integration and optimisation of HP and thermal energy storage (TES) systems at community level, with a goal of minimising peak demand, improving energy efficiency and enabling renewable energy integration.

Using the Trent Basin development in Nottingham (76 residential properties) as a case study, this research developed and evaluated multiple control strategies for coordinating HP and TES operation. A comprehensive methodology was implemented, combining building energy modelling using the intelligent Community Design tool with a custom MATLAB simulation framework. Three distinct control approaches were evaluated: a baseline model implementing conventional uncoordinated HP operation, a fixed threshold model introducing basic grid-aware control through static operational thresholds, and an active building model incorporating dynamic optimisation with daily threshold adjustments for each building.

The active building model demonstrated significant improvements across multiple performance metrics, achieving around 20% reduction in peak electrical demand (from around 500 kW_e to 400kW_e) compared to the baseline model and carbon emissions by 5% while maintaining similar total energy consumption levels. This sophisticated control approach transformed demand profiles, improving load factor from 0.35 to 0.48 and reducing demand volatility by decreasing maximum ramp rates

from 45kW/hour to 15kW/hour. HP coincidence factors during peak periods were reduced from 0.76 to 0.45, substantially improving network loading patterns.

Economic analysis revealed that while modest cost increase (1.9%) occurred under standard electricity tariffs, these decreased under time-varying pricing structures—reaching 12.1% under Economy 7 and 17.5% under Dynamic tariffs. This highlighted the importance of aligning market mechanisms with control strategies to maximize economic viability.

The research demonstrates that community-scale optimisation offers advantages beyond the aggregation of individual building benefits. Collective system benefits created by harmonised operating demonstrate that strategies to decarbonise heat should give priority to community-scale measures over the optimisation of single buildings. The results give powerful evidence that advanced control strategies can manage the grid effects of massive HP deployment and promote more penetration under current network conditions than standard analysis would yield. This has profound effects on network planning, investment in new equipment, and policy formulation to enable cost-efficient decarbonisation of heat without compromising the security of the grid.

Acknowledgments

Completing this PhD would not have been possible without the support of many people who deserve my heartfelt gratitude.

I express my sincere appreciation to my supervisors, Professor Mark Gillott and Dr Rob Shipman, for their invaluable guidance and expertise throughout this research. Their constructive feedback and support have been instrumental in shaping this work.

My deepest gratitude goes to my wife, Leen, whose love, patience, and understanding have been my anchor throughout these years. To Ward and Raya, thank you for your patience when I had to be working away from home for long periods.

I am grateful to my family for their constant encouragement, support and belief in my abilities. I also extend my appreciation to my wife's family for their understanding and support during this demanding period.

I also want to thank Philadelphia University in Jordan for providing me with the opportunity to pursue this PhD and for their support.

Finally, I want to thank my colleagues at the University of Nottingham, and everyone involved in the Trent Basin project who made this research possible.

.

Table of Contents

Abstract 4
Acknowledgments 6
Table of Contents 7
List of Figures 11
List of Tables 13
List of abbreviations 14
1. Introduction 16
1.1 Background and Context 16
1.2 Research Aim and Objectives 19
1.3 Thesis Structure 20
2. Literature Review: Heat Pumps and Thermal Storage Technologies 23
2.1 Introduction 23
2.2 Heat Pump Technologies 25
2.2.1 Working Principles and Types 25
2.2.2 Performance and Efficiency Factors 29
2.2.3 High-Temperature Heat Pumps 33
2.3 Thermal Storage Technologies 36
2.3.1 Types of Thermal Energy Storage 36
2.3.2 Integration with Heat Pumps 39
2.3.3 Integration Challenges 43
2.4 Discussion and conclusion 46
3. Literature Review: Active Buildings and Community Energy Systems. 48
3.1 Introduction 48
3.2 Grid Integration Challenges 49
3.2.1 Impact on LV Networks 50
3.2.2 Peak Demand Management 53
3.2.3 Renewable Energy Integration 58
3.3 Community Energy Systems 59
3.4 Active Buildings 62
3.5 Discussion and Conclusions 66
4. Conceptual Framework and Methodology 68
4.1 Introduction 68
4.2 Research Design 70
4.2.1 Methodological Development Process 70
4.2.2 Key Modelling Decisions 71

4.2.3 Implementation Parameters 74
4.3 Digital Twin Initial Approach 75
4.3.1 Digital Twin Framework and Capabilities 76
4.3.2 Limitations and Development Requirements 79
4.4 Simulation Framework and Control Strategy Development 80
4.4.1 Framework Architecture and Design Principles 80
4.4.2 Control Strategy Implementation 84
4.4.3 Baseline Scenario Model 84
4.4.4 Fixed Threshold Model 85
4.4.5 Active Building Model 87
4.5 Performance Evaluation Framework 93
4.5.1 Performance Metrics 93
4.5.2 Evaluation Methodology 96
4.5.3 Sensitivity Analysis Framework 97
4.6 Conclusions 99
5. Demand Modelling and Data Collection 102
5.1 Introduction 102
5.2 Heat Demand Modelling Methodology 103
5.2.1 Tool Selection and Capabilities 103
5.2.2 Simulation Parameters 104
5.2.3 Building Characterization 106
5.2.4 Implementation Process 107
5.3 Electrical Demand Data Collection 110
5.3.1 Monitoring System Architecture 110
5.3.2 Data Processing Methodology 112
5.3.3 Hourly Resolution Considerations 113
5.4 Other Data Collection 115
5.4.1 LV Substation Data 115
5.4.2 Weather Station Data 116
5.4.3 Grid Carbon Intensity Data 117
5.4.4 Electricity Pricing Data 117
5.5 Data Validation and Integration Framework 118
5.5.1 Heat Demand Validation Methodology 118
5.5.2 Integrated Dataset Development 119
5.6 Conclusions 121
6. Case Study and Simulation Analysis 123
6.1 Introduction 123

6.2 Case Study Description 124
6.3 Simulation Setup 127
6.4 Energy System Analysis 128
6.4.1 Current System Analysis 128
6.4.2 Heat Pump Integration Scenarios 130
6.5 Results Analysis 134
6.5.1 Energy Demand Patterns 134
6.5.2 Integrated Performance Assessment 140
6.5.3 Environmental Performance Summary 142
6.5.4 Economic Performance Summary 143
6.6 Conclusions 144
7. Performance Evaluation and Impact Assessment 146
7.1 Introduction 146
7.2 Energy Performance Evaluation 147
7.2.1 Dynamic Efficiency Analysis 147
7.2.2 Load Profile Characterization 149
7.2.3 Storage Utilisation Patterns 151
7.3 Grid Integration Assessment 155
7.3.1 Network Loading Analysis 155
7.3.2 Demand Rate of Change 157
7.3.3 Coincidence Factors 160
7.4 Environmental Impact Assessment 163
7.4.1 Carbon Intensity Analysis 163
7.4.2 Seasonal Carbon Performance 165
7.5 Operational Economic Analysis 167
7.5.1 Electricity Tariff Impacts 167
7.5.2 Building Type Economic Analysis 170
7.6 Sensitivity Analysis and Robustness Assessment 171
7.6.1 Impact of Forecast Error on Performance 172
7.6.2 Comparative Parameter Sensitivity 173
7.6.3 System Robustness Under Combined Uncertainties 176
7.6.4 Implications for Real-World Implementation 177
7.7 Conclusions 178
8. Discussion and Conclusions 181
8.1 Introduction 181
8.2 Summary of Key Findings 181
8.3 Completion of Research Objectives 184

8.4 Future Work 190
8.5 Conclusion 191
Bibliography 193
Appendix A: Simulation Framework MATLAB Code 206
Appendix B: HP Manufacturers' Data 229
Appendix C: Optimisation Tool: Sample of Inputs and Outputs 231
Appendix D: The UK electricity grid 234

List of Figures

Figure 1.1:Territorial UK GHG emissions by sector, 2023 (%) (UK GOV Final Figures, 2023) 16
Figure 2.1: Global residential energy demand by end-use under historical and projected scenarios (1990–2050). (IPCC Cabeza, L. F. et. al., 2023) 23
Figure 2.2:An illustration of a heat pump (Sarbu & Sebarchievici, 2014). 26
Figure 2.3: Pipe arrangements of GSHP (a) a single tier and (b) a double tier (c) slinky (Singh et al., 2010) 28
Figure 2.4: COPs at different water temperatures (Lämmle et al., 2023) 30
Figure 2.5: Comparison of heat pump cycling behaviour for a Single-Stage Heat Pump (SSHP) (left) and an Inverter-Driven Heat Pump (IDHP) (right). (Dongellini & Morini, 2019) 31
Figure 2.6: Comparison of HP COP across different heat emitters as a function of heat demand (Hu et al., 2019) 32
Figure 2.7: COP of heat pumps as a function of evaporator temperature under various condenser (output) temperatures. (Bellos et al., 2023) 34
Figure 2.8: Storage capacity vs. operating temperature for various TES technologies. (Sarbu & Sebarchievici, 2018) 39
Figure 2.9: SPF and Electrical Consumption for a HP-TES with 1 versus 2 heated zones (Glembin et al., 2015) 41
Figure 3.1: Projected annual electrical demand showing the effect of HP integration (Watson et al., 2023) 51
Figure 3.2: Different scenarios for UK electricity demand (full electrification is the green curve) (Eyre & Baruah, 2015) 55
Figure 3.3: Expected peak electricity demand with the intensive deployment of HPs (Eyre & Baruah, 2015) 55
Figure 3.4: Monthly peak electrical demand (kW) for different heating strategies, including TES integration (Ryan et al., 2022). 57
Figure 3.5: The concept of a multi-vector community energy system (Han et al., 2022) 60
Figure 3.6: Sample of the data from the Trent Basin project showing electrical energy consumption and the dominance of EV charging. (Shipman & Gillott, 2019) 62
Figure 3.7: Conceptual Representation of Active Buildings Balancing Energy and Network Services. (Vahidinasab et al., 2021) 64
Figure 4.1: 3D visualisation of the Trent Basin development generated using the iCD modelling tool. 77
Figure 4.2: Network Representation of Trent Basin buildings connected to the LV substation as visualized in the iVN tool. 78
Figure 4.3: Network Connectivity for a Single House with Individual HP as Modelled on iVN Tool. 78
Figure 4.4: System configuration of the model on both community and building levels. 81
Figure 4.5: Active building model schematic 92
Figure 5.1: Input parameters for heat demand simulation of a representative dwelling in the Trent Basin development using the iCD modelling tool. 106
Figure 5.2 : Modelled energy demand distribution for dwellings in Trent Basin, as visualized in the iCD tool. 107
Figure 5.3: Yearly Combined Space Heating and DHW Demand Profile for the Trent Basin Project in 2022 (Modelled on iCD) 109
Figure 5.4: Hourly Heat Demand in kW_{th} for 4 Buildings During Feb 2022 (Modelled on iCD). 109

Figure 5.5: Monitoring system architecture for the Trent Basin development, showing data flows from building-level sensors to cloud-based databases via the Project SCENe Gateway (Shipman and Gillott, 2019)..... 111
Figure 5.6: Comparison of modelled and measured total electrical energy consumption for 2022 at Trent Basin. 113
Figure 5.7: Comparison of modelled, hourly average, and maximum power electricity demand at Trent Basin 114
Figure 6.1: Hourly electricity demand at Trent Basin for a representative winter week, showing daily patterns and peak periods 130
Figure 6.2: Total Electricity Demand Comparison across the three scenarios throughout 2022 132
Figure 6.3: Total electrical power demand at the low-voltage (LV) substation during the coldest week of the year (7–14 January 2022) for three scenarios 133
Figure 6.4: Peak Electrical Demand comparison across the three scenarios 134
Figure 6.5: Heat demand for a Category 2 building during the coldest week of January 2022 135
Figure 6.6: Hourly peak electricity power for Category 2 building during the analysed week 136
Figure 6.7: COP and outdoor temperature for a Category 2 heat pump over the analysed week 136
Figure 6.8: Baseline scenario energy dynamics for a Category 2 building..... 137
Figure 6.9: Fixed Threshold Model energy flow in a Category 2 building..... 138
Figure 6.10: Active building model scenario energy flow in building from Category 2 139
Figure 6.11: Comparison of total peak electrical power on the LV substation between the three scenarios during the coldest week of the year. 140
Figure 6.12: Distribution of Threshold 1 and Threshold 2 values in the active building model. 141
Figure 7.1: Seasonal analysis of HP's COP under three control strategies 149
Figure 7.2: Load duration curves comparing baseline, fixed threshold, and active control strategies. 151
Figure 7.3: State of charge profiles for four dwelling categories over a full year..... 154
Figure 7.4: Annual number of hours exceeding 200 kW_e, 300 kW_e, and 400 kW_e peak electrical power for three scenarios. 157
Figure 7.5: Histogram of demand rate of change under baseline, fixed threshold, and active control strategies. 159
Figure 7.6: Distribution of heat pump coincidence factors under different control strategies. 162
Figure 7.7: Total carbon emissions across control scenarios 164
Figure 7.8: Emissions Intensity Across Control Scenarios 165
Figure 7.9: Monthly Carbon Emissions Across Control Scenarios..... 166
Figure 7.10: Annual electricity costs for HP operation under three tariff types (Standard, Economy 7, and Agile) across control scenarios. 167
Figure 7.11: Percentage cost savings relative to the baseline scenario across different tariff types. 169
Figure 7.12: Annual HP electricity costs by building category under baseline and active control strategies. 170
Figure 7.13: Impact of forecast error on Active Building Model peak reduction benefits relative to baseline scenario 172
Figure 7.14:Sensitivity of Active Building Model peak reduction benefits to parameter variations..... 174

List of Tables

Table 2.1: Summary of the most common HPs Technologies (Gaur et al., 2021) 29
Table 6.1: Building categories and characteristics in the Trent Basin development 125
Table 6.2: HP and TES configurations by building category 126
Table 6.3: Summary of the LV substation operating thresholds within the active building model during the analysed week. 138
Table 6.4: Carbon emissions summary across control scenarios. 142
Table 6.5: Annual heat pump electricity costs by tariff structure 143
Table 7.1: Quantitative sensitivity analysis results for Active Building Model performance 174
Table 0.1: Mitsubishi HTHP Performance Datasheet (MITSUBISHI ELECTRIC, 2018) .. 229
Table 0.2: Samsung HTHP Performance Datasheet for multiple available capacities (SAMSUNG, 2022) 230
Table 0.3: Sample of the Input Data into the Optimisation tool for Category 1 Building ... 229
Table 0.4: Sample of the output Data from the Optimisation tool for Category 1 Building (Active Building Model)……. 230
Table 0.5: Sample of the summary of performance metrics from the optimisation tool… 231

List of abbreviations

AB - Active Building

ASHP - Air Source Heat Pump

COP - Coefficient of Performance

CSV - Comma Separated Values

DHW - Domestic Hot Water

DNO - Distribution Network Operator

ESO - Electricity System Operator

EV - Electric Vehicle

GHG - Greenhouse Gas

GSHP - Ground Source Heat Pump

HP - Heat Pump

HTHP - High Temperature Heat Pump

iCD - Intelligent Community Design

IES - Integrated Environmental Systems

IPCC - Intergovernmental Panel on Climate Change

iVN - Intelligent Virtual Network

LV - Low Voltage

PCM - Phase Change Material

PV - Photovoltaic

PV/T - Photovoltaic/Thermal

RES - Renewable Energy Sources

SCENe - Sustainable Community Energy Networks

SPF - Seasonal Performance Factor

TES - Thermal Energy Storage

UK - United Kingdom

WSHP - Water Source Heat Pump

Units:

°C - Degrees Celsius

gCO_2 - grams of Carbon Dioxide

$kgCO_2$ - kilograms of Carbon Dioxide

kW_e - Kilowatt Electrical

kW_{th} - Kilowatt Thermal

kWh - Kilowatt-hour

L - Litre

m - Meter

MW - Megawatt

MWh - Megawatt-hour

TWh - Terawatt-hour

W/m^2K - Watts per square meter Kelvin

Chapter 1

1. Introduction

1.1 Background and Context

The global energy sector is undergoing a profound transformation driven by the urgent need to address climate change (IPCC, 2023) and achieve ambitious net-zero emissions targets. Within this transition, the decarbonisation of residential heating has emerged as a critical challenge, particularly in countries with significant heating demands such as the United Kingdom (UK). Current estimates indicate that space heating and domestic hot water contribute approximately 18% of overall UK carbon emissions (2020 UK Greenhouse Gas Emissions, Final Figures, 2023), highlighting the urgent need for innovative solutions in this sector. Figure 1.1 shows the UK greenhouse gas emissions by Sector, highlighting the significant contribution of buildings sector which mainly dominated by heating.

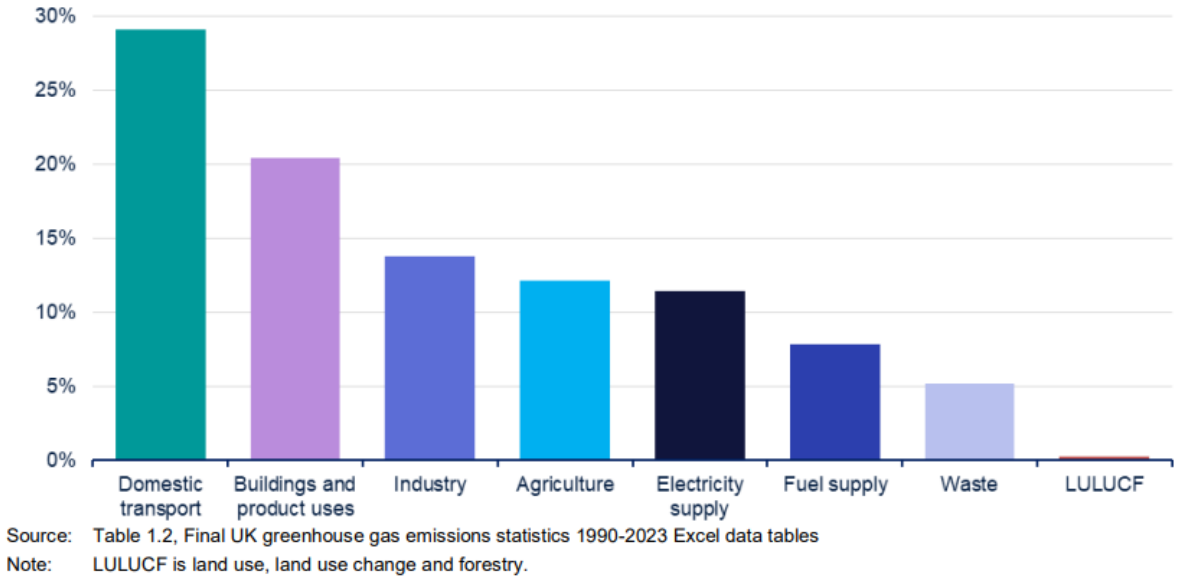


Figure 1.1:Territorial UK GHG emissions by sector, 2023 (%) (UK GOV Final Figures, 2023)

The electrification of residential heating systems, while offering a promising pathway to decarbonisation, presents significant technical and infrastructural challenges. This transition is particularly complex due to the substantial increase in electricity demand it creates, potentially straining existing low-voltage (LV) distribution networks that were not designed for such loads (Alpizar-Castillo et al., 2023). The challenge is further compounded by the concurrent electrification of transportation and the growing adoption of electric vehicles (Aschidamini et al., 2024), creating a need for sophisticated energy management solutions.

Heat Pumps (HPs) have emerged as a key technology in this transition, offering superior energy efficiency compared to traditional heating systems. With Coefficients of Performance (COP) typically ranging from three to four (Gaur et al., 2021), they represent a significant improvement over conventional electric heating solutions. However, their widespread deployment faces several obstacles, including the need to produce relatively low-temperature water (40°C to 50°C) compared to traditional gas boilers (70°C) (Chesser et al., 2021), often necessitating either substantial building retrofitting or the implementation of high-temperature HP solutions.

The transition towards renewable energy sources (RES) has become a cornerstone of global efforts to combat climate change, with many countries setting ambitious targets for RES integration into their power systems (Foggia et al., 2024). This shift in energy generation, however, creates new challenges for grid management and energy distribution, particularly as the electrification of heating adds substantial new loads to existing infrastructure while the intermittent nature of renewable sources such as wind and solar power requires more flexible and intelligent approaches to energy demand management (Henni et al., 2021).

Thermal Energy Storage (TES) systems have emerged as a potential solution to bridge the gap between variable renewable energy supply and heating demand. When integrated with HPs, TES can provide the flexibility needed to shift heating loads to periods of higher renewable energy availability or lower grid demand (Sultan et al., 2023). This approach not only supports grid stability but also enhances the economic viability of HP systems by enabling more efficient operation patterns.

The implementation of HPs and TES at a community scale presents both opportunities and challenges. While these technologies offer significant potential for reducing carbon emissions and improving energy efficiency, their successful deployment requires careful consideration of local grid capacity constraints and the development of sophisticated control strategies. The collective impact of multiple HPs operating simultaneously can potentially strain local electrical infrastructure, particularly during peak demand periods (Love et al., 2017). However, this challenge also presents an opportunity to develop innovative approaches to load management and system optimisation.

Recent advances in digital technologies and data analytics have enabled more sophisticated approaches to energy system management. Real-time monitoring and control systems can now optimise the operation of HPs and TES units based on various factors including grid conditions, renewable energy availability, and user demand patterns (O'Dwyer et al., 2020). These capabilities are particularly valuable in community-scale projects, where the aggregation of multiple systems can provide greater flexibility and efficiency gains compared to individual installations.

Policy frameworks and regulatory environments play a crucial role in facilitating this transition. Current initiatives in many countries focus on incentivising the adoption of

low-carbon heating technologies while supporting necessary infrastructure upgrades (Salite et al., 2024). However, the complex interplay between technical requirements, economic considerations, and social factors necessitates a carefully coordinated approach to ensure successful implementation at scale.

1.2 Research Aim and Objectives

The aim of this research is to develop and evaluate optimisation strategies for integrating HPs and TES systems at a community scale, focusing on minimising peak electrical demand and facilitating the integration of renewable energy sources while maintaining occupant comfort. This research seeks to answer the following research question:

Can intelligent community-scale control of integrated heat pump and thermal storage systems enable heat decarbonisation without exceeding electrical infrastructure capacity?

To achieve this aim, the following objectives have been established:

1. To collect and analyse comprehensive data from the Trent Basin case study, including electricity demand, heat demand, and relevant environmental factors, establishing a robust foundation for model development. (Chapter 5)
2. To develop and validate heat demand models for residential buildings, considering various factors such as building characteristics, occupant behaviour, and weather conditions. (Chapter 5)
3. To design an advanced simulation model that integrates HPs and TES systems within a community framework, including an optimization algorithm for

coordinating their operation based on real-time data, forecasts, and grid conditions. (Chapter 4)

4. To conduct scenario analysis comparing the performance of the optimised models against baseline (unoptimized model), focusing on peak demand reduction, energy consumption, and carbon emissions. (Chapter 6)
5. To evaluate the model's performance under various operational conditions and constraints, assessing its adaptability to different residential contexts and energy mix scenarios. (Chapter 6)
6. To assess the impact of the proposed system on low-voltage distribution networks and grid stability. (Chapter 7)
7. To evaluate the techno-economic feasibility and environmental benefits of implementing integrated HP and TES systems for residential heat decarbonisation, considering various scales of implementation and future energy scenarios. (Chapter 7)

1.3 Thesis Structure

This thesis consists of eight chapters, structured to systematically address the research objectives and present a comprehensive analysis of community heat decarbonisation strategies. The structure is as follows:

Chapter 1: Introduction The current chapter introduces the research context, establishes the aim and objectives, and outlines the thesis structure. It presents the fundamental challenges of heat decarbonisation and the role of integrated HP and TES systems in supporting renewable energy integration.

Chapter 2: Literature Review - Heat Pumps and Thermal Storage Technologies This chapter provides a comprehensive review of HP technologies, focusing on their applications, efficiency factors, and the specific challenges of high-temperature HPs. It also examines various TES technologies and their integration potential with HPs, establishing the technical foundation for the research.

Chapter 3: Literature Review - Active Buildings and Community Energy Systems The chapter explores community-scale energy systems and their role in heat decarbonisation. It examines principles of energy management at the community level and reviews relevant case studies, identifying key research gaps in the field.

Chapter 4: Conceptual Framework and Methodology This chapter presents the research design and details the development of the simulation model. It describes the optimization algorithm design and the principles underlying the control strategies for integrated HP and TES systems.

Chapter 5: Demand Modelling and Data Collection The chapter details the data collection process from the Trent Basin project and the development of heat demand models. It describes the methodology for processing and validating the data, including electricity consumption patterns and environmental parameters.

Chapter 6: Case Study and Simulation Analysis This chapter presents the implementation of the model in the Trent Basin case study. It describes the simulation setup and analyses different scenarios, comparing the performance of various control strategies for HP and TES integration.

Chapter 7: Performance Evaluation and Impact Assessment The chapter evaluates the model's effectiveness in terms of energy savings, carbon reduction, and grid impact. It

assesses the potential for renewable energy integration and examines the broader implications for community-scale heat decarbonisation.

Chapter 8: Discussion and Conclusions The final chapter synthesizes the key findings, discusses their implications for heat decarbonisation strategies, and presents recommendations for future research and implementation. It reflects on the contribution to knowledge and suggests directions for further investigation.

Chapter 2

2. Literature Review: Heat Pumps and Thermal Storage Technologies

2.1 Introduction

The decarbonisation of residential heating represents a critical challenge in achieving net-zero emissions targets. This challenge has driven significant technological advancement in both heat generation and storage systems (Knobloch et al., 2019). The building sector accounts for approximately 40% of global energy consumption, with space heating and domestic hot water production representing the majority of this demand as illustrated in Figure 2.1(Cabeza et al., 2023). HPs have emerged as a key technology for heat decarbonisation due to their ability to deliver more thermal energy than the electrical energy they consume. This efficiency advantage is quantified by the COP, which typically ranges from 3-4 in real-world applications (Carroll et al., 2020).

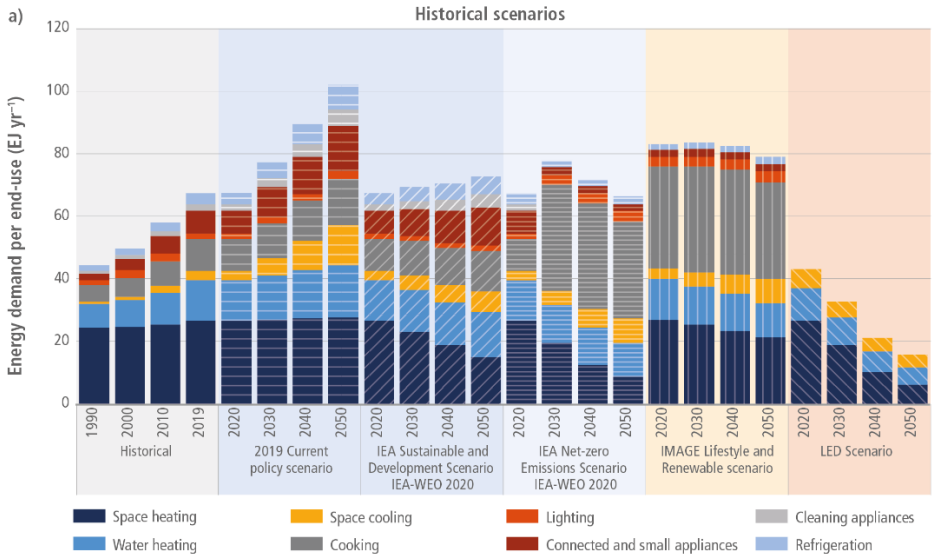


Figure 2.1: Global residential energy demand by end-use under historical and projected scenarios (1990–2050). (IPCC Cabeza, L. F. et. al., 2023)

Despite their efficiency benefits, the widespread adoption of HPs presents substantial challenges for existing electrical infrastructure. These challenges become particularly acute at the community scale, where simultaneous operation of multiple HPs can significantly impact low voltage (LV) networks through increased peak demands and potential voltage issues (Blonsky et al., 2019). Field studies have shown that HP operation can substantially increase household electricity consumption during peak heating periods—sometimes by over 200%—placing significant stress on distribution networks that were originally designed for much lower loads (Veldman et al., 2011).

The integration of HPs with TES systems has emerged as a promising approach to address these challenges. This combination extends beyond simple heat provision to offer multiple benefits including peak load reduction, enhanced system efficiency, and improved renewable energy integration (Sultan et al., 2023). By decoupling heat generation from demand, TES creates valuable flexibility in system operation, allowing HPs to run during periods of lower electricity costs or higher renewable energy availability. Such temporal flexibility becomes increasingly valuable as electricity grids incorporate higher percentages of variable renewable generation (Burkhardt et al., 2024).

Recent research has increasingly focused on optimising the interaction between HPs and TES systems, particularly in community-scale applications. This has revealed complex relationships between system performance, energy efficiency, and grid impact that warrant detailed investigation (Wang, Qu, et al., 2022). The thermal characteristics of buildings, occupancy patterns, and local climate conditions all influence system design and operation, creating a challenging multi-objective optimisation problem that extends beyond individual buildings to consider collective impacts (Nérot et al., 2023).

This chapter examines the current state of knowledge regarding HP and TES technologies, their integration, and their role in community-scale heat decarbonisation. The review begins by exploring the evolution and current state of HP technology, with particular focus on performance characteristics and high-temperature applications. It then examines developments in TES systems and their integration with HPs, highlighting different storage approaches and their respective advantages. The review continues by considering grid integration considerations and emerging approaches to system optimisation and control. Through this examination, key research gaps are identified, particularly regarding the optimisation of these integrated systems at community scale and their potential to support renewable energy integration.

2.2 Heat Pump Technologies

The electrification of residential heating has positioned HPs as a key technology in achieving decarbonisation targets. Understanding their operational principles, performance characteristics, and limitations is crucial for developing effective integration strategies, particularly at the community scale. The following subsections present a review for these topics.

2.2.1 Working Principles and Types

Heat pumps operate on the vapour compression cycle, transferring thermal energy from a low-temperature source to a higher temperature sink through the input of mechanical work. As illustrated in Figure 2.2, the basic cycle consists of four main components working in sequence (Sarbu & Sebarchievici, 2014). In the evaporator, a low-temperature liquid and vapour mixture (refrigerant) absorbs heat from the external source (e.g., air, ground, water) and becomes a low-temperature vapour. The compressor then increases both the pressure and temperature of this vapour. In the

condenser, this high-temperature vapour releases heat to the building's distribution system and condenses back to a liquid state. Finally, the expansion valve reduces the pressure, returning the refrigerant to its original low-temperature state to begin the cycle again (Sarbu & Sebarchievici, 2014).

This thermodynamic process enables HPs to deliver more thermal energy than the electrical energy they consume, as quantified by their COP (Ireneo C. Plando, Jr., 2023). For example, a COP of 3 means that for every 1 kWh of electricity consumed, the system delivers 3 kWh of heat. This fundamental efficiency advantage over direct electric heating forms the basis for their role in heat decarbonisation strategies.

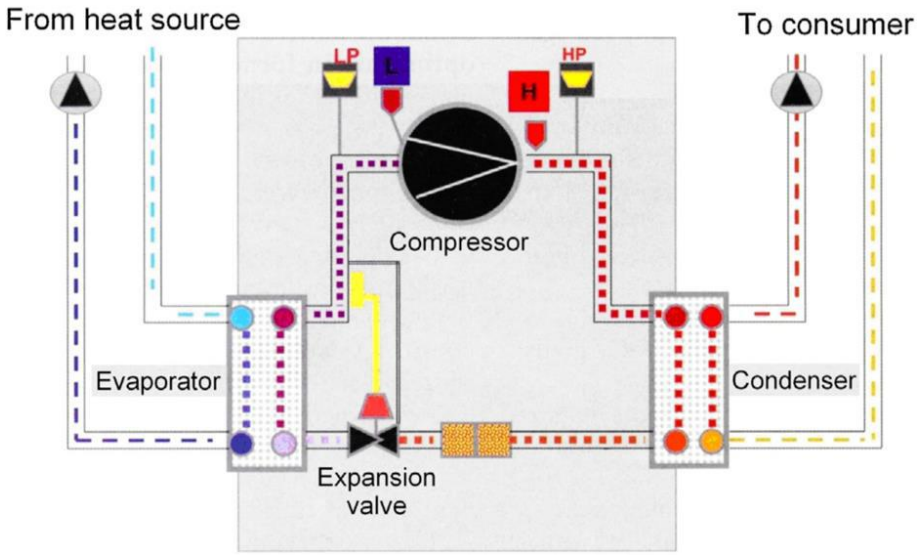


Figure 2.2:An illustration of a heat pump (Sarbu & Sebarchievici, 2014).

Several HP configurations have been developed for residential heating applications, each with distinct characteristics that affect their suitability for different contexts. Air-source heat pumps (ASHPs) extract heat from ambient air and represent the most commonly deployed type in residential settings. Their primary advantages include lower initial cost compared to other HP types and simpler installation requirements with no need for ground works (Konrad & MacDonald, 2023). However, their performance is significantly affected by ambient temperature, with efficiency

declining as external temperatures decrease, particularly below 0°C when defrost cycles are required (Rhee & Kim, 2015). (Chesser et al., 2021) conducted field trials of domestic ASHPs in the UK, finding that COP typically varies between 2-4 depending on operating conditions, with the lower end of this range occurring during the coldest periods when heating demand is highest.

Ground-source heat pumps (GSHPs) utilize the relatively stable temperature of the ground as their heat source. These systems circulate a fluid through pipes buried underground, either in horizontal trenches at depths of 1-2 meters or in vertical boreholes extending 50-150 meters deep (Gao et al., 2023). The ground temperature at depths beyond 10 meters remains relatively constant year-round, providing GSHPs with a more stable heat source than ambient air. This stability translates to more consistent performance, with typical COPs ranging from 3-5 throughout the year (Ma et al., 2024). However, GSHPs have higher initial costs and more complex installation requirements than ASHPs, including significant groundworks that may be impractical in dense urban environments with limited exterior space.

As shown in Figure 2.3, GSHP installations can use various pipe arrangements depending on available space and ground conditions. A single-tier horizontal loop is the simplest configuration but requires substantial land area. Double-tier and slinky configurations can reduce the required surface area, though at the cost of increased pipe length and installation complexity. Vertical ground loops require much less surface area but involve more expensive drilling operations (Singh et al., 2010).

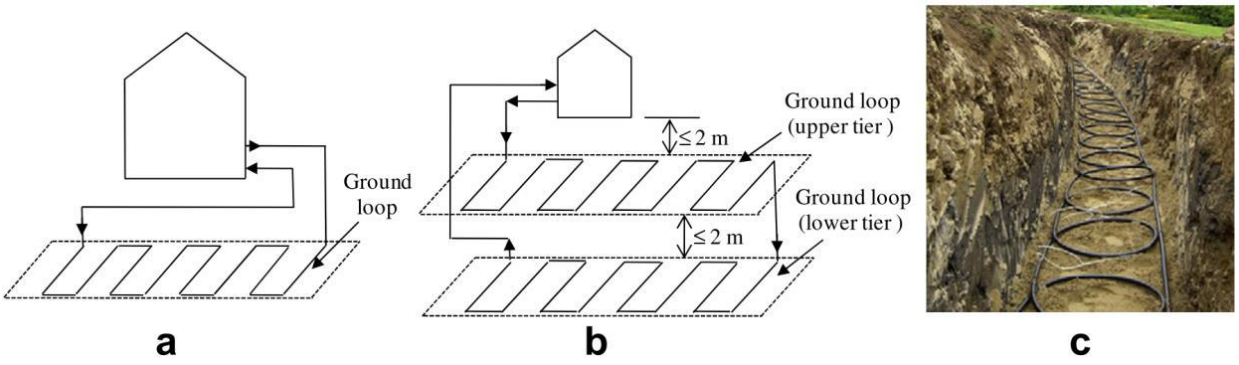


Figure 2.3: Pipe arrangements of GSHP (a) a single tier and (b) a double tier (c) slinky (Singh et al., 2010)

Water-source heat pumps (WSHPs) extract heat from water bodies such as lakes, rivers, or aquifers. When properly implemented, these systems can achieve efficiencies comparable to GSHPs while potentially requiring less extensive installation work (Wu et al., 2015). WSHPs can maintain stable performance throughout seasonal variations when drawing from deep or thermally buffered water sources, where temperatures remain relatively constant. However, their broader application is constrained by the site-specific availability of suitable water bodies and by environmental or regulatory concerns regarding water use (Wu et al., 2015).

The selection of HP type significantly influences both system performance and integration potential. This becomes particularly relevant in community-scale implementations, where factors such as space constraints, noise considerations, and collective impact on electrical infrastructure must be carefully evaluated (Reguis et al., 2021). Recent developments have also seen the emergence of hybrid systems that combine different heat sources or integrate backup heating systems to address the limitations of individual technologies, though at the cost of increased system complexity (X. Li et al., 2020).

(Gaur et al., 2021) summarized the COP, installation costs, pros, and cons of each HP technology in Table 2.1.

Table 2.1: Summary of the most common HPs Technologies (Gaur et al., 2021)

Technology	Installation cost	Average COP	Environmental Impacts	Pros	Cons
Air Source Heat Pump (ASHP)	+	3	• Highest environmental impact in cold regions • Leakage of refrigerant can cause pollution • Causes noise pollution	• Less or no pollution concerns • Simple operation • Low Maintenance Cost • High COP • Low primary energy consumption	• Frost formation on outer units • COP varies with ambient temperature • May need supplemental heat system for better performance
Water Source Heat Pump (WSHP)	++	4.5	• Can cause water pollution, stratum settlement and trigger geological disasters	• Highly efficient • Not affected by ambient conditions • Can utilise heat from rivers and lakes	• Requires water bodies or storage tanks in vicinity • Needs regulatory permission for installation
Ground Source Heat Pump (GSHP)	+++	3.5–4	• Unchecked heat transfer fluids are hazardous • Surface water can enter borehole • Can perturb groundwater temperature • Reduces emissions with low payback period	• Highly efficient and shows great energy saving potential • High COP • Utilises vast source of heat • Very reliable source of heat • Can operate in regions with extreme winters	• Needs careful assessment of local geology and requirements • COP may decrease over heating season due to saturation of soil temperature • High installation costs

2.2.2 Performance and Efficiency Factors

The effectiveness of HPs in residential heating applications depends on several factors that affect their COP. Understanding these relationships is crucial for optimising system performance, particularly in community-scale implementations where collective efficiency impacts both energy consumption and grid stability.

The primary factor affecting HP performance is the temperature difference between the source and delivery temperatures. As shown in Figure 2.4, the COP decreases as this temperature differential increases, following a non-linear relationship that fundamentally limits performance in high-temperature applications (delivery temperatures above 55°C, compared to standard HP output of 30-45°C) (Lämmle et al., 2023). The figure shows that the COP would decrease from 4.4 to 3 when the temperature lift increases from 35K to 55K.

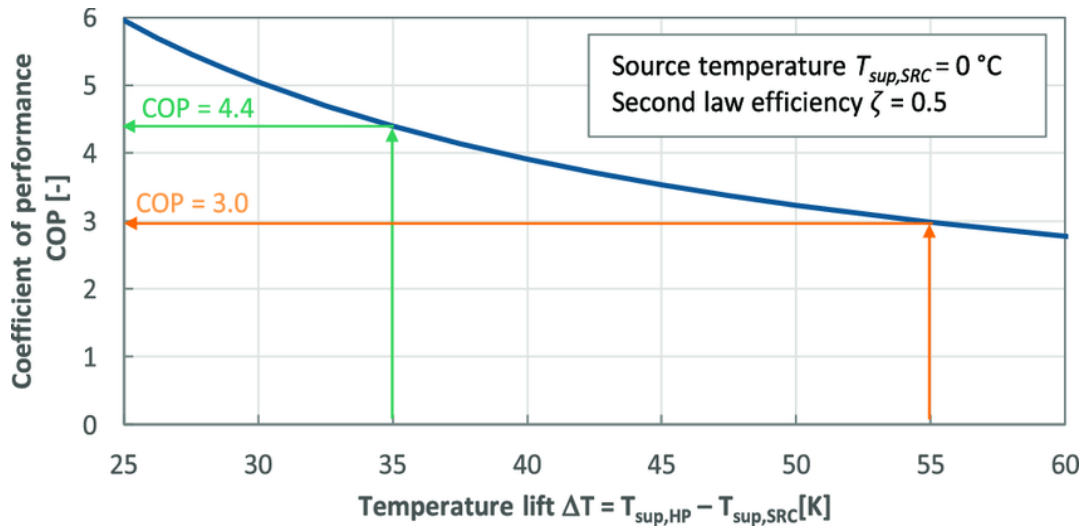


Figure 2.4: COPs at different water temperatures (Lämmle et al., 2023)

This temperature relationship becomes particularly significant in cold climates where lower ambient temperatures reduce the evaporator temperature while higher delivery temperatures may be required to maintain comfort through existing heat distribution systems (Sager et al., 2019). Demonstrated performance data shows that for a typical ASHP, increasing the temperature lift from 30K to 50K can reduce the COP by approximately 40%. This creates a challenging inverse relationship between capacity and efficiency, as HPs must work hardest (with lowest efficiency) precisely when heating demand is highest (Zhao et al., 2017) (Chesser et al., 2021)

Seasonal performance variations present specific challenges for system design and operation, particularly for ASHPs. Field studies by (Chesser et al., 2021) across 20 domestic installations found that actual seasonal performance factors often differ from rated efficiencies due to several real-world factors as variable weather conditions affect source temperatures throughout the heating season, creating fluctuating efficiency levels. Cycling losses during part-load operation reduce efficiency when systems must frequently start and stop to match variable demand (Z. Xu et al., 2021). For ASHPs specifically, defrost cycles temporarily reverse the system operation to remove ice buildup on outdoor coils, consuming energy without providing useful heat

(Dong et al., 2012). Finally, system oversizing often leads to suboptimal operation patterns with excessive cycling (Z. Xu et al., 2022).

Most residential HPs operate at part-load conditions for significant portions of the heating season, making part-load efficiency a critical consideration. Modern inverter-driven systems can modulate their output to match demand, offering significant advantages over fixed-speed systems that rely on cycling for capacity control (Mahmoudi et al., 2021).

(Dongellini & Morini, 2019) in Figure 2.5 illustrates the contrasting operational patterns of a single-stage heat pump (SSHP) and an inverter-driven heat pump (IDHP). The SSHP experiences frequent cycling—15 on/off cycles within the depicted timeframe—leading to pronounced fluctuations in supply and return water temperatures. In contrast, the IDHP maintains a stable operation with no cycling, resulting in smoother thermal output. This behavioral difference has direct implications on system efficiency: SSHPs experience higher cycling losses (around 12%), compared to just 1% for IDHPs. Consequently, seasonal COP is significantly higher for IDHPs (3.44) than SSHPs (2.88), underlining the efficiency benefits of inverter-driven systems in residential heating applications.

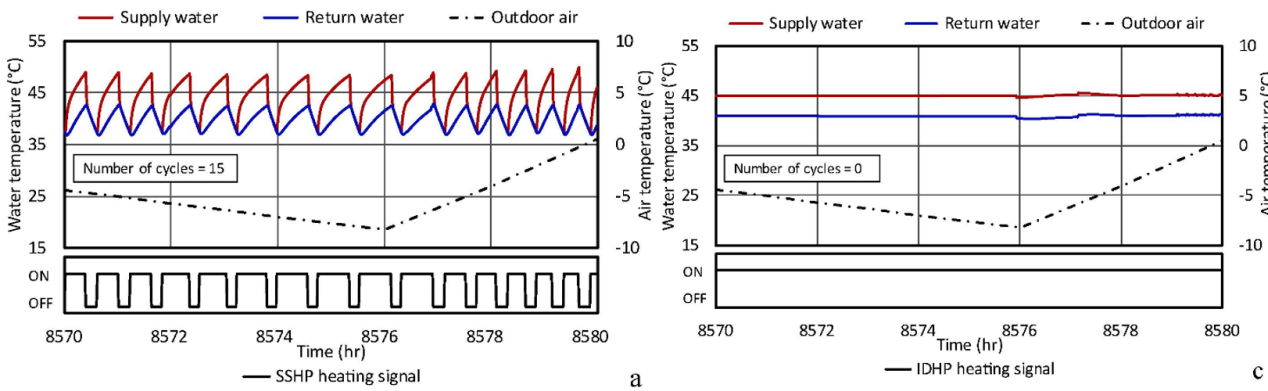


Figure 2.5: Comparison of heat pump cycling behaviour for a Single-Stage Heat Pump (SSHP) (left) and an Inverter-Driven Heat Pump (IDHP) (right). (Dongellini & Morini, 2019)

The integration of HPs within existing residential heating systems introduces additional performance considerations. Flow temperature requirements of heat emitters significantly impact system efficiency, with traditional radiator systems typically designed for temperatures of 65-75°C, well above the optimal range for standard HPs (Childs et al., 2025). Study by (Hu et al., 2019) comparing different heating terminals demonstrated that low-temperature emitters like underfloor heating can improve seasonal COP by 15-25% compared to conventional radiator systems standard (STD) fan-coil units (which are air-to-water heat exchangers that use a fan to blow air over a coil containing heated water, commonly used in commercial and some residential heating systems) which is also presented in Figure 2.6. Domestic hot water production presents another challenge, requiring higher temperatures than space heating and often necessitating additional technologies such as supplementary electric heating or specialized high-temperature HPs which will be discussed in the next subsection (Hu et al., 2019).

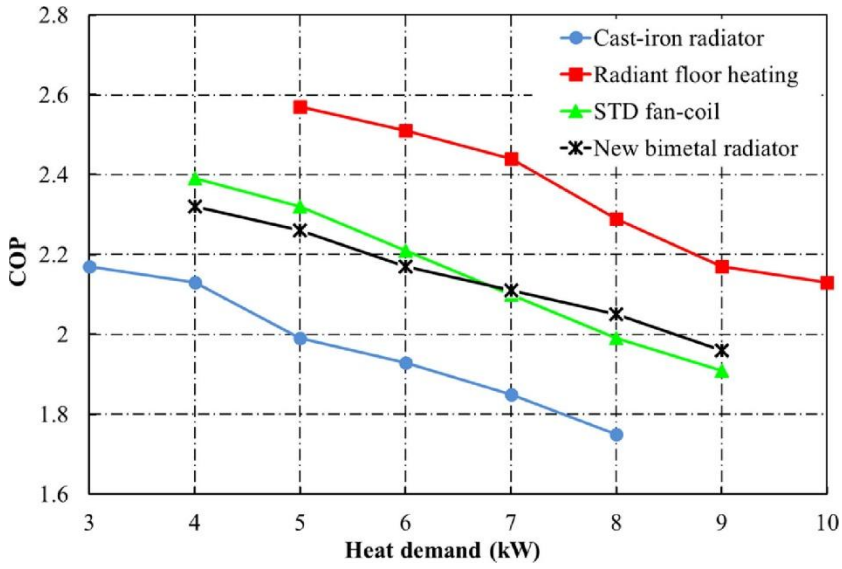


Figure 2.6: Comparison of HP COP across different heat emitters as a function of heat demand (Hu et al., 2019)

These performance factors become particularly significant when considering community-scale implementations. The diversity of demand across multiple buildings

can help smooth aggregate load profiles, while coordinated control strategies can optimize overall system performance. Simulation studies have demonstrated that coordinated operation of multiple heat pump systems can reduce peak electrical demand by 20–30% compared to uncoordinated operation, while maintaining or improving thermal comfort, (Huang et al., 2019). These findings highlight the potential benefits of community-scale approaches to HP deployment, though realizing these benefits requires sophisticated control systems and appropriate infrastructure for coordination.

2.2.3 High-Temperature Heat Pumps

The transition from conventional heating systems to HPs in existing buildings presents a significant challenge due to the temperature requirements of traditional heat emitters. While standard HPs typically deliver temperatures between 35-45°C, many existing radiator systems are designed for flow temperatures of 65-75°C (Reguis et al., 2021). This temperature disparity has driven the development of high-temperature HPs (HTHP) that can deliver output temperatures up to 75°C while maintaining acceptable efficiency levels (Arpagaus et al., 2018).

Recent technological advancements in HTHPs have focused on overcoming the inherent efficiency challenges of operating at elevated temperature differentials. These systems typically employ enhanced compression technologies and optimized refrigerant cycles to achieve higher delivery temperatures without excessive penalties to their COP (Mota-Babiloni et al., 2018). Common approaches include cascade systems that utilize multiple refrigeration cycles in series, with the condenser of the first cycle serving as the evaporator of the second (Jouhara et al., 2024). This arrangement allows each cycle to operate with a more modest temperature lift,

improving overall efficiency. Other designs use modified single-cycle configurations with enhanced compressors and novel refrigerant blends that have favourable thermodynamic properties at higher temperatures (Brendel et al., 2024).

(N. Shah & Hewitt, 2016) documented field trials of HTHPs in retrofit applications across the UK residential sector. They found that modern systems can maintain COPs with an average of 2.07 even when delivering temperatures of 65°C, though this represents a significant reduction from the performance achieved at lower delivery temperatures. Commercial systems now available from manufacturers like (SAMSUNG, 2022) and (MITSUBISHI ELECTRIC, 2018) demonstrate the market maturity of this technology, with published technical data showing COP values ranged from 2.33 at -7°C to 4.76 at 25°C for water temperature around 50°C.

Figure 2.7 highlights the inverse relationship between heat pump efficiency and required delivery temperatures—an important consideration for HTHPs applications. As shown, increasing the condenser temperature from 40 °C to 80 °C results in a marked reduction in COP across all evaporator temperatures (Bellos et al., 2023).

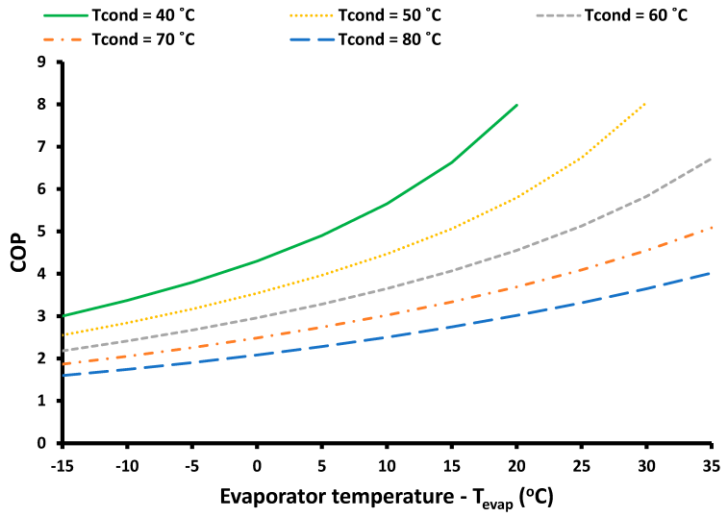


Figure 2.7: COP of heat pumps as a function of evaporator temperature under various condenser (output) temperatures. (Bellos et al., 2023)

The integration of HTHPs with TES systems offers potential for optimizing performance. Storage temperatures above 60°C enable these systems to meet both space heating and domestic hot water demands effectively, while providing opportunities for load shifting and peak demand management (Wang, Wang, et al., 2022). This strategy not only improves overall system efficiency but also reduces peak electrical demand, benefiting both system economics and grid stability. However, the lower COPs associated with high-temperature operation make the timing of storage charging cycles particularly critical for overall system efficiency (Jung et al., 2017), (Le et al., 2019).

Market adoption of HTHPs has been driven by their compatibility with existing heating systems, reducing the need for extensive modifications to building heat distribution systems (Childs et al., 2025). This advantage must be weighed against their higher capital costs and lower operational efficiency compared to standard HPs in a holistic assessment of retrofit options (Bellos et al., 2023). (Zuberi et al., 2021) conducted a comprehensive techno-economic comparison of different heat decarbonization pathways, finding that HTHPs offered advantages in certain building types where distribution system replacement would be particularly costly or disruptive. In buildings with limited space for larger radiators or underfloor heating, HTHPs may represent the only feasible electrification option without extensive renovation (Lämmle et al., 2022).

Field studies of HTHPs installations have demonstrated their viability in replacing conventional heating systems, while highlighting the importance of sophisticated control strategies to optimize their operation. (Le et al., 2019) found that appropriate control parameter selection and system integration could significantly improve operational performance in real-world conditions. These findings emphasize the need

for careful system design and operation to maximize the benefits of HTHPs deployment while managing their impact on electrical infrastructure.

2.3 Thermal Storage Technologies

The integration of TES with HPs represents a crucial strategy for enhancing system flexibility and efficiency while managing grid impact. By decoupling heat generation from demand, storage provides opportunities for both performance optimization and load management, particularly in community-scale applications where collective impacts become significant.

2.3.1 Types of Thermal Energy Storage

The selection of appropriate TES technology significantly influences system performance and integration potential. Three principal approaches to thermal storage exist - sensible, latent, and thermochemical - each offering distinct characteristics and advantages for different applications.

Sensible heat storage, which utilizes the temperature change of a storage medium, remains the most widely implemented approach in residential applications. Water-based systems dominate this category due to water's exceptional properties: high specific heat capacity (4.18 kJ/kg·K), excellent heat transfer characteristics, low cost, and compatibility with existing plumbing systems (Hutty et al., 2020). A typical domestic hot water tank can store approximately 2.1 kWh of thermal energy for each 50L of water with a 35K temperature difference, making it an efficient storage medium for residential-scale applications (Stalinski & Duquette, 2021). This simplicity and

cost-effectiveness have made water-based systems the default choice for integration with HPs operating at various temperature levels (Hutty et al., 2020).

Latent heat storage systems employ phase change materials (PCMs) that absorb or release heat during phase transitions, typically between solid and liquid states (N. Zhang et al., 2018). The primary advantage of PCMs lies in their higher energy density - they can store 2-3 times more heat per unit volume than water within the same temperature range due to the additional energy associated with phase change (Groulx et al., 2021). This compact storage potential makes PCMs particularly attractive for applications with space constraints (Zhou et al., 2024). Additionally, PCMs can store and release heat at near-constant temperatures corresponding to their phase transition point, potentially aligning well with specific HP operation points for optimized performance (Yang et al., 2021).

Despite these theoretical advantages, PCM implementation in residential settings has been limited by several practical challenges. Cost remains significantly higher than water-based storage, with premium materials adding substantial expense to system installation (Sharif et al., 2015). Long-term stability issues include degradation of thermal properties after repeated cycling, phase separation in some materials, and corrosion interactions with containment vessels (Bland et al., 2017). Heat transfer limitations also present engineering challenges, as solid-phase PCMs typically have poor thermal conductivity, potentially limiting charging and discharging rates (Shank et al., 2023). Recent developments have focused on addressing these limitations, with new materials and encapsulation methods showing promising results for building-scale applications (Osibodu et al., 2024). Organic PCMs based on paraffins, or fatty acids offer improved cycling stability, while various composite materials incorporate conductive elements to enhance heat transfer (Nazari et al., 2022).

Thermochemical storage systems represent the third approach, utilizing reversible chemical reactions to store and release heat. These systems offer theoretically higher energy densities than both sensible and latent storage - up to 10 times that of PCMs - and the potential for near-lossless long-term storage, as energy is stored in chemical bonds rather than as temperature differences (Chen et al., 2018). Common reactions include hydration/dehydration of salts, adsorption processes, and certain redox reactions (Farulla et al., 2020). During the charging process, heat input drives an endothermic reaction, typically separating a working pair of materials. These separated materials can be stored indefinitely without energy loss until they are brought together again in an exothermic reaction that releases the stored heat (Farulla et al., 2020).

While thermochemical storage holds significant promise, particularly for seasonal storage applications, current technical challenges and system complexities have limited practical implementation in residential heating systems. These challenges include managing the often corrosive materials involved, achieving sufficient reaction rates for practical power output, maintaining material stability over numerous cycles, and developing cost-effective reactor designs (Moulakhnif et al., 2024). Research in this area continues to advance, but commercial applications remain primarily at the demonstration stage rather than widespread deployment (Mukherjee et al., 2021).

Figure 2.8 from (Sarbu & Sebarchievici, 2018) compares the storage characteristics of common TES materials, plotting their energy density against operating temperature. Conventional sensible heat storage using water is limited in capacity, particularly at higher temperatures. PCMs, such as paraffins and salt hydrates, offer improved energy density by exploiting latent heat, while Thermochemical Materials, including

$MgSO_4 \cdot 6H_2O$ and zeolites, provide superior volumetric capacity—often exceeding 400–600 kWh/m³.

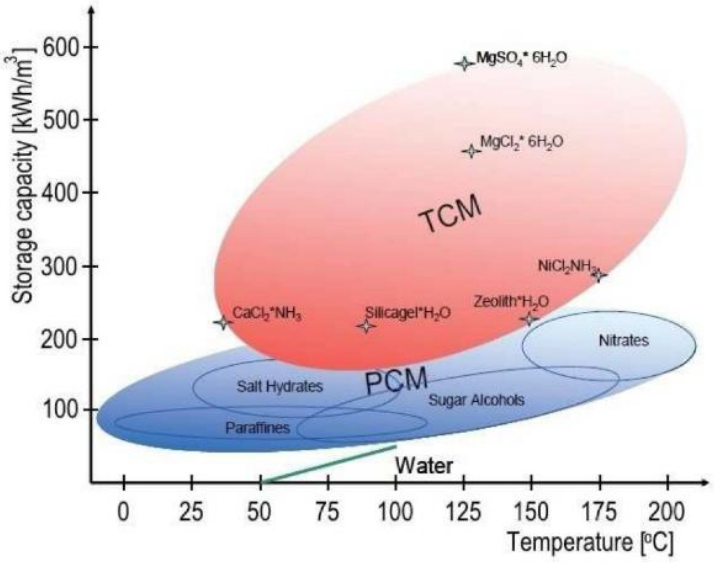


Figure 2.8: Storage capacity vs. operating temperature for various TES technologies. (Sarbu & Sebarchievici, 2018)

2.3.2 Integration with Heat Pumps

The effective integration of TES with HPs requires careful consideration of system-level temperatures, storage types, and control strategies. While physical configuration matters, the temperature regimes and control algorithms fundamentally determine overall performance, efficiency, and flexibility (Hirschey et al., 2023).

System Temperature Considerations

System temperatures represent a critical factor in integrated HP-TES systems. Which refers to the leaving water temperature from the HP through the TES temperature to the final delivery temperatures for space heating and domestic hot water. Heat pumps operate most efficiently at lower delivery temperatures, with COP declining as temperature lift increases (Tang et al., 2024). A 10K increase in delivery temperature

can reduce COP by 15-25%, creating a fundamental trade-off between storage capacity and system efficiency (Rony & Gladen, 2021).

The stratification temperature profile within storage systems significantly influences overall performance. A well-stratified tank maintains distinct temperature zones, allowing the heat pump to operate with lower return temperatures while providing higher delivery temperatures to the distribution system (Haller et al., 2019a). Experimental studies have shown that maintaining a 5-10K temperature difference between top and bottom zones can improve system efficiency by 3-8% compared to fully mixed tanks (Zinsmeister et al., 2023). Active stratification management through specialized inlet diffusers, baffle plates, or multiple tank arrangements has proven particularly effective in larger installations (Bouzaher et al., 2019).

For high-temperature applications, the storage temperature selection becomes particularly critical. Heat pumps designed for higher output temperatures (65-75°C) can directly meet DHW requirements but operate with lower efficiency (Trinchieri et al., 2020).

(Glembin et al., 2015) used detailed TRNSYS simulations of an 8-kW_e HP serving a solar-assisted combi-store TES to compare one heated zone (single-temperature) with two heated zones: a space-heating (SH) zone held at ≈ 43 °C and a DHW zone held at ≈ 57 °C. By allowing the HP to operate most of the year at the lower SH set-point, the average condenser outlet temperature dropped by 6 K, raising the HP seasonal performance factor (SPF) from 3.35 → 3.67 and the whole-system SPF which includes the HP plus all auxiliary components such as circulation pumps, controls, and system thermal losses from 3.15 → 3.48 as presented in Figure 2.9. The corresponding reduction in compressor electricity consumption was ≈ 10 %.

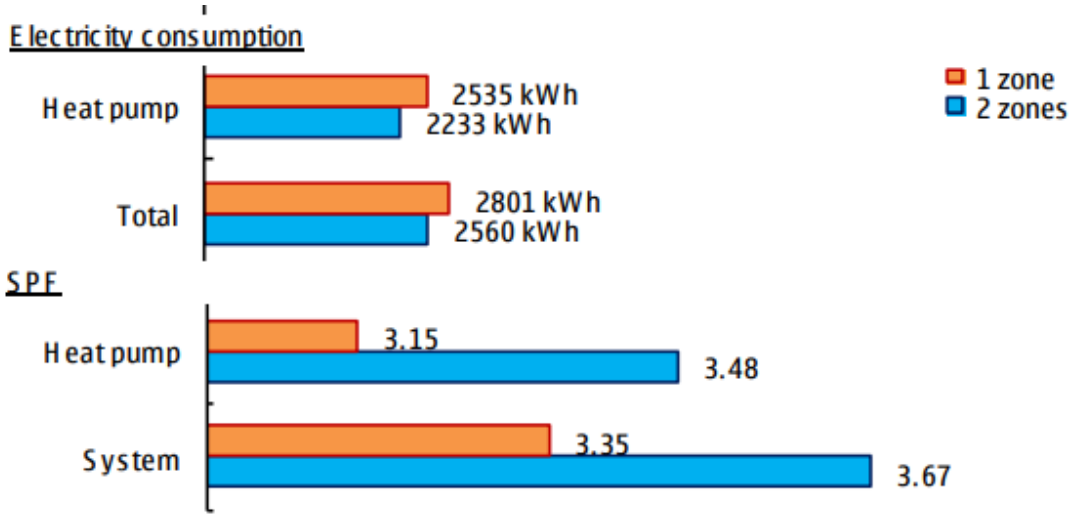


Figure 2.9: SPF and Electrical Consumption for a HP-TES with 1 versus 2 heated zones (Glembin et al., 2015)

Control Strategies for Different TES Types

Different TES technologies require specific control approaches to maximize performance. For sensible water-based storage, predictive control algorithms that incorporate weather forecasts, occupancy patterns, and electricity pricing have demonstrated advantages (D. Lee et al., 2020). (Kargar & Bahamin, 2025) implemented model predictive control for water tank storage, achieving around 18% reduction in operating costs compared to conventional thermostat-based approaches.

Latent heat storage systems utilizing PCMs require control strategies that account for their non-linear charging and discharging characteristics. According to (Caron-Soupart et al., 2016) and (Peng et al., 2021), the effective control of PCM-based storage must consider:

1. State-of-charge estimation, which is more complex than for sensible storage due to the non-linear temperature-enthalpy relationship during phase transition.
2. Charging rate limitations during phase transition periods.

3. Optimal temperature matching between the HP output and PCM melting point.

For thermochemical storage, which offers higher energy density but more complex operation, control strategies must manage the chemical reaction rates and temperatures carefully. These systems typically require multi-stage control approaches that balance reaction completeness with system efficiency (Y. X. Xu et al., 2022).

Community-Scale Implementation

At the community scale, coordinated control becomes particularly valuable for managing collective grid impacts. Simulation studies have shown that staggered charging or operation of heat pumps across multiple buildings can reduce peak electrical demand at substations by 20–35% compared to uncoordinated operation. (Gonzato et al., 2019).

Advanced coordination approaches including hierarchical control structures enable both local optimization and community-wide constraints to be considered. (Renaldi et al., 2017) demonstrated that optimization-based control at community scale could identify load shifting opportunities that balance multiple objectives including:

1. Minimizing operating costs under time-variable electricity pricing.
2. Reducing peak electrical demand on the local network.
3. Maximizing heat pump efficiency through optimal storage utilization.
4. Ensuring thermal comfort requirements are maintained across all buildings.

Sizing and Performance Considerations

Appropriate sizing of TES tanks relative to HP capacity is pivotal for both efficiency and economics. The principal European design standard BS EN 15450:2007

recommends 12–35 L · kW_{th}^{-1} of buffer volume for water-based storage in HP systems, a range echoed by BS EN 14511's defrost-cycling guidance at ≈ 25 L · kW_{th}^{-1} (homemicro.co.uk, 2016).

Larger storage volumes offer greater flexibility for load shifting but introduce higher standby losses and capital costs (Baeten et al., 2017). While larger TES volumes offer increased flexibility, studies have shown that beyond a certain point, the additional benefits diminish. In many residential systems, excessively large storage capacities may not yield proportional economic returns, due to higher capital costs and thermal losses (Felten & Weber, 2018).

Through appropriate temperature management, advanced control strategies, and proper sizing, integrated HP-TES systems can significantly enhance both technical performance and grid flexibility while minimizing operational costs. The selection of specific control approaches should be determined by the storage technology, application requirements, and operational objectives.

2.3.3 Integration Challenges

The practical implementation of HP-TES systems faces several challenges that influence their effectiveness in residential applications. These challenges include heat losses, space requirements, system complexity, and economic considerations that must be addressed in system design and operation (N. N. Shah et al., 2018).

Heat losses from storage can significantly impact system efficiency, particularly in applications requiring high-temperature storage (above 60°) (Brunelli et al., 2024). Insulation quality plays a crucial role in minimizing these losses, while (Janakarajan et al., 2019) noted that even with effective insulation, an insulated water tank can experience a significant temperature drop, with a predicted loss of approximately

6.29°C over a 24-hour period. These losses become more critical in HTHPs applications, where storage temperatures above 65°C may be required for DHW provision. Since HPs operate with lower efficiency when producing these elevated temperatures, any heat loss represents premium energy that required additional electrical input to generate (Kropp et al., 2025).

Space requirements frequently constrain the installation of water-based TES in dwellings. Manufacturer datasheets like (Rheem, 2023) and (Vaillant UK, 2022) show that a 200 – 300 L unvented hot-water cylinder has a shell diameter of roughly 0.53 – 0.60 m and a height of 1.3 – 2.1 m, giving a bare footprint near 0.22 – 0.30 m². This challenge becomes particularly relevant in retrofit applications, where available space for storage tanks may be limited by existing building layouts. Various compact and slim-line tank designs have emerged to address these constraints, though often at higher cost and with some compromise in performance (Bourne & Novoselac, 2015). The trade-off between storage volume and space constraints influences the potential for load shifting and peak demand management, affecting the overall effectiveness of the integrated system (Reguis et al., 2021).

System complexity increases with the integration of TES, requiring additional components such as valves, pumps, sensors, and controls beyond those needed for stand-alone HP systems (Rendall et al., 2023). This complexity not only adds to initial installation costs but also creates potential maintenance and reliability concerns over the system lifetime (N. N. Shah et al., 2018). Ensuring proper commissioning becomes particularly important for integrated systems, as suboptimal configuration can significantly reduce realized benefits (Y. Li et al., 2023). Studies of field installations have shown that actual performance often falls short of design expectations, with

improper valve sequencing, inadequate sensor placement, or suboptimal control parameters frequently identified as contributing factors (N. N. Shah et al., 2018).

Economic considerations ultimately determine the viability of integrated HP-TES systems in residential applications. While TES can provide valuable operational flexibility and reduce electricity costs through load shifting, the additional capital expense must be justified through tangible benefits such as peak demand reduction, increased self-consumption, or participation in dynamic pricing schemes (Sultan et al., 2023). In markets with time-of-use electricity pricing or demand charges, the economic case for storage becomes stronger as peak-period electricity use can be reduced (Romero Rodríguez et al., 2018). Similarly, in applications where renewable self-consumption is valued, storage can improve economic returns by increasing the proportion of self-generated electricity used on-site (L. Zhang et al., 2025). However, in markets with flat electricity rates and no financial incentives for load flexibility, the economic justification may rely primarily on reduced equipment cycling and potential lifetime extension, benefits that are more difficult to quantify in standard economic assessments (Jung et al., 2017).

Despite these challenges, the integration of HPs with TES continues to advance through both technological improvements and market developments. Enhanced insulation materials, more sophisticated controls, and evolving electricity market structures are gradually improving the value proposition for integrated systems (Jung et al., 2017). As renewable energy penetration increases and grid flexibility becomes more valuable, the economic case for storage is likely to strengthen further, driving continued innovation in this area (Enescu et al., 2020).

2.4 Discussion and conclusion

This chapter has reviewed HP and TES technologies for residential heat decarbonisation, examining their operational principles, performance characteristics, and integration challenges. The analysis reveals that while individual technologies are technically mature, significant knowledge gaps remain in their integrated application.

Heat pump efficiency fundamentally depends on the temperature differential between source and delivery points, with COPs declining from 3-5 to below 2.5 as delivery temperatures increase to the 65-75°C range required by conventional heating systems. For practical implementation without extensive retrofits, HTHPs from manufacturers like Samsung and Mitsubishi offer a viable solution, delivering the higher temperatures needed by existing radiator systems while maintaining acceptable efficiency. These systems represent a pragmatic approach for widespread deployment across existing housing stock.

The integration of thermal storage, particularly PCM-based solutions such as Sunamp's Thermino systems, provides significant advantages in residential applications where space is constrained. These systems offer 2-3 times higher energy density than conventional water tanks, addressing practical installation limitations while enabling effective load shifting capabilities. However, the literature reveals critical gaps in understanding how to optimise these integrated systems effectively.

Most notably, there is limited research on optimisation algorithms that coordinate HP operation with TES charging and discharging cycles to minimise peak electrical demand while maintaining thermal comfort. Furthermore, real-world performance data for HTHP operating at 65-75°C when integrated with TES remains limited,

particularly regarding actual COP values achieved in practice and the optimal control strategies for different building types.

Additionally, the validation of heat demand models for integrated HP-TES systems across diverse building characteristics remains incomplete. Most studies rely on standardized assumptions about building thermal properties and occupancy patterns, without comprehensive validation against measured data from operational systems. This gap is particularly significant for existing UK housing stock, where varied construction standards and thermal characteristics create complex optimization challenges.

These knowledge gaps directly inform the research approach undertaken in this thesis, emphasizing the need for comprehensive data collection from real deployments and the development of modelled heat demands.

Chapter 3

3. Literature Review: Active Buildings and Community Energy Systems.

3.1 Introduction

This chapter extends the analysis beyond individual HP systems to examine their collective implementation at the community scale. While Chapter 2 focused on technical aspects of HPs and TES at the building level, here we address the broader challenges and opportunities that emerge when these technologies are deployed across entire communities.

The collective operation of multiple HPs presents significant challenges for electrical distribution networks. As (Quiggin & Buswell, 2016) demonstrate, traditional LV networks designed for predictable power flows, now face unprecedented stresses from electrified heating loads that can increase household electricity demand up to six times during peak periods. This challenge is compounded by the increasing integration of variable renewable generation, creating a fundamental mismatch between supply and demand patterns that must be managed effectively (McGarry et al., 2024).

TES offers a promising solution for addressing these temporal misalignments, enabling heat demand to be shifted to periods of higher renewable availability or lower network stress. However, realizing these benefits requires coordinated approaches that extend beyond individual building optimization to consider community-wide impacts and opportunities (Tito et al., 2023).

Recent developments in community energy systems have shown that coordinated control strategies can reduce peak electrical demands compared to uncoordinated operation (Srithapon & Månsson, 2023), while simultaneously increasing renewable self-consumption and providing valuable grid services. These approaches leverage demand diversity across multiple buildings and enable more efficient use of shared infrastructure.

This chapter examines how HPs and TES can be optimally integrated within community energy frameworks, focusing on network impacts, peak demand management, renewable energy integration, and practical implementation approaches. By addressing these community-scale considerations, we can develop more effective strategies for heat decarbonization that balance technical performance, grid integration, and economic viability.

3.2 Grid Integration Challenges

The widespread adoption of HPs introduces significant challenges for low voltage distribution networks that were historically designed for much lower electrical loads. These challenges become particularly acute at the community scale, where the simultaneous operation of multiple HPs can create substantial peaks in electricity demand. Understanding these impacts is crucial for developing effective integration strategies and avoiding costly network reinforcement requirements that could otherwise impede the pace of heat decarbonisation.

3.2.1 Impact on LV Networks

The electrification of residential heating through HP deployment fundamentally changes the demand characteristics that electrical distribution networks must accommodate. Unlike traditional electrical loads such as lighting and appliances, HPs typically draw higher power for extended periods, especially during colder weather. This characteristic creates new challenges for grid capacity and load management.

Field studies and modelling work have shown that HP operation can significantly increase household electricity consumption, particularly during heating seasons. For instance, an energy mapping study in Oxford (UK) reported that deploying ASHPs led to a 200% increase in mean daily electricity demand per household (Gupta & Gregg, 2023). Another field study found that peak electricity use increased by 23% after retrofitting social housing with HPs, even though average daily use declined overall (Gupta & Zahiri, 2020).

Large-scale analyses also estimate that nationwide HPs adoption could more than double the electricity demand, especially during cold spells, due to sustained and synchronized operation patterns (Watson et al., 2023). Figure 3.1 illustrates this impact, showing how the introduction of HPs can substantially alter both the magnitude and temporal profile of electrical demand at the household level.

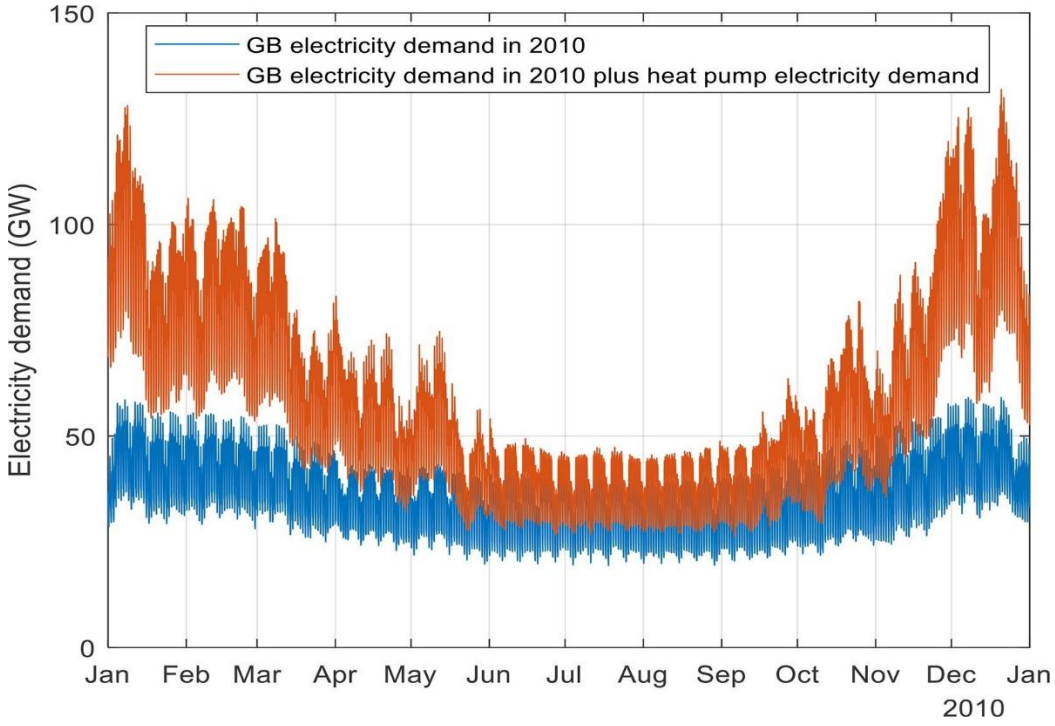


Figure 3.1: Projected annual electrical demand showing the effect of HP integration (Watson et al., 2023)

When aggregated across multiple households within a community, these increased loads can approach or exceed the thermal limits of LV network components, particularly distribution transformers and cables (Haque et al., 2017). Distribution substations in residential areas typically have capacity ratings based on historical demand patterns, with limited headroom for additional load and has been conventionally developed in a 'fit-and-forget' approach due to the relatively longer lifetime of the network assets enabling a much longer planning horizon for the network operators (Harkin & Turton, 2017). Similar capacity constraints exist in distribution cables, particularly in older networks where conductor sizing may already be operating near thermal limits during peak periods (Navarro-Espinosa & Mancarella, 2014).

The temperature dependency of HP operation further complicates their grid impact. During cold weather periods, when HPs operate at lower COPs, their electrical demand increases precisely when the network may be experiencing higher overall

loading (Milev et al., 2023). This correlation between weather conditions and peak demand creates challenges for network capacity planning and management. (Chesser et al., 2021) documented this effect in field trials, showing that the electrical consumption of HPs can increase by up to 50% during periods of extremely low temperatures compared to average winter operation. This weather sensitivity creates a "double impact" where more units operate simultaneously at lower efficiency, potentially creating demand peaks that exceed even conservative planning estimates.

The seasonal variation in HPs demand patterns creates challenges for electricity network planning and operation. Unlike conventional electrical loads, which typically follow relatively stable seasonal trends, HP electricity demand can fluctuate significantly between summer and winter, due to strong dependency on outdoor temperatures. Field studies and system modelling have shown that during the winter season, HP loads can be several times higher than in summer months, creating sharp seasonal peaks in electricity consumption (Peacock et al., 2023).

The combination of these impacts necessitates a comprehensive approach to network planning and operation that considers both immediate technical constraints and longer-term infrastructure requirements. Traditional approaches to network reinforcement, where capacity is increased based on worst-case scenarios, may prove prohibitively expensive if applied universally to accommodate heat pump adoption. More sophisticated approaches that incorporate smart control, storage, and flexible operation offer potential pathways to higher heat pump penetration while managing network impacts, as will be explored in subsequent sections of this chapter.

3.2.2 Peak Demand Management

The coincidence of HP operation across multiple households presents a critical challenge for LV electricity networks—one that traditional diversity factors are ill-equipped to address. Conventional network planning often assumes that not all household electrical appliances will operate simultaneously, allowing planners to apply diversity factors that reduce expected peak loads. However, the weather-dependent and synchronous nature of HP operation disrupts this assumption. During cold periods, many or most HPs within a community may activate at the same time in response to temperature drops, creating coincidence factors far higher than those used in standard household load modelling (Navarro-Espinosa & Mancarella, 2014).

High coincidence of heat pump operation during cold periods poses a major challenge for distribution networks. Probabilistic modelling and field studies in the UK and Europe have shown that, unlike conventional residential loads, heat pump usage is strongly synchronized by temperature, leading to coincidence factors much higher than those used in traditional load planning. During extreme cold, the simultaneous activation of heat pumps across multiple households can result in coincident peak loads approaching unity, dramatically increasing demand at the feeder and transformer level (Johnson & Mayfield, 2022).

Building thermal characteristics play a critical role in shaping HP operation patterns and the resulting electrical demand profiles. Well-insulated buildings with high thermal mass can delay the need for heating, allowing indoor temperatures to remain within comfort thresholds for longer without active HP operation. This thermal inertia introduces opportunities for load shifting and demand smoothing, potentially reducing peak coincidence during high-demand periods (Ellerbrok, 2014).

The temporal distribution of heating demand across a community presents both challenges and opportunities for peak management. Analysis of residential heating patterns typically reveals two daily peaks: a morning peak as buildings recover from nighttime temperature setbacks, and an evening peak coinciding with occupant return and increased activity. These heating demand peaks often align with existing electricity demand patterns from lighting, cooking, and other household activities, creating compounded system stress. Field measurements by (Perelli-Rocco et al., 2024) showed that these extended periods of high demand can last for several hours during cold weather, particularly in poorly insulated buildings or during extreme weather events, creating sustained high loads that exceed network capacity rather than brief demand spikes that might be more easily managed.

Network capacity constraints necessitate more sophisticated approaches to managing peak HP demand beyond simply expanding infrastructure. Traditional reinforcement strategies are costly and time-consuming, particularly in dense urban areas where asset replacement may be disruptive. Consequently, utilities are increasingly turning to demand-side flexibility and smart control strategies to mitigate peak loads and enhance grid resilience (El Feghali et al., 2022).

(Eyre & Baruah, 2015) modelled several scenarios to explore pathways for decarbonising residential heating in the UK, one of which was the full electrification of heat and transport (EHT). As shown in Figure 3.2, the EHT scenario (green line) projects a significant and continuous increase in electricity demand, reaching over 70 TWh by 2050, driven by the widespread adoption of electric heating and electrical transportation technologies and the decline of the gas grid. In contrast, other scenarios such as Minimum Policy Intervention (MPI), Local Energy and Biomass (LEB), and Deep Decarbonisation with Balanced Transition (DDBT) show more modest or even

declining electricity demand, reflecting varying levels of efficiency improvements, decentralised energy use, and alternative heating fuels like biomass or district heating. While figure 3.3 shows the growing peak electricity demand over years for the full electrification and hybrid solutions scenarios. The peak demand is expected to be at least doubled following the deep electrification of the heating

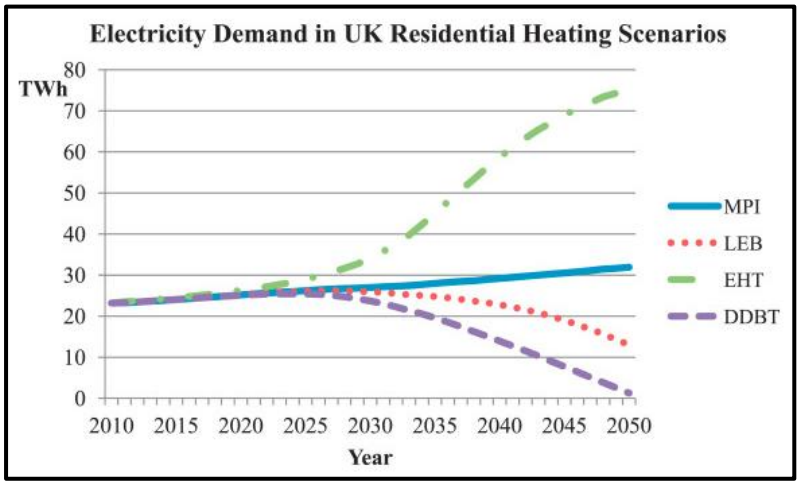


Figure 3.2: Different scenarios for UK electricity demand (full electrification is the green curve) (Eyre & Baruah, 2015)

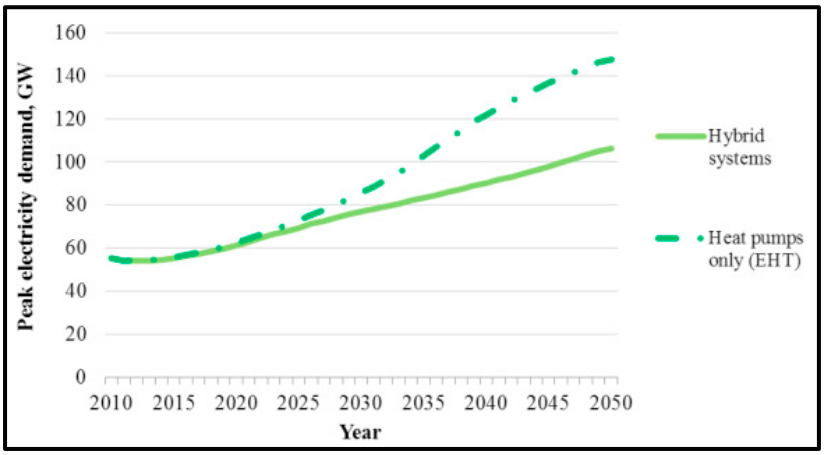


Figure 3.3: Expected peak electricity demand with the intensive deployment of HPs (Eyre & Baruah, 2015)

Time-of-use control strategies, which encourage HP operation during lower-tariff periods, have been shown to offer some benefits. However, these approaches often rely on rigid schedules, causing many systems to switch on at the same time when

cheaper tariffs begin. This synchronised behaviour can unintentionally generate new periods of high demand—sometimes comparable to or exceeding the peaks they were intended to reduce—if not carefully managed (Sweetnam et al., 2019). The challenge lies in developing control strategies that stagger HP operation intelligently across households and distribute load over longer periods, while maintaining both user comfort and energy efficiency (Georges et al., 2017).

The integration of thermal energy storage (TES) offers substantial potential for managing peak electricity demand by decoupling heat generation from heat delivery. This temporal flexibility enables HPs to operate during periods of lower grid stress—such as overnight or midday—and store thermal energy for use during peak periods, thereby alleviating pressure on the distribution network. Studies of residential and community-scale systems have shown that appropriately sized TES systems can reduce peak electrical demand by 20–50%, depending on climate, control strategy, and storage configuration (Hirschey et al., 2023). Figure 3.4 shows the monthly peak electrical demand for different heating system configurations, highlighting the impact of TES during the heating season. Systems without TES reach peak demands exceeding 10,000 kW, while storage-based configurations reduce these peaks significantly. On average, TES reduces peak demand by approximately 25–30% which demonstrates the effectiveness of thermal storage in flattening demand curves and enhancing system efficiency during high-load periods.

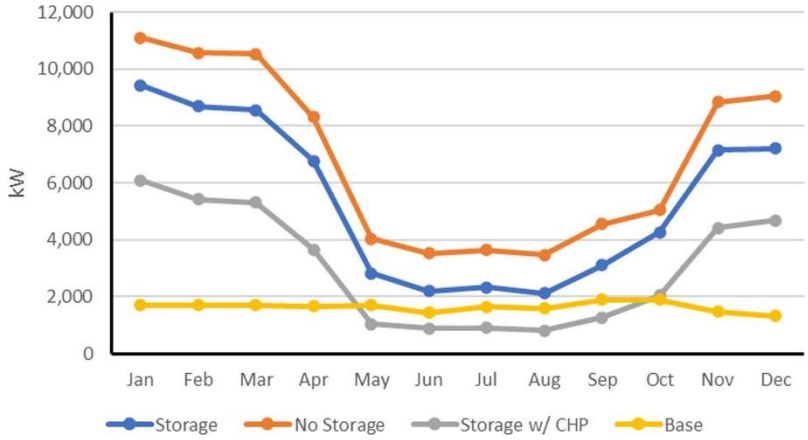


Figure 3.4: Monthly peak electrical demand (kW) for different heating strategies, including TES integration (Ryan et al., 2022).

Advanced forecasting and predictive control strategies have emerged as critical tools for managing peak electricity demand in community-scale HP deployments. By incorporating weather forecasts, building thermal response, and occupancy patterns, predictive controllers can anticipate future conditions and schedule HP operation to avoid network congestion while maintaining occupant comfort. Unlike fixed time-of-use schedules, these systems can pre-heat buildings during periods of lower network stress, reducing the need for simultaneous operation during constrained periods (Dou et al., 2023).

Economic considerations play a central role in selecting appropriate strategies for managing peak demand from HP deployment. While advanced control systems and TES offer significant potential to reduce network stress, their costs must be weighed against the investment required for conventional grid reinforcement. Simulation studies have shown that coordinated smart control strategies—such as optimized HP scheduling and flexible demand response—can often deliver equivalent or better performance at lower cost than upgrading physical infrastructure (Pudjianto et al., 2013).

3.2.3 Renewable Energy Integration

The accelerating deployment of electric HPs in community energy systems heightens the imperative to align variable renewable generation with highly variable space- and water-heating loads. A growing direction of peer-reviewed work shows that combining on-site renewables—principally photovoltaics (PV), photovoltaic-thermal collectors (PV/T) and, at district scale, surplus wind power—with HPs and TES can yield benefits, while also exposing new operational constraints.

Recent empirical studies of PV-assisted HP dwellings indicate that matching the PV array to roughly the annual household electricity demand can halve the need for grid imports and cut operational CO_2 emissions by nearly 50 % relative to an HP-only baseline (Rabczak et al., 2024). Optimisation work by (L. Zhang et al., 2025) demonstrates that adding a modest two-hour TES buffer increases self-consumption of rooftop PV by a further 12 % and permits a net-zero balance in three UK climate regions without oversizing the solar array. These findings confirm that even relatively small storage volumes can time-shift solar surpluses to the evening heating peak and thereby dampen distribution-network stress.

Hybrid PV/T–HP configurations extend this synergy. Experimental campaigns in northern Europe record seasonal performance factors above 4.0 and exergy efficiencies 15–20 % higher than conventional ASHP, because the liquid-cooled PV/T collectors both raise evaporator temperatures and boost electrical yield (Obalanlege et al., 2022). Such dual-function collectors are attractive for urban retrofit where roof area is limited, as they exploit the same surface for heat extraction and electricity production.

At the community or micro-grid level, multi-energy optimisation reveals even greater gains. Using a mixed-integer model for fifty UK homes, (Ling & Mulani, 2024) found that co-optimising HP dispatch with communal PV and a 160 kWh stratified tank lifted renewable utilisation from 42 % to 73 % while shaving the distribution-transformer winter peak by 30 %. Equally compelling evidence arises from district-heating studies. (Desguers et al., 2024) show that a power-constrained heat-network equipped with large-scale TES can absorb up to 48 % of otherwise curtailed wind energy, reducing system-wide emissions by 12 % and lowering wholesale operating cost for the network operator. These results position power-to-heat as a flexibility sink that enhances renewable value while decarbonising heat.

Overall, the literature portrays renewable-integrated electrified heating as a technically complementary and increasingly cost-effective pathway for community decarbonisation. The synergy hinges on leveraging TES and smart scheduling to reconcile variable supply with comfort-driven demand while respecting network limits. Remaining gaps centre on seasonally skewed resources, distribution-network headroom, optimal storage sizing, and socio-technical design. Future research should therefore integrate high-resolution weather hindcasts with behavioural models and marginal-emissions signals to craft control strategies that maximise carbon abatement per installed kilowatt of renewables and storage, ensuring that community-scale heating genuinely advances the transition to a net-zero energy system.

3.3 Community Energy Systems

The community energy concept covers a range of topics where people of one community work together to achieve energy-related goals (van der Schoor & Scholtens, 2015). This might include energy generation, saving or management, while

usually, it is related to achieving sustainable communities with net-zero emissions or even with positive emissions (Bauwens et al., 2022). In the UK alone there are more than 5000 community energy projects with initiatives starting from generating electricity from RES locally to benefit the community, while others have more complex systems with energy storage and heat networks (*Community Energy - GOV.UK*, n.d.).

(Han et al., 2022) presented the concept of a multi-vector community energy system (Figure 3.5) to achieve an electrified energy supply and demand. Besides, the model presented an electrified heating network utilising GSHP and thermal storage with decentralised PV generation with EV charging stations and electric batteries for storage. In the results, it was mentioned that optimized community energy systems could help limit the expected peak demand increase in fully electrified scenarios to only 33%.

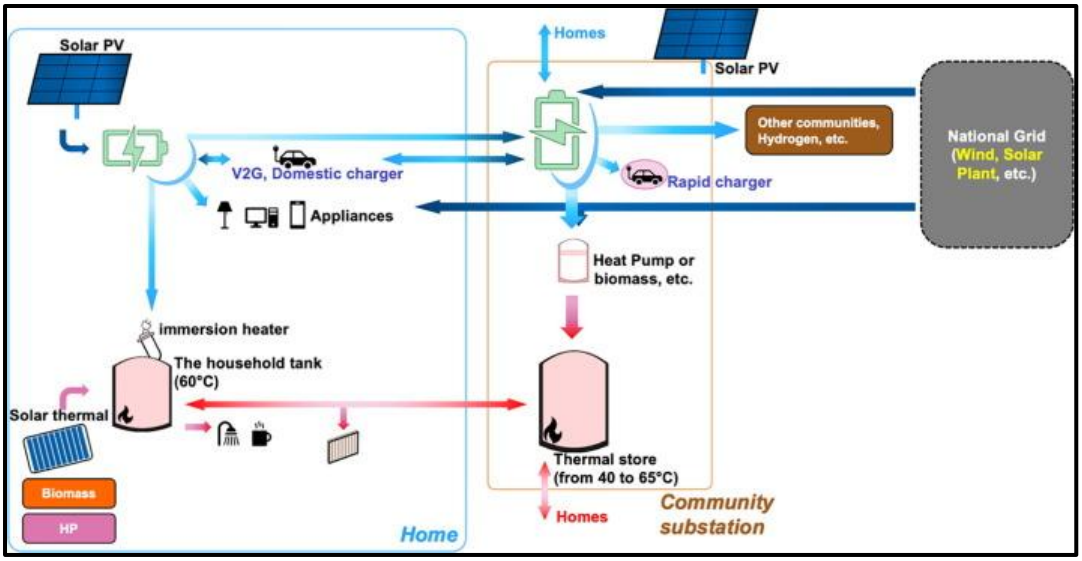


Figure 3.5: The concept of a multi-vector community energy system (Han et al., 2022)

Other references also suggested such systems to achieve net-zero targets. (Fan et al., 2022) introduced a net-zero community energy system that comprised electricity, heating, cooling, and hydrogen, with storage for each form of energy. Additionally,

multi-objective optimization was used to manage energy flow between the different components.

Trent Basin project is one of the examples of community energy in the UK, which is a development of low-energy houses located on the riverside in Nottingham. The project has multiple phases where the first 2 phases have 76 houses already sold and occupied and phase 3 is still under development at the time of writing, while the total number of houses after finishing the whole development will be 500 (Trent Basin Project, n.d.). The community energy project consists of a 2.1 MWh Tesla battery that will be charged from the PV systems on the rooftops of the participating houses (*Trent Basin · Project Scene (Sustainable Community Energy Networks)*, n.d.).

Additionally, the houses are being monitored through a set of sensors installed in each property to measure thermal energy (for both space heating and DHW), electrical energy, occupancy, temperature and set points for heating. (Shipman & Gillott, 2019) introduced this Internet of Things (IoT) based monitoring system and presented samples of the resulted data. Figure 3.6 shows the electricity consumption (kWh) for 21 properties over 24 hours period while categorizing the electricity loads in colours. This set of data shows the dominance of EV charging over other electrical loads in such energy-efficient houses which also gives a glimpse on how HP integration would affect such community.

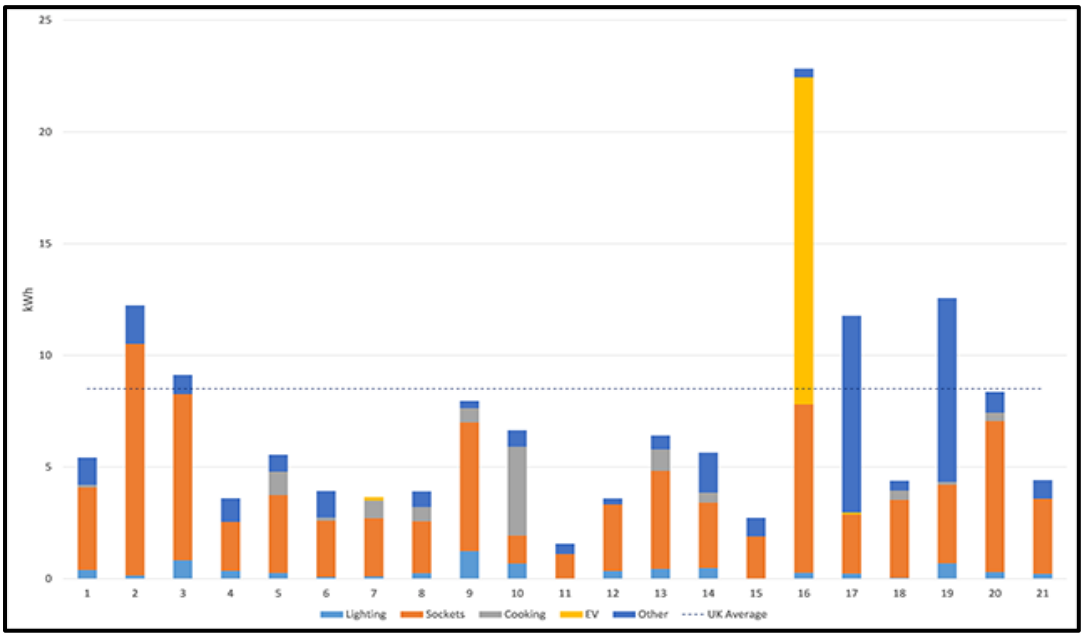


Figure 3.6: Sample of the data from the Trent Basin project showing electrical energy consumption and the dominance of EV charging. (Shipman & Gillott, 2019)

3.4 Active Buildings

The UK research community defines an Active Building (AB) as one that "supports the energy network by intelligently integrating renewable generation, electrical and thermal storage, and smart controls for heat, power and transport" (Clarke et al., 2020). Six design principles underpin the approach: (1) high-performance fabric and passive design, (2) monitored energy-efficient systems, (3) on-site renewables, (4) on-site storage, (5) EVs and HPs integration and (6) managed import/export to micro- and national grids. These elements move buildings from being passive electrical loads to dynamic, grid-responsive assets.

(Fosas et al., 2021) developed ABCode1 framework positions ABs as grid-servicing assets that must move beyond "nearly-zero" energy to four concurrent objectives: (i) minimise demand, (ii) maximise on-site generation, (iii) provide verifiable network services and (iv) limit embodied carbon. In their rating method, hours-of-autonomy

are used as a pragmatic proxy for grid services until market baselines for flexibility are formalised, explicitly rewarding buildings that combine controllable electric loads with thermal and electrical storage.

(Vahidinasab et al., 2021) extend this view, treating an AB as a multi-vector energy system whose optimisation variables include thermal state, electrical state and comfort. Their synthesis of 273 publications shows that the most mature control strategies revolve around heat-pump (HP) dispatch coupled to thermal energy storage (TES), because these technologies offer the widest operating envelope for shifting demand without undermining occupant comfort. Importantly, they emphasise that HP-TES pairs unlock the lowest-cost flexibility per kWh. Figure 3.7 illustrates the dual role of active buildings in both consuming and managing energy while supporting grid stability. It highlights how real-time data exchange and secure control mechanisms enable buildings to optimize their own operation (e.g., heating, cooling, and storage) while simultaneously offering grid services like demand-side response, flexibility, and voltage/frequency support. The balance point signifies optimal operation where user needs and network requirements are effectively aligned.

Recognising the systemic value of ABs, UK Research & Innovation invested £36 million in the Active Building Centre (ABC) under the Transforming Construction Challenge in 2019. In its first four years ABC delivered >100 real-world schemes worth ~£300 million and produced open-access design guides on integrating PV, batteries, HPs and TES in new and retrofit housing (*Active Building Centre (ABC) - Energy Systems Catapult*, n.d.).



Figure 3.7: Conceptual Representation of Active Buildings Balancing Energy and Network Services. (Vahidinasab et al., 2021)

Government policy now explicitly links flexibility to heat decarbonisation. The Smart Systems & Flexibility Plan 2021 states that "smart technologies and flexibility are essential to integrating low-carbon power, heat and transport onto the system" (*Transitioning to a Net Zero Energy System: Smart Systems and Flexibility Plan 2021*, 2021) and proposes mandatory interoperability standards for energy-smart appliances such as HPs and thermal stores.

Field demonstrations reinforce the modelling insights.

- The Trent Basin development in Nottingham aggregates rooftop PV, Europe's largest residential community battery (2.1 MWh Tesla), domestic HPs and smart metering. After phase 1 (76 homes) the scheme is saving ≈34 t CO_2 yr^{-1}, and 83 % of residents would recommend the storage-led approach (*ERA: The Trent Basin Community Energy Project - Midlands Innovation*, n.d.).

- ESC's Electrification of Heat trial retrofitted 742 HPs across a representative UK housing mix and reported reliable operation, good seasonal COPs and positive consumer experience, demonstrating the technical feasibility of mass HP deployment when paired with smart controls (*ELECTRIFICATION OF HEAT DEMONSTRATION PROJECT SUMMARY REPORT,* 2024)

Flexibility ultimately relies on household trust. The HeatFlex UK pilot (Berry et al., 2023) remote-controlled 12 domestic HPs via a smart thermostat that pre-heated homes before a peak-time turn-down. Nine out of ten participants found third-party automation acceptable, and no significant comfort loss was recorded. While small-scale, the study signals that well-designed automation combined with clear opt-out options can secure public buy-in—critical for scaling AB services.

These findings align with ESC's Living Lab surveys, where early HP adopters reported high satisfaction and willingness to provide demand response when bill savings were transparent (*ELECTRIFICATION OF HEAT DEMONSTRATION PROJECT SUMMARY REPORT,* 2024). Together they suggest that engagement programmes, intuitive interfaces and service-based business models (e.g. Heat-as-a-Service) are as important as technical optimisation.

The UK experience shows that active buildings are a practical, people-centred pathway to reconcile mass electrification of heat with grid stability. Supported by a clear policy direction (Smart Systems Plan), dedicated innovation infrastructure (ABC/ESC) and encouraging trial evidence, ABs can cut peak demand by around a fifth, deliver tangible CO_2 savings and maintain occupant comfort. Remaining barriers lie less in technology than in scaling standards, interoperability and equitable business models. Embedding AB principles into forthcoming building standards, tariff reforms

and consumer protections will be pivotal to unlocking community-wide flexibility and progressing toward the UK's 2050 net-zero goal.

3.5 Discussion and Conclusions

The literature reviewed in this chapter demonstrates that large-scale deployment of HPs and thermal energy storage can be reconciled with distribution network constraints when buildings are treated as flexible, grid-interactive assets rather than passive loads. Across empirical and modelling studies, a consistent finding emerges: while coincident HP operation threatens LV network capacity during cold periods, coordinated control supported by thermal storage can effectively manage peak demands without costly grid reinforcement.

The evidence shows that TES plays a central role in enabling cost-effective flexibility. By decoupling heat generation from heat delivery, storage allows HPs to operate during periods of lower electrical demand or higher renewable availability, improving seasonal efficiency while reducing peak coincidence. Community-scale coordination multiplies these benefits through diversity effects, with simulations showing potential peak reductions of 20-40% when aggregated control is properly implemented.

The Active Building framework provides a coherent approach for implementing these concepts, making flexibility an explicit performance criterion alongside efficiency and carbon reduction. Real-world demonstrations at sites like Trent Basin validate the technical feasibility, though they also reveal critical gaps in current understanding.

The literature reveals three critical gaps that this research directly addresses:

First, there is limited evidence on practical optimization algorithms for coordinating multiple HP-TES systems at the community scale. While theoretical frameworks exist, there is insufficient research on implementable control strategies that can manage diverse building types with varying thermal characteristics and storage capacities while respecting grid constraints. This thesis addresses this gap through the development and testing of three distinct control strategies using real operational data (Objectives 3 and 4).

Second, existing studies lack comprehensive validation using real-world data from operational community energy systems. Most research relies on simulated or laboratory data, with limited validation against actual consumption patterns, weather conditions, and grid loading from functioning communities. This research fills this gap by utilizing extensive monitoring data from 76 homes at Trent Basin, providing empirical validation of model predictions (Objectives 1 and 2).

Third, the quantitative impact of different control strategies on LV network infrastructure remains poorly understood. While studies acknowledge grid constraints, few provide detailed analysis of how optimized HP-TES operation affects transformer loading, demand ramp rates, and coincidence factors at the community scale. This thesis provides systematic evaluation of these grid impacts across different control approaches (Objectives 6 and 7).

These gaps directly informed the research approach, emphasizing the need for data-driven optimization strategies validated through real-world implementation. By addressing these specific knowledge gaps, this research contributes practical insights for enabling heat decarbonization without exceeding electrical infrastructure capacity, as explored through the methodology presented in the following chapter.

Chapter 4

4. Conceptual Framework and Methodology

4.1 Introduction

The development of an effective methodology for optimizing community-scale heat pump systems required a thoughtful progression from conceptual frameworks through to detailed simulation models. This chapter describes the methodological approach undertaken to address the research objectives, focusing on the development and implementation of control strategies for integrated heat pump and thermal storage systems.

The methodological evolution in this research reflected growing understanding of system complexity and optimization requirements. Initial investigations employed commercial digital twin software using the IES (Integrated Environmental Systems) toolset (*Digital Twins for the Built Environment | IES*, n.d.), which provided valuable insights into system behaviour while revealing limitations in optimization capabilities. These limitations prompted development of a more sophisticated custom model implemented in MATLAB, enabling advanced control algorithms and dynamic optimization approaches.

This progression from commercial to custom modelling reflects a fundamental challenge in community energy system research: the need to balance computational efficiency with optimization flexibility. Commercial tools offer robust simulation environments but often constrain control strategy sophistication, while custom models can implement advanced algorithms but require significant development effort. The

methodology described in this chapter navigated this tension to create an effective framework for system analysis and optimization.

The methodological approach centred on three distinct control scenarios, each representing progressively more sophisticated approaches to system management:

1. A baseline scenario implementing uncontrolled heat pump operation, providing reference performance levels for comparison
2. A fixed threshold model introducing basic grid-aware control through static operational thresholds
3. An active building model incorporating dynamic optimization with daily threshold adjustments

These scenarios enabled systematic evaluation of how control strategy sophistication influences system performance across multiple metrics. The simulation framework supported detailed analysis of energy consumption, peak demand reduction, thermal storage utilization, and grid impact, providing comprehensive understanding of system behaviour under different control approaches.

This chapter first outlines the research design principles that guided methodological development. It then describes the simulation model frameworks, detailing both the initial digital twin approach and the subsequent custom model implementation. The control scenario development section explains the theoretical foundations and implementation of each control strategy, while the final sections address performance evaluation methodologies and validation approaches.

4.2 Research Design

The research design for this study evolved through systematic exploration of simulation approaches and control algorithms tailored to the Trent Basin community. This section outlines the methodological decisions and implementation approaches forming the foundation of this research.

4.2.1 Methodological Development Process

The research methodology progressed through several distinct phases, each addressing specific requirements:

Phase 1: Digital Twin Implementation

Initial modelling using IES software (iVN and iCD components) established baseline understanding of system behaviour and constraints. This phase revealed important system characteristics while identifying limitations in optimization capabilities.

Phase 2: Requirements Definition

Based on digital twin limitations, specific requirements emerged for advanced analysis:

- Dynamic optimization algorithms responsive to changing conditions
- Temperature-dependent HP performance modelling
- TES control strategy
- Building-level optimisation with community-scale coordination

Phase 3: Custom Framework Development

Development of MATLAB-based simulation framework incorporating:

- Modular architecture separating physical models from control logic
- Hourly temporal resolution matching available data
- Scalability to community-level analysis

Phase 4: Control Strategy Implementation

Development of three control approaches, from baseline through to dynamic optimisation, enabling systematic performance comparison.

The final model implemented three distinct control approaches to enable systematic performance comparison: a baseline scenario where HPs responded directly to heat demand without coordination; a fixed threshold model using static thresholds to govern heat pump operation; and an active building (Dynamic Optimisation) model that performed daily optimization of building-specific thresholds. This phased approach enabled development of increasingly sophisticated control strategies while maintaining consistent evaluation frameworks across scenarios.

4.2.2 Key Modelling Decisions

The research design incorporated several critical modelling decisions that shaped the methodology:

The model operated at hourly intervals, aligning with available monitoring data while enabling practical computational implementation. This resolution captured essential diurnal patterns in both electricity demand and heat requirements while enabling simulation across full annual cycles. The hourly timestep provided sufficient detail to

model both morning and evening peak periods while remaining computationally feasible for community-scale analysis.

The model boundaries were defined to include the 76 residential buildings of varying types within Trent Basin, HPs sized according to building heating requirements, TES systems with capacities proportional to building size, and the 800 kW_e local LV substation (National Grid, 2023). These boundaries created a well-defined system for analysis while capturing the essential components influencing heat pump integration and control strategy effectiveness.

Simplifying Assumptions

Several important simplifications were necessary to facilitate the community-scale analysis. First, while the LV substation serves additional loads beyond the Trent Basin development, the collective load of the 76 houses was considered to represent the total demand on the substation. This simplification was necessary due to limited access to comprehensive substation data, with only the capacity rating (800kW) available. Second, in the active building model (Dynamic Optimisation) scenario, historical data served as a proxy for forecasts, allowing for the simulation of predictive control strategies without implementing complex forecasting algorithms. Finally, thermal comfort was assumed to be maintained whenever the heat demand was met, linking system performance directly to occupant satisfaction. This approach facilitated focus on the electrical and thermal system dynamics without introducing additional complexity from detailed comfort modelling.

The model incorporated additional technical simplifications regarding TES and HP operations. TES systems were represented using energy capacity (kWh) rather than volumetric models with detailed internal temperature gradients, flow rates, or heat

exchanger configurations. This approach treated TES as an energy buffer with simplified charging/discharging characteristics and standardized thermal losses (5% daily).

Similarly, HP performance was implemented through temperature-dependent COP values derived from manufacturer data without modelling detailed refrigeration cycle dynamics, defrost cycles, or transient responses during startup and shutdown periods. Part-load operation was represented through proportional adjustments to maximum capacity rather than detailed compressor modulation behaviours. These technical abstractions maintained essential system response characteristics while enabling community-scale analysis over extended timeframes.

The research incorporated specific control algorithms addressing identified optimisation objectives. For the fixed threshold model, this involved simple threshold comparison with two static values. For the active building model, this entailed daily optimisation through parameter sweep to identify optimal thresholds. These algorithm selections balanced sophistication with computational feasibility while enabling clear performance comparison between approaches.

The research established quantitative metrics to evaluate control performance, including peak electrical demand reduction, total electrical energy consumption, carbon emissions based on grid carbon intensity, TES utilization rates, and grid loading patterns. These metrics enabled systematic comparison between control strategies while addressing multiple system objectives.

4.2.3 Implementation Parameters

The model implementation incorporated specific parameters essential for simulating the Trent Basin community:

Heat pump configuration was based on building categories, with capacities ranging from 5-16 kW_e. Temperature-dependent COP values ranged from 2.33 at -7°C to 4.76 at 25°C, following manufacturer performance data. Maximum flow temperatures were set at 55°C to ensure domestic hot water compatibility. These parameters reflected commercially available high-temperature heat pumps suitable for the UK climate similar to the ones mentioned in Chapter 2.

TES implementation included capacities ranging from 10-30kWh based on building category, with maximum charging rates limited to 50% of HP capacity. This charging limitation serves multiple technical purposes: preventing secondary demand peaks during coordinated charging periods and enhancing thermal stratification within storage systems. As demonstrated by (Haller et al., 2019b), reduced charging rates improve stratification efficiency by minimizing mixing and maintaining distinct temperature zones within storage tanks, thereby increasing overall system effectiveness. TES temperature requirements were set at 55°C for hot water compatibility, with thermal losses approximated at 5% daily.

Control parameters for LV substation threshold optimisation ranged from 30-200kW_e, with step sizes of 10 kW_e for parameter sweep optimisation which will be described in detail in section 4.4. This range was determined through initial testing to encompass suitable threshold values while maintaining computational efficiency. The optimisation process also incorporated priority rules for heat demand satisfaction

versus storage charging, ensuring occupant comfort while supporting grid stability objectives.

Network parameters centred on the substation capacity of 800 kW_e and baseline building electrical demands derived from monitoring systems. This focused approach to network modelling aligned with the research emphasis on aggregate demand impacts rather than detailed power flow analysis.

This research design created a structured approach to investigating community-scale heat pump integration, with methodological decisions tailored to the Trent Basin context. The approach balanced theoretical rigor with practical implementation considerations, enabling systematic evaluation of control strategy effectiveness.

4.3 Digital Twin Initial Approach

The research began with implementation of commercial digital twin software to model the Trent Basin community energy system. This section describes the capabilities, implementation process, and limitations encountered with the IES toolset.

In this research context, a digital twin refers to a dynamic simulation model of the Trent Basin community that replicates the thermal and electrical behaviour of all 76 buildings. The digital twin serves three primary purposes: (1) to establish baseline heat demand profiles for buildings where direct heat metering was unavailable, (2) to enable testing of control strategies without disrupting actual residents, and (3) to provide a validated simulation environment for scenario analysis. Unlike static models, the digital twin incorporates real-time weather data and can be updated with

actual consumption patterns, though in this implementation it operates on historical data at hourly resolution.

4.3.1 Digital Twin Framework and Capabilities

The initial modelling phase employed the Integrated Environmental Solutions (IES) digital twin toolset with two key components: Intelligent Community Design (iCD) and Intelligent Virtual Network (iVN). This approach established a foundation for understanding system behaviour while revealing limitations that informed subsequent development.

The iCD component enabled energy modelling of all 76 houses within the Trent Basin development. Using a simplified physics-based simulation engine, this tool captured building-level characteristics including construction details, occupancy patterns, and heating systems. This approach is described in detail in Chapter 5.

Figure 4.1 illustrates the layout and building configuration of the Trent Basin site as generated by the IES digital twin toolset, which then used within the iCD tool for spatial and energy system modelling within the study.

Building geometries were simplified to rectangular forms based on developer floor plans, with each dwelling modelled as a single thermal zone. Complex features were simplified to equivalent flat surfaces. These simplifications were necessary for computational efficiency when modelling 76 homes.



Figure 4.1: 3D visualisation of the Trent Basin development generated using the iCD modelling tool.

The iVN tool was used to develop the digital twin at the level of the LV substation. This allowed for a comprehensive analysis of the electrical network, taking into consideration both the real data collected from the buildings and the modelled data. Initially, an evaluation of the current state of the electrical network was conducted using the data sources. This assessment enabled a thorough understanding of the existing conditions and energy demands within the LV substation area. Figure 4.2 shows the network representation of Trent Basin buildings connected to the LV substation as visualized in the iVN tool.

The developed model incorporated essential network parameters, including the 800 kW_e capacity rating of the LV substation obtained from National Grid's Connected Data Portal. This capacity constraint represented a crucial boundary condition for subsequent scenario analysis. The digital twin enabled mapping of energy flows (both electrical and thermal) throughout the community, with network nodes representing individual buildings connected through electrical distribution infrastructure to the central substation.

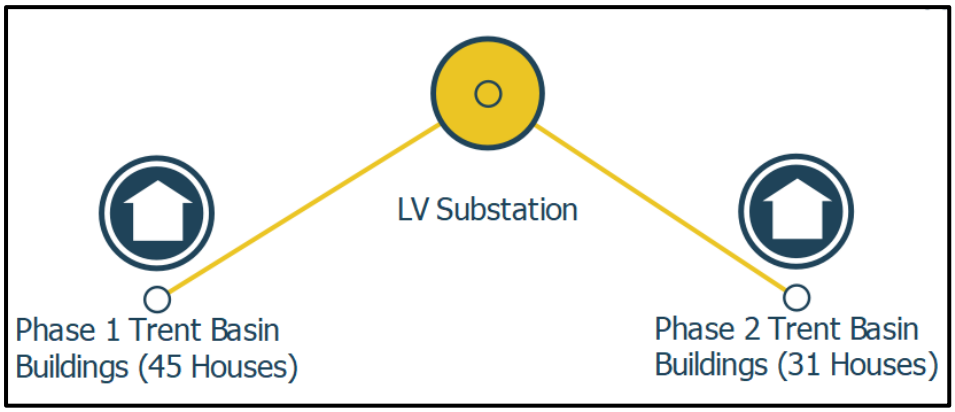


Figure 4.2: Network Representation of Trent Basin buildings connected to the LV substation as visualized in the iVN tool.

At the building level, the iVN tool facilitated detailed representation of energy system components and their interactions. Figure 4.3 illustrates the network connectivity for a single house, showing the integration points between electrical systems, heat demands, and potential heat pump installation. This detailed building-level modelling was replicated across all 76 properties, creating a comprehensive community-scale digital twin.

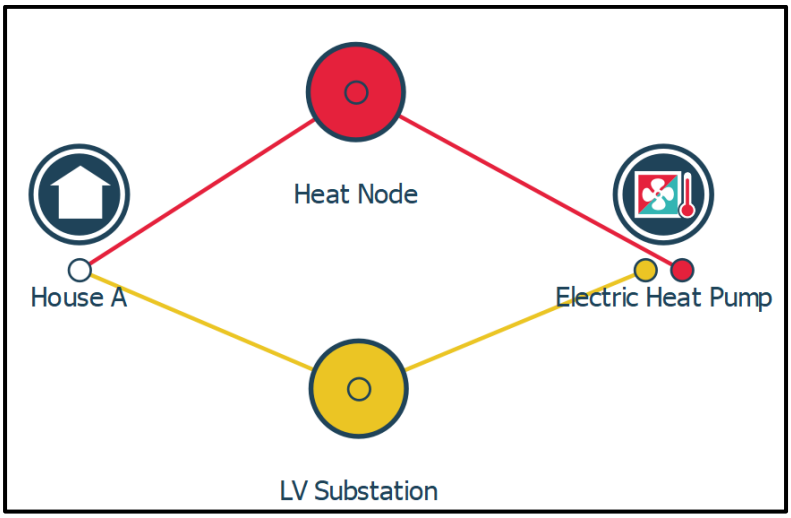


Figure 4.3: Network Connectivity for a Single House with Individual HP as Modelled on iVN Tool.

The digital twin implementation followed a hierarchical approach that captured both individual building characteristics and community-scale interactions. This multi-level

methodology enabled analysis of system behaviour at different scales while supporting insight into emergent properties from building aggregation. The implementation process progressed systematically from individual building characterization through to network integration and validation against available data.

This initial digital twin implementation provided valuable insights into community-scale energy dynamics and potential challenges of HP integration. The visualization capabilities and network analysis functions revealed patterns of distribution system loading and potential constraints that would inform subsequent model development. While not sufficiently flexible for implementing advanced control strategies, this approach established essential understanding of the physical system behaviour that would guide the development of more sophisticated optimization approaches.

4.3.2 Limitations and Development Requirements

Despite its utility for initial analysis, the digital twin implementation revealed several limitations that necessitated development of a more sophisticated approach. These constraints directly influenced subsequent methodological decisions.

The IES toolset provided limited optimization capabilities. The software supported fixed operational thresholds but lacked functionality for implementing dynamic control algorithms responsive to changing conditions. This limitation was particularly problematic for community-scale optimization, where coordination across multiple buildings and adaptation to varying grid conditions are essential.

System integration challenges further limited the digital twin approach. The simplified TES modelling constrained exploration of sophisticated charging strategies, while

limited inter-building coordination restricted community-scale optimization potential. Additionally, fixed coefficient of performance assumptions inadequately captured heat pump efficiency variations under changing environmental conditions.

These limitations led to specific requirements for advanced model development:

- Dynamic optimization of operational LV substation thresholds
- Coordinated control across multiple buildings
- Integration of weather-dependent HP performance
- Advanced thermal storage management

These requirements directly informed the development of a customized model capable of addressing the complexities of community-scale heat decarbonization.

4.4 Simulation Framework and Control Strategy Development

4.4.1 Framework Architecture and Design Principles

The custom MATLAB model developed in response to identified limitations integrated multiple system components while enabling implementation of advanced control strategies. This framework represented the physical and operational characteristics of the community energy system while supporting sophisticated optimization approaches.

System Configuration

The model incorporated three interconnected subsystems:

1. **Building-level components**: Heat demand profiles, TES systems, and HPs with temperature-dependent performance characteristics
2. **Electrical network**: The LV substation with 800 kW_e capacity and connections to individual buildings
3. **Control system**: Hierarchical control framework implementing different operational strategies

The system configuration of the model is illustrated in Figure 4.4, showcasing the community infrastructure and the individual building system. At the community level, it shows the Trent Basin project with 76 houses connected to the LV substation via the electrical network. The figure also shows the communication between the buildings and the LV substation, highlighting the data exchange that provides the buildings with the necessary information about substation capacity to make decisions regarding optimising the thresholds, as described in the model development section.

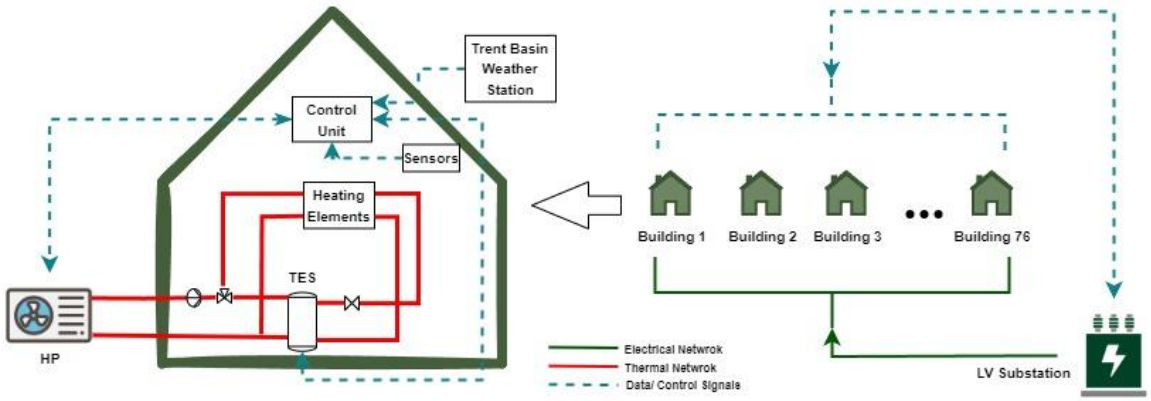


Figure 4.4: System configuration of the model on both community and building levels.

At the individual building level, each building is equipped with an individual heating system consisting of a HTHP, capable of producing water at temperatures up to 55 °C, suitable for space heating and domestic hot water, and coupled with TES units for each house. The HP and TES units are connected to the heating elements, which, in the model, represent the heat consumers, such as the space heating system (radiators or

underfloor heating) and DHW system. While the control unit manages the operation of the HP and TES units based on the heating demand, grid conditions, and the real-time data from the sensors utilise the algorithm mentioned in the model development section.

Mathematical Framework

The MATLAB framework adopted modular architecture separating physical system representation from control logic. This separation enabled consistent comparison between control strategies while maintaining computational efficiency.

The framework operated on all control scenarios and on three levels:

Component Level

HP Electrical Demand:

$$E_{HP}(t) = \frac{Q_{Heat}(t)}{COP\ (T_{ambient}(t))} \rightarrow \text{Eq. 4.1}$$

Where $E_{HP}(t)$ represents heat pump electrical demand, $Q_{Heat}(t)$ indicates heating requirement, and $COP\ (t)$ reflects heat pump efficiency based on ambient temperature $T_{ambient}$ at time t.

TES model:

$$S(t) = S(t-1).(1-\eta_{loss}) \pm Q_{Charge/Discharge}\ (t) \rightarrow \text{Eq. 4.2}$$

Tracking thermal energy stored based on previous state and charge/discharge operations, where $\eta_{loss} = \frac{0.05}{24}$ represents hourly thermal losses.

Heat Pump Charging Operation:

$$E_{HP(charging)}(t) = \frac{E_{HP(MAX)}/2}{COP\ (t)} \rightarrow \text{Eq. 4.3}$$

Limiting charging power to 50% of the HP capacity as mentioned in section 4.2.3. While this is only applied when no immediate heat demand exists as mentioned in control scenarios in sections 4.4.3-4.4.5 for priority logic.

Building Level

Total Electrical Demand:

$$E_{Peak,total}(\mathrm{t}) = E_{HP}(t) + E_{other}(t) \rightarrow \text{Eq. 4.4}$$

Combining $E_{HP}(t)$ with other building loads (peak load each hour) $E_{other}(t)$.

Community Level

Substation loading:

$$LV_{Peak\ Demand}\ (t) = \sum_{i=1}^{76} E_{Peak,total,i}(\mathrm{t}) \rightarrow \text{Eq. 4.5}$$

These formulations enabled comprehensive system simulation while supporting optimization of control strategies.

The novelty of this methodological approach lies in three key aspects: Firstly, the implementation of building-specific daily optimization that accounts for individual thermal characteristics rather than applying uniform control across all buildings, secondly, the use of comprehensive real-world operational data from an actual community rather than general or laboratory data, and finally the systematic comparison of control strategies at increasing levels of sophistication using identical boundary conditions. Unlike previous studies that optimize individual buildings or use

simplified community models, this framework maintains building-level detail while coordinating community-wide operation.

4.4.2 Control Strategy Implementation

The model implemented a hierarchical control structure that operated at both building and community levels. Individual controllers monitored local conditions including heat demand, storage state, and electrical consumption, while interfacing with community-level optimization that considered aggregate impacts on the LV substation.

Three distinct control scenarios were implemented:

1. **Baseline Scenario**: HPs operated directly in response to building heat demand without consideration of grid impacts or storage optimization.
2. **Fixed Threshold Model**: Two static LV substation threshold values governed HP operation and storage charging based on substation loading.
3. **Active Building Model**: Daily optimisation of LV substation thresholds for each building based on predicted demand patterns and environmental conditions.

The upcoming subsections describe each model scenario in detail.

4.4.3 Baseline Scenario Model

The baseline scenario implemented conventional HP operation without coordinated control or advanced optimisation. This approach represented typical current practice in residential HP installations and established reference performance levels for evaluating more sophisticated control strategies.

In this scenario, each building's HP operated independently to meet heating demand through simple thermostatic control. The operational logic followed a direct demand-response approach where HPs activated whenever building temperature fell below setpoint thresholds, operating until demand was satisfied. This basic control approach made no attempt to coordinate operation across multiple buildings or consider grid loading conditions.

The mathematical representation of HP electrical demand under this scenario was straightforward and similar to the equations presented in the previous section.

The baseline scenario made no use of TES systems, focusing solely on direct HP operation to meet immediate heating requirements. This approach prioritized simplicity and responsiveness to thermal comfort requirements without consideration of grid impacts or system optimisation.

This scenario served as a benchmark by establishing reference performance metrics across multiple dimensions. The unoptimized operation provided clear indication of potential grid impacts from widespread HP adoption while establishing baseline levels for energy consumption, peak demand, and operational patterns.

4.4.4 Fixed Threshold Model

The fixed threshold model introduced basic grid-aware operation through implementation of static control thresholds governing HP operation and TES charging decisions based on the LV substation loading. This intermediate approach introduced coordination between buildings while maintaining operational simplicity, enabling assessment of how basic grid awareness influences system performance.

This control strategy implemented two fixed thresholds that remained constant throughout the simulation period:

- Threshold 1 (T1): 140 kW
- Threshold 2 (T2): 180 kW

These thresholds were determined through iterative analysis of historical demand patterns to identify values that balanced peak reduction with heating system performance. The control logic operated according to three distinct conditions based on current LV substation loading:

Mode 1: Normal Operation (LV demand < 140 kW)

When substation demand remained below T1 (140 kW), the system entered normal operation mode. In this state, HPs could operate freely to meet immediate heating requirements and charge TES if capacity was available. This operational state prioritized maintaining TES charge levels while ensuring responsive heating provision.

Mode 2: Restricted Operation (140 kW_e ≤ LV demand < 180 kW_e)

As substation demand increased above T1 but remained below T2 (140-180 kW_e), the system entered managed operation mode. In this state, TES charging was restricted while direct heating operation continued. This intermediate state began to limit non-essential operations while maintaining essential heating functionality.

Mode 3: Peak demand reduction (LV demand ≥ 180 kW_e)

When substation demand exceeded T2 (180 kW_e), the system entered Peak demand reduction mode. In this state, HP operation was restricted with priority given to TES

discharge for meeting heating demands. This operational state minimized grid impact during peak periods by utilizing stored thermal energy instead of electrical input.

The decision logic for this control strategy can be represented as:

For LV peak demand < T1:

- Direct HP operation permitted for heating
- TES charging allowed if capacity available

For T1 < LV peak demand < T2:

- Direct HP operation permitted for heating
- TES charging restricted to prevent additional load

For LV peak demand > T2:

- HP operation restricted
- Priority given to TES discharge for heating
- HP operation only if TES insufficient

This approach implemented basic grid-aware control while maintaining operational simplicity. The fixed nature of the thresholds meant the system could not adapt to changing conditions or optimise operation based on forecast information, but it provided an improvement over uncoordinated baseline operation.

4.4.5 Active Building Model

The active building model represents the most sophisticated control approach implemented in this research, incorporating dynamic optimisation and predictive elements to achieve superior system performance. Unlike the fixed threshold model's hierarchical structure, this approach implements a dual-parameter optimisation

strategy that treats threshold selection as an optimisation problem solved independently for each building.

Fundamental Approach

The core innovation involves recognising that buildings with different thermal characteristics, storage capacities, and usage patterns benefit from individualised control parameters rather than community-wide values. This building-specific approach emerged from the observation that uniform thresholds create artificial synchronisation points where multiple systems respond simultaneously, generating secondary demand peaks that undermine the coordination benefits.

The optimisation formulation aims to minimise peak electrical demand over a 24-hour horizon while maintaining thermal comfort requirements. The problem structure incorporates peak demand minimisation as the primary objective, heat demand satisfaction as an essential constraint, and two independent threshold values as decision variables for each building. This daily optimisation operates with hourly resolution across the 24-hour prediction horizon.

Threshold Functions and Control Logic

The two optimised thresholds serve distinct control purposes within the system architecture. Threshold 1 (T1) governs HP operation when heating demand exists, permitting direct operation when grid loading remains below this value while prioritising storage discharge when loading exceeds it. Threshold 2 (T2) controls TES charging during periods without immediate heating requirements, allowing storage charging at reduced HP capacity when grid loading falls below this threshold while prohibiting charging when loading exceeds it.

These thresholds operate independently, enabling T1 to exceed or fall below T2 depending on optimisation outcomes. This independence provides greater flexibility in control strategy development, allowing the system to separately optimise conditions for direct heating provision versus storage preparation activities. For instance, a building might optimise with Threshold 1 at 150 kW_e and Threshold 2 at 90 kW_e, creating more restrictive conditions for storage charging than for direct heating.

Optimisation Implementation

The algorithm employs an exhaustive search strategy across a discretised threshold space to ensure global optimality within the defined range. Both threshold parameters can range from 30 to 200 kW_e with 10 kW_e increments, creating 18 possible values per threshold and yielding 324 total combinations per building. This optimisation executes daily at midnight for the upcoming 24-hour period.

The optimisation process follows a structured sequence:

- **Initialisation phase:** Current storage states are retrieved, 24-hour weather forecasts are processed to calculate hourly COP values, and predicted heat demand profiles are extracted
- **Evaluation phase:** Each of the 324 threshold combinations is systematically tested by simulating 24-hour operation under the threshold-based control logic, tracking peak electrical demand and heat satisfaction rates
- **Selection phase:** All combinations achieving adequate heat demand satisfaction are identified, with the combination producing the lowest peak demand selected for implementation

Control Operation with Optimised Thresholds

Once daily optimisation determines building-specific thresholds, operational control follows structured logic:

When heating is required:

- If LV demand < T1: Operate HP directly at required capacity
- If LV demand ≥ T1: Use stored thermal energy first, supplement with HP only for any shortfall

When no heating is required:

- If LV demand < T2 and storage available: Charge storage at 50% HP capacity
- If LV demand ≥ T2 or storage full: No HP operation

This control structure enables responsive operation while considering grid constraints, with daily recalculation allowing adaptation to forecast ambient temperatures affecting HP efficiency, expected occupancy patterns influencing demand timing, and day-of-week variations in community electrical consumption.

Mechanisms for Enhanced Performance

Several interconnected mechanisms contribute to the model's effectiveness beyond simple threshold application. Building-specific thresholds naturally distribute control actions across the community, preventing synchronised responses that create demand spikes. The array of threshold values means that buildings with lower Threshold 1 values curtail operation first during demand increases, while higher Threshold 2 values distribute storage charging activities throughout daily cycles.

The 24-hour optimisation horizon enables anticipatory behaviour through forward-looking decisions including pre-charging storage before anticipated evening peaks, reducing morning storage charging when high afternoon demand is expected, and

adjusting thresholds based on forecast temperature variations. Although buildings optimise independently, community-level coordination effects emerge naturally through the implicit coordination created by diverse threshold values and the shared grid loading signal.

Implementation Considerations

The exhaustive search approach provides global optimality guarantees within the defined search space while maintaining computational feasibility. Processing requirements remain practical with approximately 8 seconds per building for 324 combinations across 24 hours of calculations, totalling roughly 10 minutes for all 76 buildings on standard computer hardware. The daily execution frequency avoids real-time computational constraints while enabling responsive adaptation to changing conditions.

This threshold-based control framework effectively translates optimisation objectives into implementable actions through discrete threshold values that align with practical building management system capabilities. The approach creates straightforward operational rules through daily threshold determination, maintains clear physical interpretation of threshold values, and provides reliability through exhaustive search elimination of solution quality uncertainty.

Figure 4.5 illustrates the complete active building model framework, demonstrating the integration of optimisation algorithms, control logic, and verification procedures within the broader community energy system context.

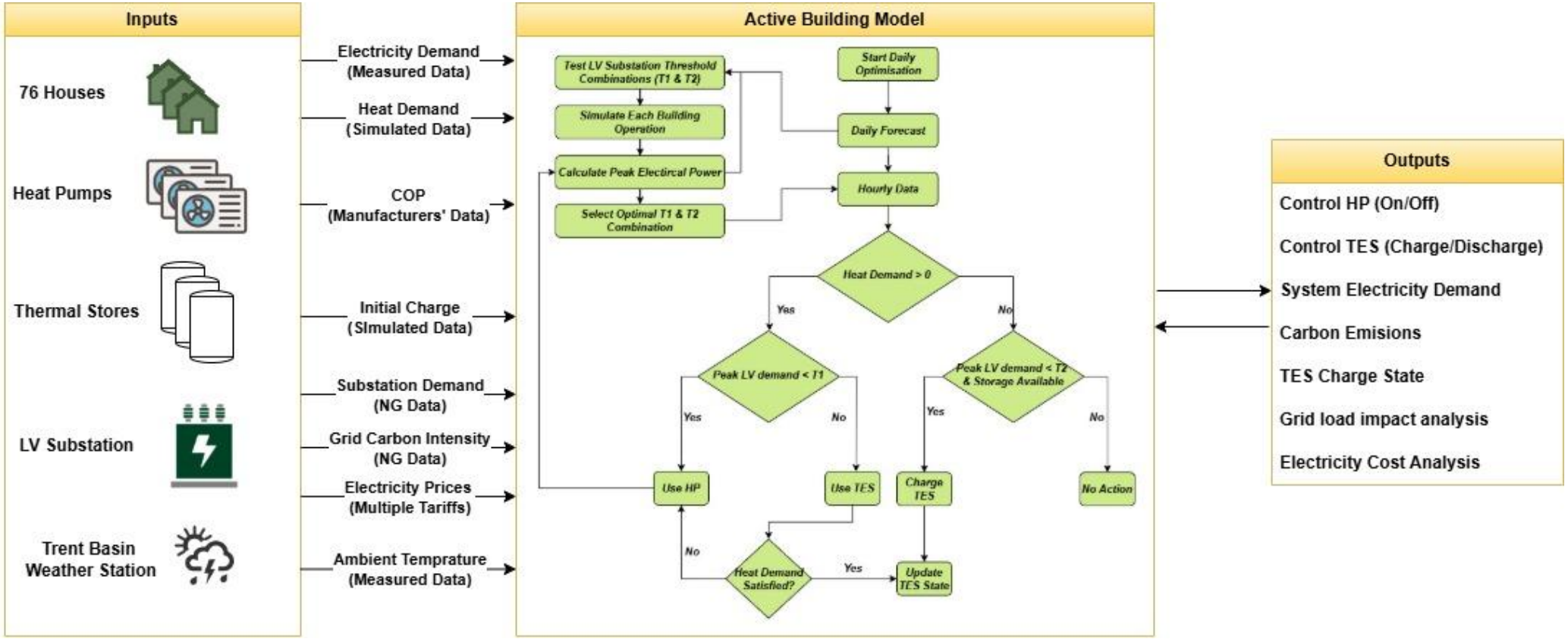


Figure 4.5: Active building model schematic

4.5 Performance Evaluation Framework

The evaluation of different control strategies required a comprehensive assessment framework addressing multiple aspects of system performance. This section describes the methodological approach to performance evaluation, detailing the metrics, evaluation procedures, and validation methods employed in the study. This framework enabled systematic comparison between control scenarios while maintaining focus on key research objectives.

4.5.1 Performance Metrics

The evaluation framework incorporated multiple complementary metrics designed to capture different aspects of system performance. These metrics addressed energy consumption, grid impact, environmental performance, and system operation characteristics.

Energy performance metrics focused on both total consumption and temporal distribution patterns. Primary energy metrics included:

- Total electrical (HP) energy consumption (kWh) over annual operation
- Peak LV electrical demand (kW_e) throughout the simulation period
- Load factor (ratio of average to peak demand)
- HP operational efficiency (COP) under different control strategies

The Load factor is the ratio of average electrical demand to peak demand over a specified period, expressed as a decimal between 0 and 1. A higher load factor indicates more efficient infrastructure utilization, as it means the system operates

closer to its peak capacity throughout the period rather than experiencing brief, extreme peaks.

Grid impact assessment metrics addressed the influence of HP operation on the LV substation and electrical infrastructure. Key grid metrics included:

- Duration and frequency of high-demand events
- Rate of change in electrical demand (kW_e/hour)
- Coincidence factor of HP operation across multiple buildings
- Distribution of demand throughout daily and seasonal cycles

Coincidence factor represents the proportion of HPs operating simultaneously at any given time, ranging from 0 (no systems operating) to 1 (all systems operating together). Lower coincidence factors indicate better load distribution and reduced stress on the electrical network.

Carbon Emissions

Environmental performance metrics incorporated carbon emissions analysis based on grid carbon intensity data. This approach enabled assessment of how different control strategies influenced overall environmental impact through both energy consumption patterns and temporal alignment with grid carbon intensity. The primary environmental metric was:

- Total carbon emissions ($kgCO_2$) calculated as:

$$CO_{2\,Emissions} = \sum_{t=1}^{T} CI\,(t) \times E_{HP}(t) \rightarrow \text{Eq. 4.6}$$

Where $CI\,(t)$ represents grid carbon intensity at time t.

Emissions intensity (also called carbon intensity) measures the grams of CO_2 emitted per kilowatt-hour of energy delivered (g CO_2/kWh). For HPs, this reflects both the

grid's carbon intensity at the time of operation and the system's efficiency in converting electricity to useful heat.

Economic Performance

Economic performance metrics addressed the financial implications of different control strategies across various electricity pricing structures. The evaluation incorporated multiple tariff frameworks representative of UK market conditions, enabling assessment of how operational patterns influenced system economics. Primary economic metrics included:

- Total operational costs (£) under standard flat-rate tariffs
- Cost variations under time-of-use pricing structures (Economy 7)
- Dynamic cost impacts under variable pricing schemes (Like Octopus "Agile Tariff")
- Cost-effectiveness ratios comparing expenditure to thermal energy delivered

The economic assessment utilized real electricity pricing data from 2024/2025 UK market conditions. Standard rate calculations employed a flat rate of 24.5p/kWh throughout all periods. Economy 7 analysis incorporated off-peak rates of 13.32p/kWh (00:00-07:00) and peak rates of 30.5p/kWh (07:00-00:00). Dynamic tariff evaluation used dynamic hourly pricing reflecting wholesale market conditions.

Economic performance was calculated as:

$$Total\ Cost\ = \sum_{t=1}^{T} Tariff\ rate\ (t) \times\ E_{HP}(t) \rightarrow \text{Eq. 4.7}$$

Where Tariff Rate (t) indicates the applicable electricity rate at time t. This approach enabled assessment of how different control strategies influenced operational costs while revealing the sensitivity of economic benefits to pricing structure design.

This multi-dimensional approach to performance assessment ensured comprehensive evaluation of control strategies across all relevant aspects of system operation. The integrated metric framework enabled identification of trade-offs between different performance objectives while supporting holistic assessment of system effectiveness.

4.5.2 Evaluation Methodology

The performance evaluation methodology followed a systematic approach to ensure consistent assessment across different control scenarios. This process incorporated several key elements that supported robust comparison while maintaining methodological rigor.

Comparative scenario analysis formed the foundation of the evaluation approach. Each control scenario underwent identical simulation using consistent input data, enabling direct comparison of performance outcomes. The baseline scenario provided reference performance levels for unoptimised HP operation, while the fixed threshold and active building models demonstrated progressive improvements in control sophistication. This structure enabled clear identification of how control strategy development influenced system performance.

Temporal scale analysis examined system performance across multiple timescales to capture both immediate operational dynamics and longer-term patterns. The evaluation considered:

- Hourly operation dynamics capturing demand peaks

- Daily patterns revealing diurnal variations in system performance
- Seasonal trends demonstrating system adaptation to changing environmental conditions
- Annual performance metrics providing comprehensive assessment of long-term operation

This multi-scale approach enabled detailed understanding of system behaviour while ensuring that short-term dynamics did not obscure longer-term performance patterns.

Statistical analysis of performance metrics supported rigorous evaluation of control strategies. Beyond simple comparison of total or peak values, the evaluation incorporated detailed statistical analysis including:

- Distribution analysis of demand patterns and operational states
- Correlation assessment between environmental conditions and system performance
- Time-series analysis identifying system response to changing conditions
- Performance variation analysis across different building types and operational scenarios

This statistical approach enabled more nuanced understanding of performance differences while supporting robust conclusions regarding control strategy effectiveness.

4.5.3 Sensitivity Analysis Framework

To evaluate the robustness of control strategies under parameter uncertainties, a systematic sensitivity analysis framework was developed. This framework addresses

a key limitation of the primary simulations—the assumption of perfect parameter values and forecasting—by examining system performance under realistic variations.

Parameter Selection and Justification

Four critical parameters were identified for sensitivity testing based on their potential impact on system performance and uncertainty in real-world applications:

- **COP**: ±20% variation to account for manufacturer tolerances, degradation over time, and operational variations from rated conditions.
- **Heat Demand**: ±20% variation to capture uncertainties in occupancy patterns, behavioural differences, and modelling assumptions.
- **TES Capacity**: ±20% variation to represent installation tolerances and degradation of storage media over operational lifetime.
- **Forecast Error**: 0-20% range to address the assumption of perfect 24-hour ahead prediction, representing realistic forecasting uncertainties.

Methodological Approach

The sensitivity analysis employed a one-at-a-time approach, where each parameter was varied independently while others remained at baseline values. This approach was selected over factorial designs due to:

- Computational efficiency given the scale of simulation (76 buildings × 8760 hours)
- Clear identification of individual parameter impacts
- Sufficient insight for validating control strategy robustness

The analysis focused on the coldest week of the year as a worst-case scenario, when system stress is highest and control strategy effectiveness most critical. For each

parameter perturbation, all three control scenarios (Baseline, Fixed Threshold, Active Building Model) were re-simulated to enable comparative assessment.

Performance Assessment

Peak demand reduction was selected as the primary metric for sensitivity assessment, as it represents the core objective of the control strategies and directly influences grid infrastructure requirements.

The robustness of each control strategy was evaluated based on:

- Maintenance of positive benefits across all parameter variations
- Magnitude of performance degradation under adverse conditions
- Identification of critical parameters requiring careful management

This sensitivity framework ensures that the performance benefits identified in the primary simulations represent robust improvements achievable under real-world uncertainties rather than idealized assumptions.

4.6 Conclusions

This chapter has presented the development and implementation of a methodological framework for optimizing community-scale HP systems. The progression from initial digital twin modelling to a sophisticated simulation framework reflects the complex challenges inherent in community energy system optimization.

The research design established a structured approach to investigating HP integration at the Trent Basin community, with specific modelling decisions tailored to address key research questions. The digital twin implementation demonstrated the feasibility

of community-scale modelling while revealing significant limitations in optimisation capabilities. These limitations drove development of an enhanced modelling approach capable of implementing sophisticated control strategies across multiple buildings.

The resulting simulation framework enabled investigation of three distinct control approaches. The baseline scenario established reference performance levels for traditional HP operation. The fixed threshold model demonstrated potential benefits of basic grid-aware control strategies. The active building model, incorporating dynamic optimization and predictive elements, represented the most sophisticated approach to system management.

The performance evaluation framework established comprehensive metrics and assessment methodologies to enable systematic comparison between control strategies. This approach addressed multiple aspects of system performance including energy efficiency, grid impact, environmental performance, and operational characteristics. The validation methodology ensured reliable model operation across varying conditions, providing confidence in the simulation results.

The sensitivity analysis framework established in Section 4.5.3 provides essential validation of control strategy robustness. By systematically examining performance under parameter uncertainties particularly forecast error which addresses a key assumption limitation. This framework ensures that the simulation results presented in subsequent chapters represent achievable real-world benefits rather than theoretical optimums dependent on perfect conditions.

This methodological foundation enables detailed investigation of system performance and optimization potential, as explored in subsequent chapters. The developed framework provides a robust platform for evaluating different approaches to

community-scale heat decarbonization while maintaining practical applicability for real-world implementation.

Chapter 5

5. Demand Modelling and Data Collection

5.1 Introduction

Accurate energy demand characterization forms the foundation for effective community-scale heat decarbonization strategies. This chapter presents the methodological approach to demand modelling and data collection at the Trent Basin development, comprising 76 houses across two construction phases.

The research methodology integrated two complementary approaches: direct measurement of electrical consumption through installed monitoring systems, and thermal modelling to establish heat demand baselines. This dual approach created a comprehensive framework that balanced theoretical precision with empirical validation.

Hourly temporal resolution was selected as the optimal balance between computational feasibility and analytical detail, capturing essential consumption patterns while enabling practical simulation at the community scale. The integration of multiple data streams—building-level electrical consumption, modelled heat demands, weather patterns, and network loading—provided the essential inputs for the simulation model described in Chapter 4.

This chapter examines the heat demand modelling methodology, details the electrical data collection approach, and presents the framework for integrating these diverse data streams to support the optimization strategies evaluated in subsequent chapters.

5.2 Heat Demand Modelling Methodology

The heat demand modelling for the Trent Basin community required detailed thermal simulation while maintaining computational efficiency for community-scale analysis. With directly measured heat demand data unavailable, a robust modelling approach was essential to establish baseline heating requirements for all 76 houses.

5.2.1 Tool Selection and Capabilities

The IES Intelligent Community Design (iCD) tool version 2023 was selected for heat demand simulation based on its capacity for community-scale analysis. This tool employs the same physics-based simulation engine that underpins the Virtual Environment software but allows for scalability with simplified parameters for large-scale projects (*Digital Twins for the Built Environment | IES*, n.d.). The approach enabled simultaneous modelling of multiple buildings while maintaining sufficient accuracy for system-level analysis.

The iCD tool generates simulated heat demand data with hourly resolution, distinguishing between space heating and domestic hot water (DHW) components. This provides complete coverage of seasonal variations and daily demand patterns essential for system sizing and control strategy evaluation. The simulation data calculated at an hourly resolution aligns with the temporal requirements for the analysis of peak demand periods and optimization strategies.

IES-VE was selected over alternatives (EnergyPlus, TRNSYS, DesignBuilder) for the following reasons: first, its iCD tool is specifically designed for community-scale analysis with simplified inputs suitable for multiple buildings, it also offers computational efficiency when modelling 76 buildings simultaneously. While

EnergyPlus provides more detailed HVAC modelling capabilities, the additional complexity was unnecessary given that heat demands rather than detailed system dynamics were required. TRNSYS would have required extensive custom model development for each building type.

5.2.2 Simulation Parameters

In this research, the default ASHRAE template was used, and the following parameters were set:

- **Type of building/house**: This parameter identified the specific characteristics and layout of each building or house within the Trent Basin project, this includes building type, floor area, number of bedrooms, number of storeys, storey height and roof type.
- **Hours of use**: The tool accounted for the typical hours of occupancy and utilisation of the buildings. Default house profiles from the tool were utilised which are typically between 6 – 10 AM and 4 – 11 PM. It is important to note that using default profiles resulted in duplicated profiles in terms of hours of use. This duplication, although unlikely in a real-life scenario, allowed testing of a worst-case scenario and assessment of its potential impact on energy demand. By considering such extreme cases, we could gain insights into the system's performance under challenging conditions and ensure robustness in our analysis.
- **Type of heating**: Information regarding the heating system employed in each building, such as underfloor heating or radiators. For this case study, all houses utilised gas boilers with radiators.

- **Heating System**: Details regarding the type and efficiency of the boilers utilized for heating purposes were considered to accurately simulate energy consumption. For this case study the highest boiler efficiency of 95% assumed given the recent construction.
- **DHW system and demand profile**: The DHW demand profile was dependent on the hours of use mentioned above and the occupancy of the house.
- **U-values for walls, windows, and roof**: The thermal properties of the building envelope, including U-values for walls, windows, and roofs, were input into the tool. Assumptions were made based on the UK building standards for the respective years of construction (2017 for phase 1 and 2020 for phase 2) with the external wall u-value assumed to be 0.18 W/m^2K and the external window u-value assumed to be 1.4 W/m^2K.
- **Temperature Setpoints:** Comfort thresholds followed standard residential requirements with living spaces maintained at 21°C during occupied periods, bedrooms at 18°C, and a setback temperature of 16°C during unoccupied periods.
- **Lighting**: The lighting system and its characteristics, such as the type of bulbs or fixtures, were accounted for in the modelling. The default house lighting profile based on the house hours of use was assumed with the highest efficiency LED lighting system.
- **Occupancy**: To estimate occupancy levels, the number of occupants per dwelling was assumed to be equal to the number of bedrooms plus one (n_bedrooms + 1).

Figure 5.1 presents the building-level simulation parameters used within the iCD modelling environment to estimate heat demand for the Trent Basin development.

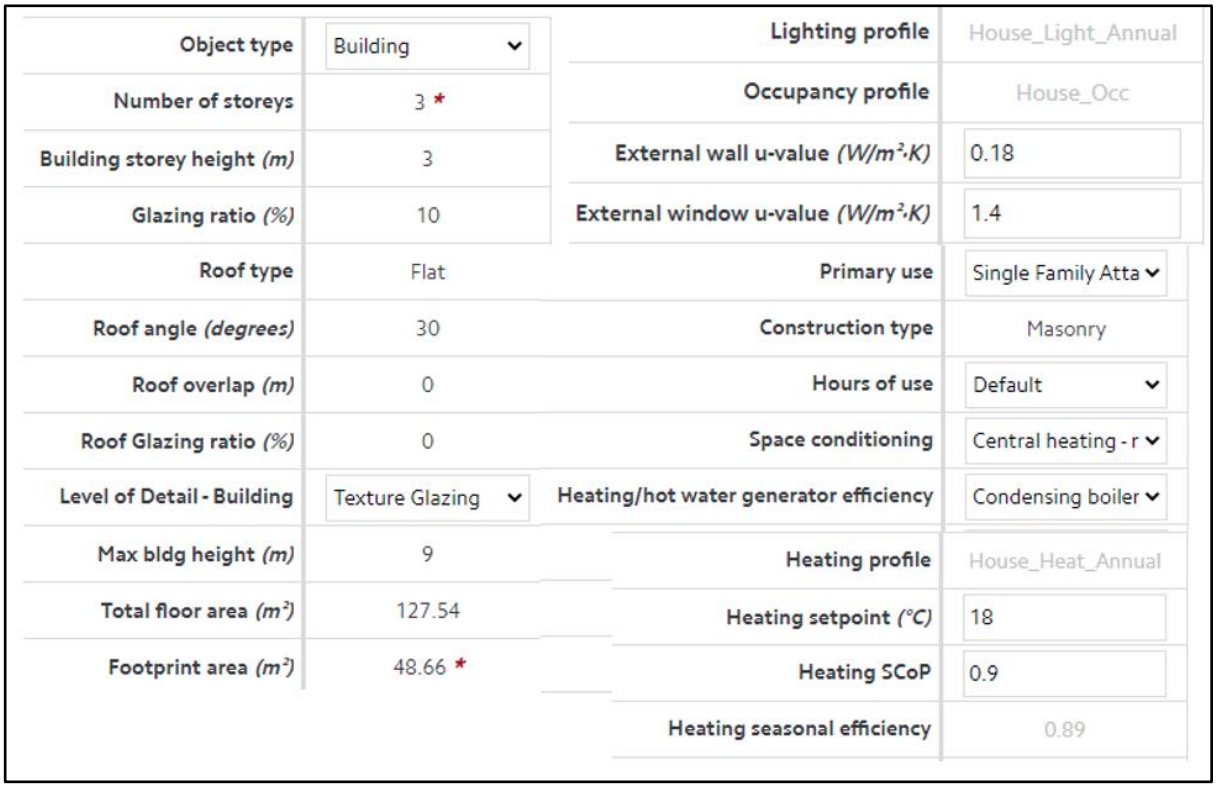


Figure 5.1: Input parameters for heat demand simulation of a representative dwelling in the Trent Basin development using the iCD modelling tool.

5.2.3 Building Characterization

The 76 houses at Trent Basin were categorized based on construction phase, size, and type. Phase 1 comprised 45 houses completed in 2017, while Phase 2 added 31 houses completed in 2020. To enable effective heat demand modelling and system planning, the dwellings were further grouped into four categories, each reflecting a range of thermal profiles:

- Category 1: peak heat demand of 4-6 kW_{th}.
- Category 2: peak heat demand of 7-9 kW_{th}.
- Category 3: with peak heat demand of 10-12 kW_{th}.
- Category 4: peak heat demand of 17-19 kW_{th}.

These classifications were not only informed by available construction and performance data but also used consistently in the system-wide analysis and optimisation discussed in Chapter 6. Figure 5.2 visualises the spatial distribution of modelled energy demand across the development using the iCD simulation tool. The colour coding corresponds to the relative magnitude of thermal demand during the simulation process, highlighting the variation in consumption patterns across different building forms and configurations.

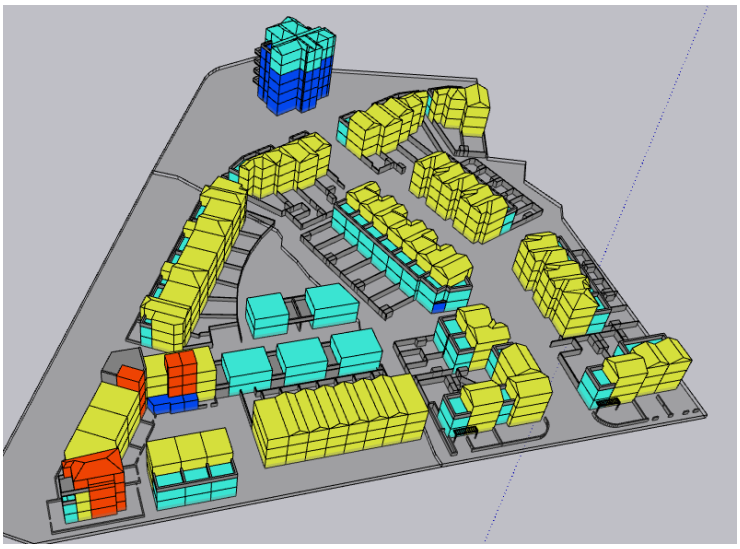


Figure 5.2 : Modelled energy demand distribution for dwellings in Trent Basin, as visualized in the iCD tool.

5.2.4 Implementation Process

The modelling followed a systematic process starting with individual building characterization based on the four defined categories. Local weather data from the Trent Basin weather station was incorporated to represent actual environmental conditions affecting heat demand throughout 2022.

The simulation employed hourly timesteps aligned with the temporal resolution required for control strategy evaluation. Complete annual simulations were conducted for all 76 houses, capturing both peak winter demands and reduced summer requirements. This comprehensive approach ensured the model accounted for seasonal

variations in heating demand and their implications for heat pump operation and storage utilization.

The yearly heat demand profile for the entire Trent Basin project is illustrated in Figure 5.3. This chart provides an overview of the heat demand patterns observed throughout 2022. The data reveals significant seasonal fluctuations, with peak demand reaching 850 kW_e in January during the coldest period, while summer months show reduced demand between 120-150 kW, primarily for domestic hot water. These variations highlight the dynamic nature of energy consumption in response to seasonal changes, temperature fluctuations, and occupancy patterns.

A closer examination of heating patterns was conducted by analysing demand profiles for sample properties. Figure 5.4 shows the hourly heat demand for four representative buildings during a week in February 2022. The chart provides detailed visualization of daily heat demand fluctuations and highlights variations among different property types. These differences are primarily driven by floor area, as the simulated heating systems and building envelopes share common thermal characteristics across the development. The daily patterns reveal characteristic morning and evening peaks corresponding to the implemented occupancy schedules.

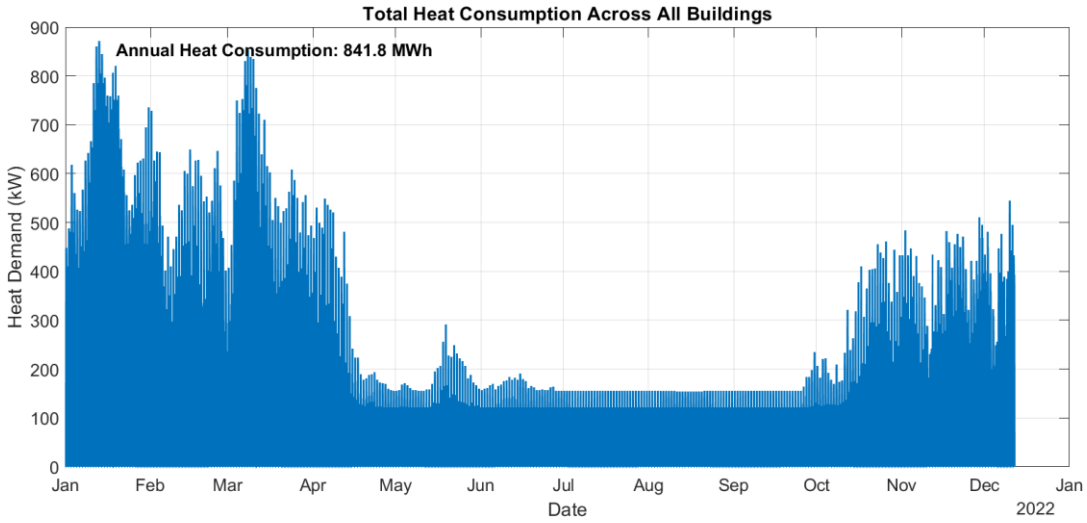


Figure 5.3: Yearly Combined Space Heating and DHW Demand Profile for the Trent Basin Project in 2022 (Modelled on iCD).

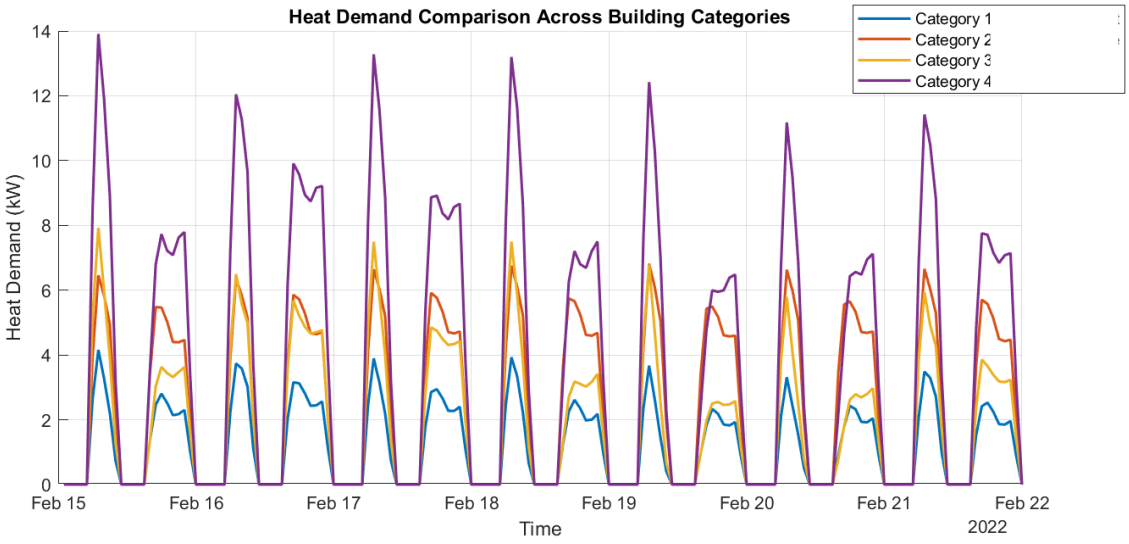


Figure 5.4: Hourly Heat Demand in kW_{th} for 4 Buildings During Feb 2022 (Modelled on iCD).

The validation process compared modelled outputs with established benchmarks for UK residential buildings and assessed internal consistency across different building types and operational patterns. Heat demand intensity values (kWh/m²/year) were verified against typical values for energy-efficient new-build properties (mentioned in Section 5.5), confirming appropriate representation of building performance. This

validated demand data provided the foundation for system sizing and the development of control strategies described in the previous chapter.

5.3 Electrical Demand Data Collection

5.3.1 Monitoring System Architecture

The Trent Basin development incorporated extensive monitoring infrastructure to capture detailed energy consumption data. Each property was equipped with monitoring devices collecting three key electrical consumption metrics: hourly average power consumption (kW), maximum power demand per hour (kW), and cumulative energy consumption (kWh). This comprehensive approach enabled detailed analysis of both typical usage patterns and peak demand events.

Data collection utilized a networked system that transmitted measurements to a central database through a publicly accessible Application Programming Interface (API). This infrastructure facilitated the retrieval of both real-time and historical data at varying granularities from hourly to yearly intervals, providing extensive coverage of consumption patterns throughout the monitoring period.

Sensors within each home were specifically configured to record the maximum power usage for each hour, focusing on peak usage instances rather than solely average consumption. This approach ensured that potential stress on electrical infrastructure could be properly evaluated by operating under a worst-case scenario assumption, wherein each house reaches its maximum demand simultaneously.

Figure 5.5 illustrates the monitoring system architecture deployed in the Trent Basin development (Shipman & Gillott, 2019). The diagram shows the end-to-end data

collection pathway from in-home sensors—such as electricity meters, indoor environment sensors, and radiator controllers—through the Project SCENe (Sustainable Community Energy Networks) Gateway and local wireless networks, to cloud-based databases. Project SCENe is a research initiative focused on developing and demonstrating community-scale energy monitoring and management systems (*Trent Basin · Project Scene (Sustainable Community Energy Networks)*, n.d.). Data is transmitted via multiple communication protocols: Wi-Fi for standard internet connectivity, EnOcean for low-power wireless sensor networks optimized for building automation, and M-Bus (Meter-Bus) for utility meter communication following the EN 13757 standard. The collected data ultimately feeds into the University of Nottingham and Honeywell cloud platforms for further analysis and system optimisation.

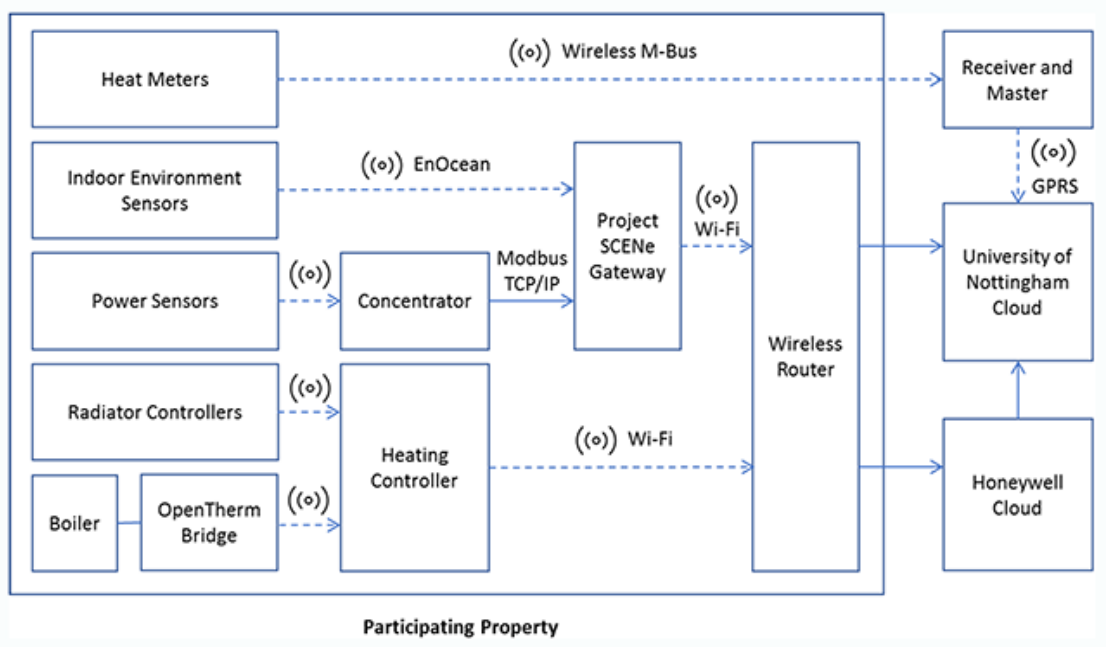


Figure 5.5: Monitoring system architecture for the Trent Basin development, showing data flows from building-level sensors to cloud-based databases via the Project SCENe Gateway (Shipman and Gillott, 2019).

5.3.2 Data Processing Methodology

Raw electrical consumption data underwent several processing steps to ensure quality and consistency for subsequent analysis. The first stage involved identification and removal of anomalous readings, including sensor disconnections, extreme values, and measurement errors.

Gap filling was implemented for missing data points using contextual interpolation methods that considered both temporal patterns (time of day, day of week) and environmental conditions. This approach maintained data continuity while minimizing the introduction of artificial patterns that could influence subsequent analysis.

Temporal alignment was particularly important when working with data from multiple meters across the development. The processing methodology ensured consistent timestamp conventions and corrected for any measurement drift between devices. This alignment was crucial for accurate assessment of coincident demands and their impact on network infrastructure.

The modelling approach for heat demand using iCD also generated modelled electricity demand. Figure 5.6 presents a comparison between the modelled and measured total electrical energy consumption for the year 2022, illustrating the alignment between simulated predictions and actual monitored data. This comparison validates the efficacy of the modelling process and highlights areas requiring further calibration or detailed investigation.

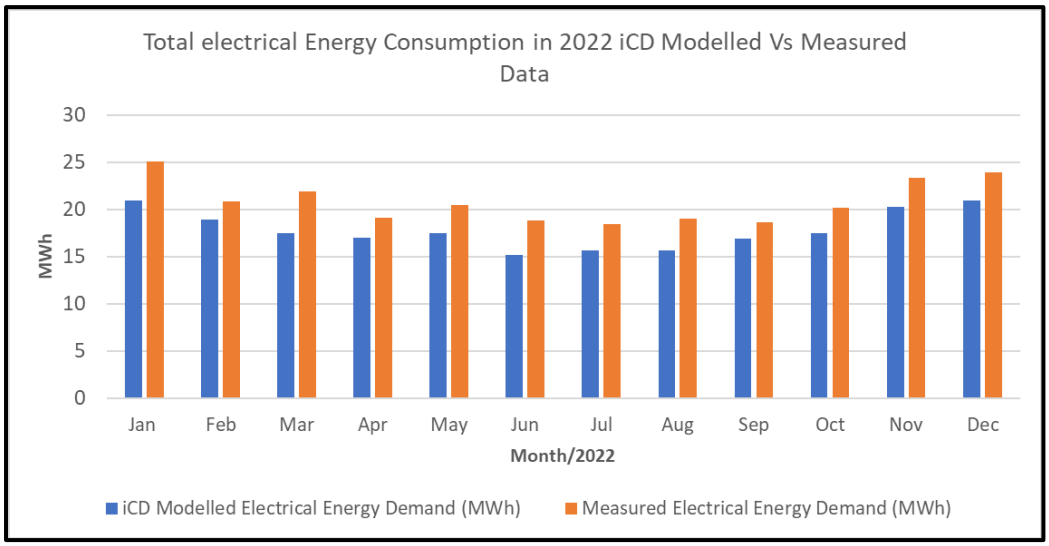


Figure 5.6: Comparison of modelled and measured total electrical energy consumption for 2022 at Trent Basin.

5.3.3 Hourly Resolution Considerations

The selection of hourly temporal resolution for electrical data represented a balance between analytical detail and practical implementation considerations. This resolution enabled capture of daily consumption patterns, including morning and evening peaks, while maintaining manageable data volumes for long-term analysis across multiple buildings.

For peak demand assessment, the hourly maximum power measurement proved particularly valuable, as instantaneous peaks within each hour were captured rather than being averaged out. This approach revealed that maximum power demands frequently exceeded average consumption by a factor of three or more, highlighting the importance of considering peak events when evaluating network impacts.

The electrical demand data revealed characteristic daily patterns with significant implications for system design:

- Morning peak (06:00-09:00): 150-200 kW

- Midday demand (10:00-15:00): 100-150 kW
- Evening peak (17:00-20:00): 250-300 kW
- Night-time base (23:00-05:00): 45-50 kW

While sub-hourly resolution might provide additional insights into very short-duration peaks, the hourly maximum measurement approach captured the essential characteristics needed for system sizing and control strategy development. The focus on hourly maximum power rather than average consumption ensured that critical peak demands were properly represented in the analysis.

Further analysis highlighted the importance of using maximum measured power rather than average or modelled values, as only the maximum measurements accurately capture the instantaneous peaks critical to grid stability. Figure 5.7 illustrates these differences clearly, emphasizing why maximum power values were prioritized in the analysis.

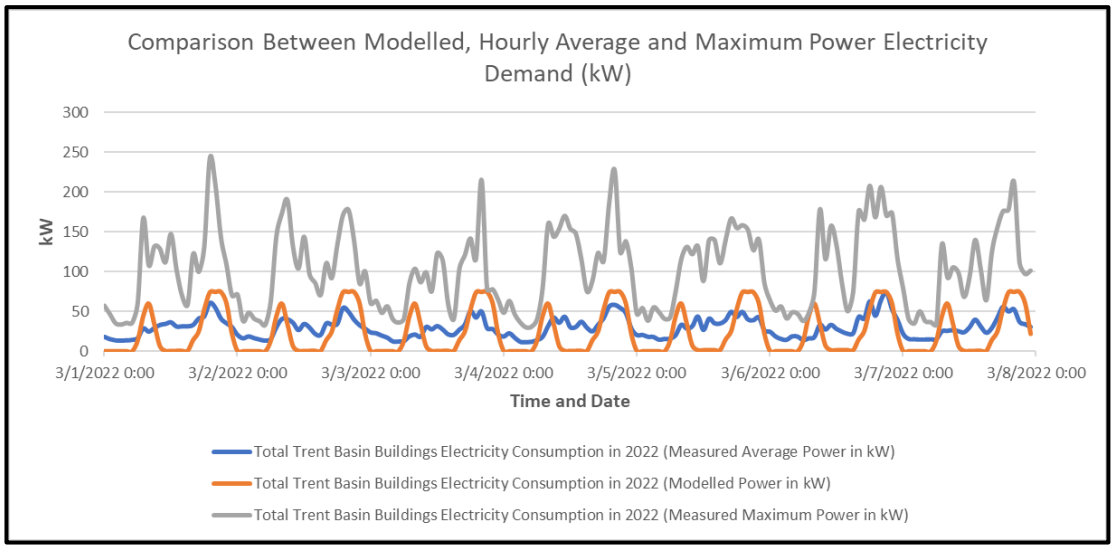


Figure 5.7: Comparison of modelled, hourly average, and maximum power electricity demand at Trent Basin

5.4 Other Data Collection

5.4.1 LV Substation Data

The LV substation serving the Trent Basin development represented a critical infrastructure element in the analysis, establishing fundamental constraints for heat pump integration strategies. Information regarding the substation was limited to its rated capacity of 800 kW, which was obtained from the National Grid's Connected Data Portal. This capacity rating established an essential upper boundary for system loading in the simulation model.

Despite extensive efforts to access comprehensive loading data for the substation, including inquiries to the Distribution Network Operator, full operational data proved unavailable for research purposes. Consequently, as detailed in Chapter 4, the methodology employed an important simplification: the aggregate electrical demand from the 76 Trent Basin buildings was used as a proxy for substation loading. This approach allowed for consistent analysis of relative loading changes while acknowledging that, in reality, additional loads beyond the Trent Basin development are likely connected to this infrastructure.

The electrical demand measurements from individual buildings provided the foundation for estimating community-scale impact on the network. Aggregating these measurements revealed characteristic patterns:

- Pronounced evening demand peaks (typically 17:00-20:00)
- Minimal loading during early morning hours (23:00-05:00)
- Distinct weekday-weekend consumption variations
- Seasonal fluctuations with higher winter demands

This building-level data, combined with the known substation capacity limit, enabled assessment of network headroom availability and evaluation of potential capacity constraints under heat pump deployment scenarios. While this approach necessarily simplified actual network conditions, it provided a pragmatic basis for analysing relative impacts of different control strategies on infrastructure loading.

5.4.2 Weather Station Data

The on-site weather station at Trent Basin provided crucial ambient temperature data that directly influenced HP efficiency calculations. Temperature readings were collected at 5-minute intervals and subsequently processed to hourly resolution to align with the simulation framework.

This temperature data proved essential for determining the dynamic COP values for HPs throughout the analysis period. Using manufacturer performance specifications, each hourly temperature reading was converted to a corresponding COP value according to established performance curves. The relationship showed significant variation, with COP values ranging from 2.33 at -7°C to 4.76 at 25°C, highlighting the substantial influence of environmental conditions on system efficiency.

The direct relationship between ambient temperature and heat pump performance represented a critical parameter in the simulation model. By incorporating actual temperature data rather than statistical averages, the analysis captured realistic efficiency variations that would affect both energy consumption and capacity requirements under real-world operation.

5.4.3 Grid Carbon Intensity Data

Real-time grid carbon intensity data was obtained from the National Grid ESO—Electricity System Operator—Data Portal (*Historic Generation Mix and Carbon Intensity | ESO*, n.d.), providing hourly carbon emission factors for the East Midlands region electricity grid. This dataset enabled assessment of how different control strategies aligned with varying grid carbon intensity patterns, supporting evaluation of environmental performance beyond simple energy consumption metrics.

The carbon intensity data ranged from approximately 35-320 gCO_2/kWh throughout the analysis period, reflecting the variable contribution of renewable generation and fossil fuel sources to the electricity grid. This temporal variation in carbon intensity became particularly important for evaluating the environmental benefits of load shifting strategies, as HP operation during periods of lower carbon intensity could significantly improve overall emissions performance.

5.4.4 Electricity Pricing Data

Economic performance evaluation required representative electricity tariff structures reflecting UK residential market conditions in 2024/2025 as published by The Office of Gas and Electricity Markets (Ofgem) (*Energy Price Cap | Ofgem*, n.d.). Three distinct pricing frameworks were incorporated:

- **Standard rate tariff**: A flat rate of 24.5p/kWh representing conventional fixed pricing

- **Economy 7 tariff**: Time-of-use pricing with off-peak rates (13.32p/kWh, 00:00-07:00) and peak rates (30.5p/kWh, 07:00-00:00)
- **Dynamic tariff**: Dynamic hourly pricing reflecting wholesale market conditions, obtained from Octopus Energy (electricity supplier) Agile Tariff scheme (*Agile Portal*, n.d.)

These tariff structures enabled comprehensive assessment of how different control strategies influenced operational costs while revealing the sensitivity of economic benefits to pricing structure design.

5.5 Data Validation and Integration Framework

5.5.1 Heat Demand Validation Methodology

Model outputs were benchmarked against recent UK evidence for both annual and peak loads. At category level the simulation produced peak space-plus-water-heating demands of 5.5 kW, 8.7 kW, 11 kW_{th} and 18 kW_{th} for small-apartment through to premium-house typologies (Figures 5.3–5.4). These fall well inside, or at the upper tail of, the 2–15 kW_{th} per-dwelling range reported from half-hourly gas-meter data in (Watson et al., 2019) and therefore capture realistic winter-design conditions.

Annual heat-demand totals of 6.4 MWh, 10.4 MWh, 7.4 MWh and 17.3 MWh compare favourably with monitored means for new-build dwellings: (Beis, n.d.) statistics for 2017 show a weather-corrected average of c. 9.3 MWh for gas-heated houses and 6–8 MWh for modern flats, while the (Innovate UK, 2016) Building Performance Evaluation (BPE) programme reports median delivered-thermal energy of 71 kWh m^{-2} yr^{-1} (≈7–11 MWh for the floor-areas modelled). Normalising the

simulated results by the floor areas specified in Section 5.2.2 gives intensities of roughly 60–100 kWh m^{-2} yr^{-1}, comfortably within the 60–130 kWh m^{-2} band observed across low-energy developments monitored by the BPE, yet still well above the Passivhaus limit of 15 kWh m^{-2} yr^{-1} (Passivhaus Trust, 2017), indicating scope for further fabric improvements.

While the buildings currently operate with gas boilers and radiators, the validation approach remains applicable for HP analysis. The building heat demands are independent of the heat generation technology - the thermal energy required to maintain comfort conditions remains the same whether delivered by boilers or HPs. HP electrical demands were calculated from these validated heat demands using temperature-dependent COP curves from manufacturer data, with COP values ranging from 2.5 to 3.8 depending on ambient temperature.

Taken together, these comparisons confirm that the iCD-based demand model reproduces both the magnitude and seasonal dynamics expected for contemporary, gas-heated UK housing and hence provides a credible baseline for the system-sizing and optimisation studies in Chapter 6.

5.5.2 Integrated Dataset Development

The development of an integrated dataset combining multiple data streams required careful consideration of temporal alignment, resolution harmonization, and quality assurance. All data sources were standardized to hourly resolution, with appropriate averaging or maximum value extraction depending on the parameter's characteristics.

Timestamp conventions were unified across all data streams to ensure accurate temporal relationships.

The integration methodology followed a systematic process:

1. Synchronization of all data streams to a common temporal framework
2. Quality assurance checking across integrated parameters
3. Creation of unified data structures for simulation input
4. Implementation of consistent naming conventions and units

The final integrated dataset structure included:

- Building-level electrical consumption (average and maximum hourly power).
- Modelled hourly heat demands.
- Weather parameters.
- Substation loading conditions.
- Grid carbon intensity data.
- Electricity tariffs for the economic analysis.

This comprehensively integrated dataset provided the essential foundation for the simulation model described in Chapter 4, enabling evaluation of different control strategies for HP and TES systems while maintaining consistent temporal relationships between all parameters.

5.6 Conclusions

This chapter has presented the methodological approach to demand modelling and data collection that underpins the simulation framework for community-scale heat decarbonization at Trent Basin. The integration of modelled heat demands with measured electrical consumption data provided a robust foundation for analysing community-scale HP deployment strategies.

The heat demand modelling, implemented through the IES iCD tool, successfully captured both temporal and magnitude characteristics of building heating requirements. The validation process demonstrated the model's capability to represent realistic demand patterns while accounting for building-specific characteristics and occupancy behaviours. The resulting demand profiles, with peak community heating demands reaching 850 kW_{th} during winter periods, established crucial baseline requirements for system sizing and control strategy development.

The extensive monitoring infrastructure at Trent Basin provided valuable insights into actual energy consumption patterns. Electrical demand data revealed significant variations between average and peak power requirements, with maximum demands frequently exceeding three times the average consumption levels. This finding highlighted the importance of considering peak demand events in system design and optimization.

Weather station data proved essential for understanding environmental influences on both building thermal performance and potential HP operation. The relationship between ambient temperature and HP COP, varying between 2.33 at -7°C and 4.76 at 25°C under typical conditions, emerged as a crucial factor in system optimization.

The LV substation data provided critical context for network constraints, with the 800 kW_e capacity limit establishing clear boundaries for system operation. The analysis of current loading patterns, showing peak demands around 300 kW, indicated available capacity for HP integration while highlighting the need for careful demand management to avoid network overload.

This detailed understanding of demand patterns and system constraints forms the foundation for the simulation analysis and optimization strategies presented in subsequent chapters. The combination of modelled and measured data ensures that the proposed control strategies address real-world operational conditions while maintaining practical feasibility.

The datasets developed in this chapter directly feed into the simulation and optimisation in Chapters 6 and 7. The validated hourly heat demands for each building type, measured baseline electrical consumption patterns, weather data and LV substation constraints form the foundation for evaluating the three control strategies presented in the next chapter

Chapter 6

6. Case Study and Simulation Analysis

6.1 Introduction

The integration of HPs with TES systems at community scale requires practical validation to assess the effectiveness of theoretical control strategies. This chapter presents a detailed case study implementation and simulation analysis of the Trent Basin development in Nottingham, examining how the control strategies developed in Chapter 4 perform when applied to real-world building configurations and energy demands outlined in Chapter 5.

The Trent Basin development provides an ideal testing ground for community-scale heat decarbonisation strategies, comprising 76 residential units of varying sizes and configurations connected to a single LV substation. This diversity of building types creates realistic variations in heating demands and thermal characteristics, challenging the control strategies to maintain effective performance across different operating conditions.

This chapter examines three distinct control approaches that represent progressively more sophisticated system management:

1. A baseline scenario implementing uncontrolled HP operation, establishing reference performance metrics for comparison
2. A fixed threshold model introducing basic grid-aware control through static operational thresholds

3. An active building model incorporating dynamic optimization with daily threshold adjustments

Each control strategy undergoes comprehensive performance assessment across multiple dimensions including peak demand reduction, energy consumption patterns, system efficiency, grid stability impacts, and carbon emissions. This multifaceted evaluation provides insight into the practical effectiveness of different control approaches while revealing important interactions between system components and operational objectives.

The chapter first describes the specific characteristics of the Trent Basin development that influence system performance, followed by detailed explanation of simulation implementation. The results analysis then examines both immediate performance outcomes and broader implications for community-scale heat decarbonisation strategies. This structured approach enables systematic evaluation of control strategy effectiveness while maintaining focus on practical implementation considerations.

6.2 Case Study Description

The Trent Basin development represents a modern approach to sustainable residential construction in Nottingham's waterside regeneration zone. The development consists of 76 residential properties across two completed construction phases, with Phase 1 comprising 45 houses completed in 2017 and Phase 2 adding 31 houses completed in 2020. These properties are connected to a single 800 kW_e LV substation, creating a well-defined electrical network boundary for analysis.

The residential units span four distinct building categories with varying thermal characteristics and heating requirements as summarized in Table 6.1:

Table 6.1: Building categories and characteristics in the Trent Basin development

Category	Number of Properties	Peak Heat Demand (kW)
1	6	3-4
2	31	5-6
3	16	7-8
4	23	12-16

The sizing strategy adopted in this research is simplified, aiming to ensure each element is adequately dimensioned to meet energy demands while facilitating the optimisation process. Also, it is only specific to the Trent Basin project and may not be directly applicable to other scenarios without adaptation.

While community-scale district heating could potentially offer greater efficiency, this study focuses on individual HTHPs and TES units. This choice reflects a more realistic solution for the existing UK building stock, requiring lower infrastructure and cost investment compared to community-scale systems. Cost considerations were not factored into the sizing methodology, although efforts were made to maintain realistic sizes for both HPs and TES units.

HP capacity is determined based on the average heat demand observed during the coldest days, providing a buffer for colder-than-average periods. TES units are sized to independently meet the heat demand for a 3 h duration, based on the average

demand during cold days. The resulting HP and TES configurations for each building category are shown in Table 6.2:

Table 6.2: HP and TES configurations by building category

Category	HP Capacity (kW)	TES Capacity (kWh)	Charging Rate (kW)
1	5	10	2.5
2	6	15	3
3	8	20	4
4	16	30	8

These configurations enable approximately three hours of autonomous heating operation from TES during peak demand periods, providing flexibility for demand management while remaining practical for domestic installation.

The electrical infrastructure centres on a single 800 kW_e LV substation serving all 76 properties. Current peak electrical demands typically reach 300 kW_e during winter evenings, providing theoretical headroom for HP integration, though the coincident operation of multiple HPs could rapidly approach this capacity without effective control strategies.

Occupancy patterns follow typical residential profiles with primary heating demand during morning (06:00-10:00) and evening (16:00-23:00) periods. Weekend patterns show more distributed demand, reflecting varied activity schedules. These patterns

create characteristic demand profiles that influence optimization strategy effectiveness.

The local climate data from 2022 shows ambient temperatures ranging from -2°C to 25°C throughout the year, directly affecting HP performance. During the coldest periods when heating demand peaks, HP COPs vary between 2.6 and 3.4, significantly influencing electrical demand patterns and system efficiency.

This operational context creates both challenges and opportunities for system optimization:

- Morning pickup loads after night setback periods generate potential demand peaks
- Evening coincidence of heating and non-heating electrical loads stresses grid capacity
- Weekend demand diversity offers opportunities for load shifting
- Seasonal variation in HP efficiency influences optimal control strategies

6.3 Simulation Setup

The simulation implementation applied the methodological framework established in Chapter 4 to the Trent Basin case study. The three control strategies—baseline scenario model (Section 4.4.3), fixed threshold model (Section 4.4.4), and active building model (Section 4.4.5)—were implemented using the performance evaluation framework detailed in Section 4.5.

Case study-specific parameters included the 76 residential properties with HP and TES configurations summarized in Table 6.2. The simulation utilized operational data for

a full calendar year at hourly temporal resolution, incorporating real weather data from the on-site Trent Basin weather station, modelled heat demands and actual electricity consumption patterns from the community monitoring system described in Chapter 5.

All scenarios operated under identical boundary conditions to ensure systematic comparison, with building characteristics, environmental data, and baseline electrical demands held constant across control approaches.

6.4 Energy System Analysis

The analysis examined multiple scenarios to evaluate system performance under both current operational conditions and projected future states. This systematic examination enabled understanding of immediate implementation impacts while providing insight into longer-term system evolution and grid integration challenges.

6.4.1 Current System Analysis

The electricity demand profile at Trent Basin demonstrates significant temporal variation across daily and seasonal timescales. Analysis of the full annual dataset from 2022 reveals pronounced seasonal patterns that directly influence the potential integration of heat pump systems. Winter months exhibit substantially higher demand patterns compared to the summer period, reflecting increased lighting requirements, longer indoor occupancy periods, and existing electrical heating supplements during colder weather.

The LV substation serving the community experiences variable loading throughout the year, with current peak demands of approximately 300 kW_e during winter evenings.

This represents approximately 37.5% utilization of the substation's rated capacity, suggesting theoretical headroom for additional electrical loads. However, the coincident nature of heating demands during cold periods warrants careful consideration of potential network stress points.

Examination of typical daily profiles reveals consistent characteristics throughout the year with more pronounced variability during colder months:

- Morning peak (06:00-09:00): 150-200 kW, corresponding with household morning activities
- Midday demand (10:00-15:00): 100-150 kW, reflecting reduced occupancy during typical working hours
- Evening peak (17:00-20:00): 250-300 kW, coinciding with highest occupancy and activity levels
- Night-time base (23:00-05:00): 45-50 kW, representing background and standby loads

Figure 6.1 illustrates these peak power demand patterns for a representative winter week, highlighting the distinct daily cycles and the relationship between demand peaks and typical occupancy periods. The consistent night-time base load of 45-50 kW_e represents approximately 15-17% of peak demand, indicating significant potential for load shifting to off-peak periods if suitable storage systems were implemented.

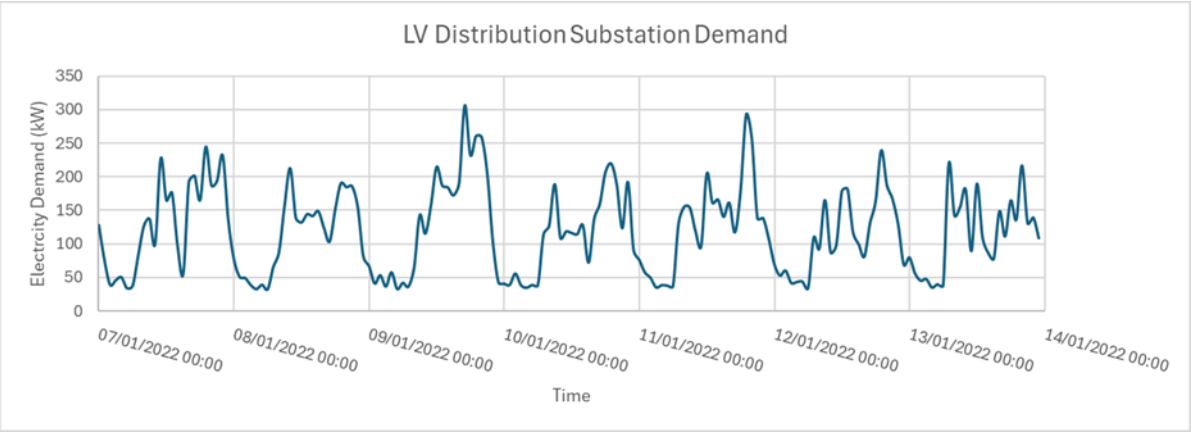


Figure 6.1: Hourly electricity demand at Trent Basin for a representative winter week, showing daily patterns and peak periods

These baseline demand patterns and environmental conditions establish the foundation for evaluating potential heat pump integration strategies. The identified daily and seasonal variations will significantly influence both the capacity requirements for heat pump systems and the potential optimization strategies for managing their grid impact.

6.4.2 Heat Pump Integration Scenarios

The introduction of heat pumps fundamentally transforms electrical demand patterns across the Trent Basin community. Figure 6.2 illustrates the comparative impact of three distinct control approaches over the entire annual cycle, demonstrating significant variations in both peak demand and temporal distribution patterns.

Baseline Heat Pump Operation

Under uncontrolled operation, heat pumps create substantial demand spikes during peak heating periods. As shown in Figure 6.2, the coincidence of heat pump activation during morning pickup periods results in peak demands reaching 497.45 kW_e during winter days, representing approximately a 66% increase over current maximum

demands. These peaks are particularly pronounced during January and February, with multiple instances exceeding 450 kW.

The baseline electricity consumption from HP operation for the year reached 245 MWh, with demand patterns closely following heating requirements. The uncoordinated operation creates characteristic 2 peaks during morning and evening hours. This operational pattern demonstrates clear potential for network capacity exceedance, particularly during cold weather periods when heat pump efficiency decreases.

Fixed Threshold Implementation

Implementation of fixed operational thresholds moderates peak demands through basic load shifting and storage utilization. This approach reduces maximum demands to 421.93 kW, representing a 15.18% improvement over the baseline scenario. The annual profile in Figure 6.2 shows more consistent demand patterns with fewer extreme peaks, particularly during winter months.

The fixed threshold model increased total electrical consumption from HP operation to 270 MWh, approximately 10% higher than the baseline scenario. This increase stems from suboptimal operational timing, where HPs sometimes operate during periods of lower efficiency to maintain system constraints. Despite this energy consumption increase, the approach demonstrates meaningful peak reduction capabilities, though the static nature of these thresholds limits their effectiveness during extreme weather conditions.

Active Building Model

The active building model, utilizing daily optimized thresholds and predictive control elements, achieves the most substantial peak reduction. Maximum demands under this

scenario reach 403.48 kW, demonstrating approximately 20% improvement over baseline operation. The annual profile in Figure 6.2 shows remarkably consistent demand patterns across all seasons, with significantly reduced peak-to-average ratio compared to other scenarios.

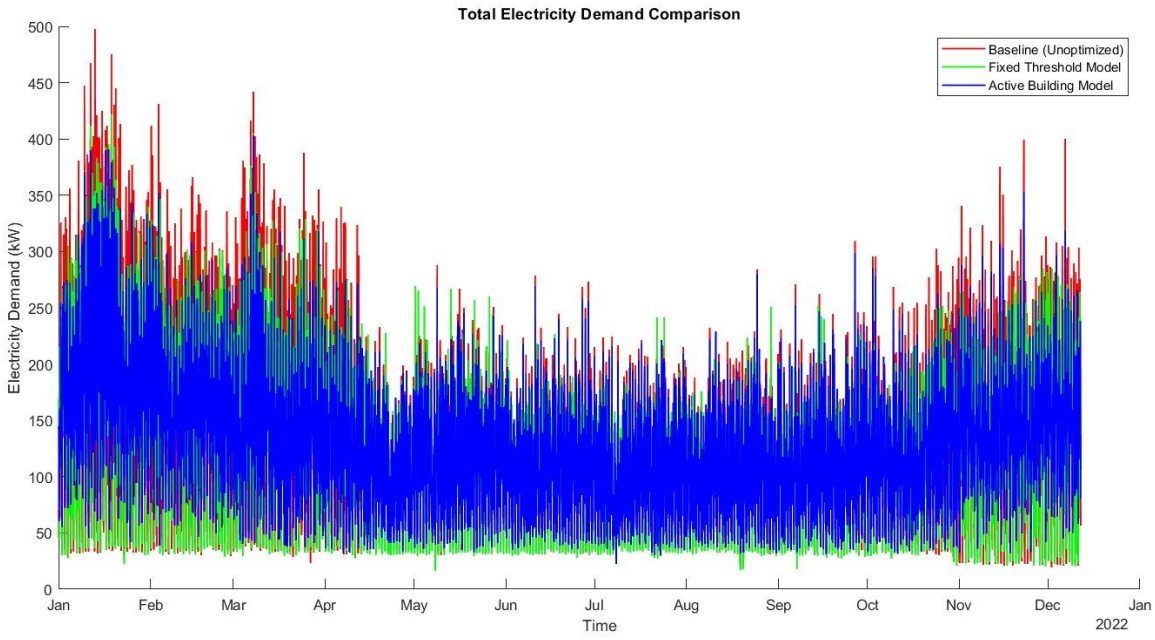


Figure 6.2: Total Electricity Demand Comparison across the three scenarios throughout 2022

Total electrical consumption (HP only) under this model was 248 MWh, a slight 1.3% increase from the baseline. This modest increase reflects the trade-off between peak demand management and total consumption, where the control strategy prioritises grid stability objectives over energy minimisation.

Figure 6.3 provides a closer examination of the three scenarios during the coldest week of January 2022, when heating demands reached their annual maximum. During this critical period, the baseline scenario exhibited frequent sharp peaks exceeding 450 kW_e and around 500 kW_e on January 13th. These severe demand spikes represent the

most challenging conditions for network integration. The fixed threshold model demonstrated moderate improvement with peaks between a 400-450 kW_e range, while the active building model maintained substantially smoother profiles predominantly below 400 kW_e even during this extreme period. This performance during the highest demand week of the year highlights the robustness of the active control strategy under worst-case conditions, with peak reductions of 15-20% compared to baseline operation while maintaining effective heat provision.

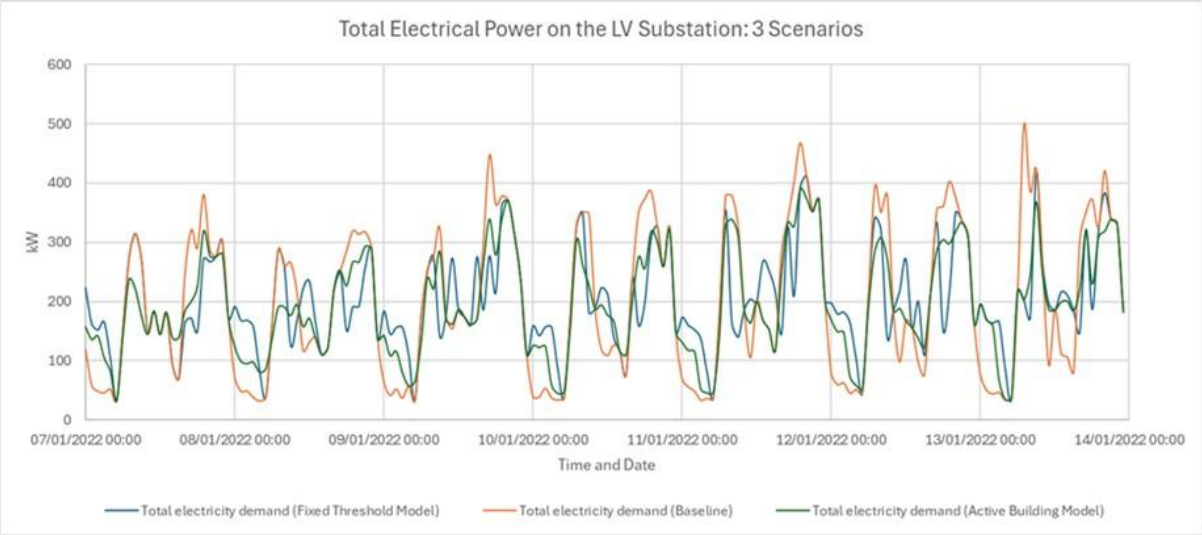


Figure 6.3: Total electrical power demand at the low-voltage (LV) substation during the coldest week of the year (7–14 January 2022) for three scenarios

Figure 6.4 presents a direct comparison of peak electrical demand across the three scenarios. The substantial reduction from 497.45 kW_e in the baseline case to 403.48 kW_e under the active building model represents a potentially significant benefit for network integration. These reductions maintain effective heat provision across all properties, demonstrating that sophisticated control strategies can successfully manage the grid impact of heat pump deployment without compromising occupant comfort.

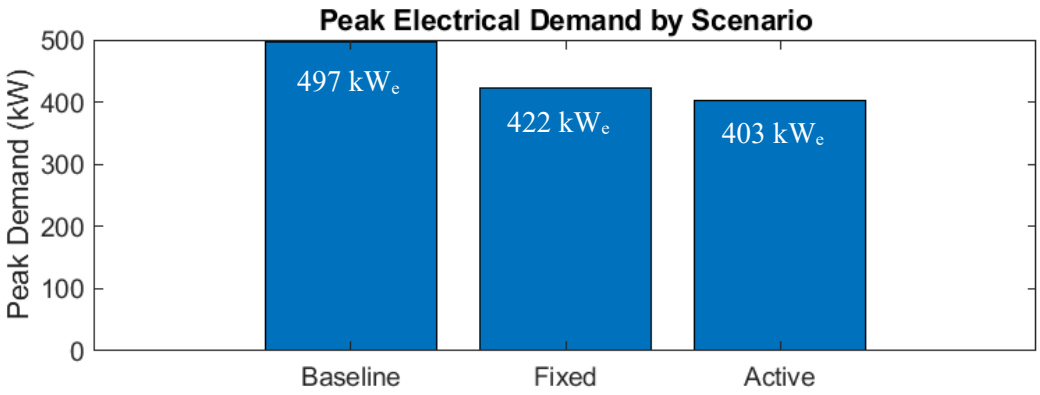


Figure 6.4: Peak Electrical Demand comparison across the three scenarios

6.5 Results Analysis

6.5.1 Energy Demand Patterns

The analysis of energy demand patterns provides essential insight into both current consumption characteristics and the transformative impact of heat pump integration. At the building level, heat demand follows distinct daily and seasonal cycles that directly influence heat pump electricity consumption and storage utilization patterns.

Figure 6.5 illustrates the heat demand profile for a representative Category 2 building (mid-sized house) during the coldest week of January 2022 (Friday 07/01/2022 – Thursday13/01/2022). The demand pattern exhibits characteristic morning and evening peaks, typically reaching 6-7 kW_{th} during early morning hours (06:00-09:00) and evening periods (17:00-22:00). These peaks correspond to recovery from night setback temperatures and increased thermal comfort requirements during peak occupancy periods. Midday demand generally stabilizes between 2-4 kW_{th}, while night demand drops to minimal levels, often close to 0.

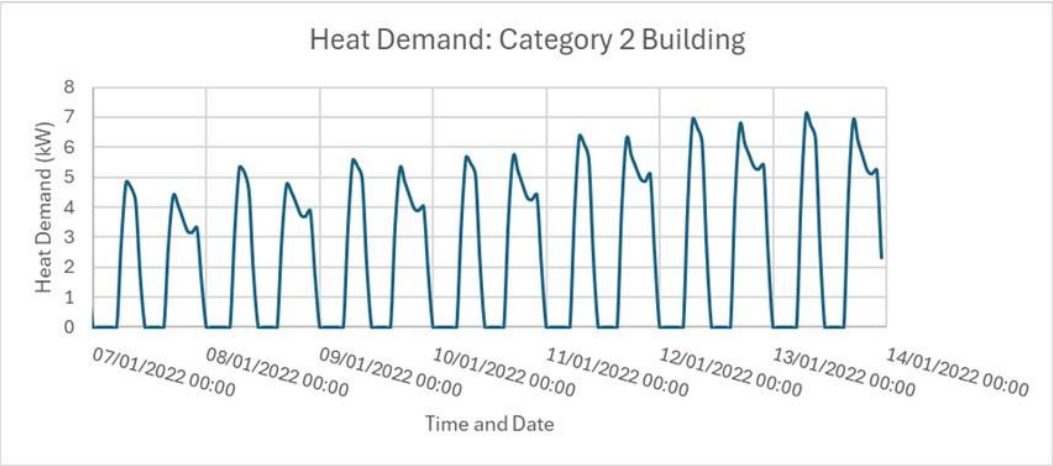


Figure 6.5: Heat demand for a Category 2 building during the coldest week of January 2022

Heat demand patterns vary significantly across building categories due to differences in floor area, occupancy, and thermal characteristics which was thoroughly described in Chapter 5.

Subsequently, Figure 6.6 displays the hourly peak electrical power for this building during the same period as previously noted. This chart captures the maximum power usage for each hour, detailing daily fluctuations and highlighting peak demand times.

The sharp spikes seen across the graph occur at various times throughout the week, illustrating the building's maximum electrical load under current conditions without the influence of HPs. This detailed insight into hourly peaks is crucial for understanding the building's energy consumption patterns, allowing for more precise energy management and planning to efficiently handle peak loads and enhance overall energy efficiency during extreme weather conditions.

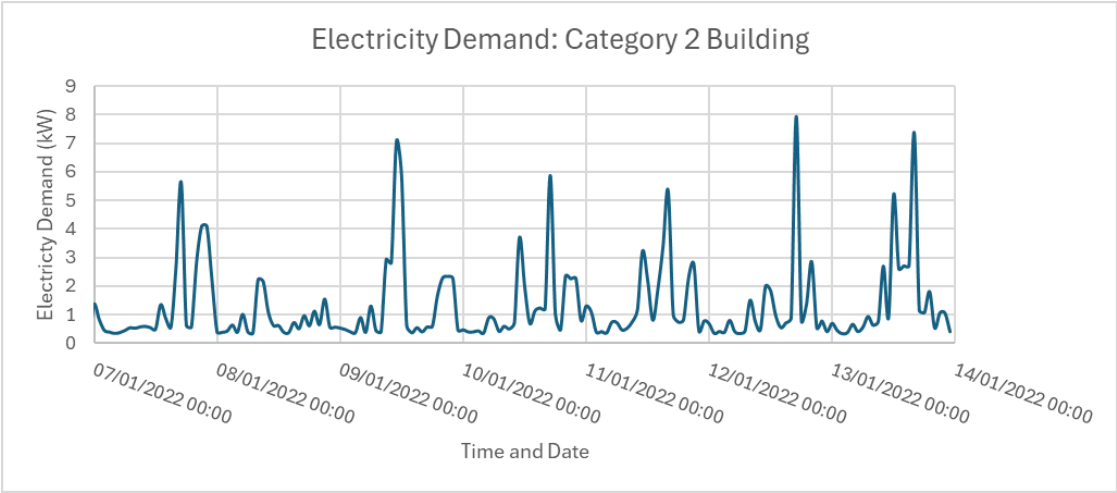


Figure 6.6: Hourly peak electricity power for Category 2 building during the analysed week

The relationship between outdoor temperature and heat pump efficiency plays a crucial role in determining electricity demand patterns. Figure 6.7 illustrates how COP values for a Category 2 heat pump fluctuate with ambient temperature during the analysed week. With outdoor temperatures ranging from approximately 0°C to 10°C, COP values varied between 2.9 and 3.4, directly influencing the electricity required to meet heating demands.

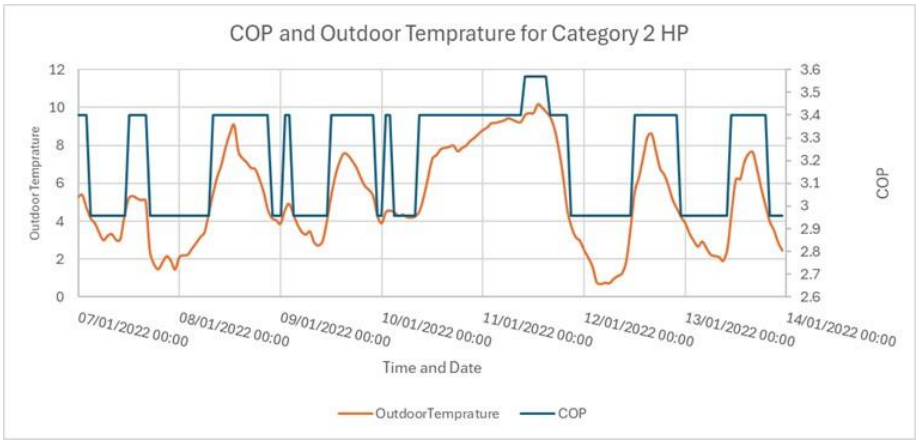


Figure 6.7: COP and outdoor temperature for a Category 2 heat pump over the analysed week

When translated to electricity consumption under the baseline scenario, these heating requirements create significant demand patterns. Figure 6.8 displays the electricity demand for the same Category 2 building, showing how HPs operation directly

correlates with heat demand profiles. The electricity demand follows a similar temporal pattern to the heat demand but at a reduced magnitude due to the heat pump's COP. Peak electrical demands reach approximately 10 kW_e during the coldest periods, with additional consumption from non-heating loads creating compound peaks during evening hours.

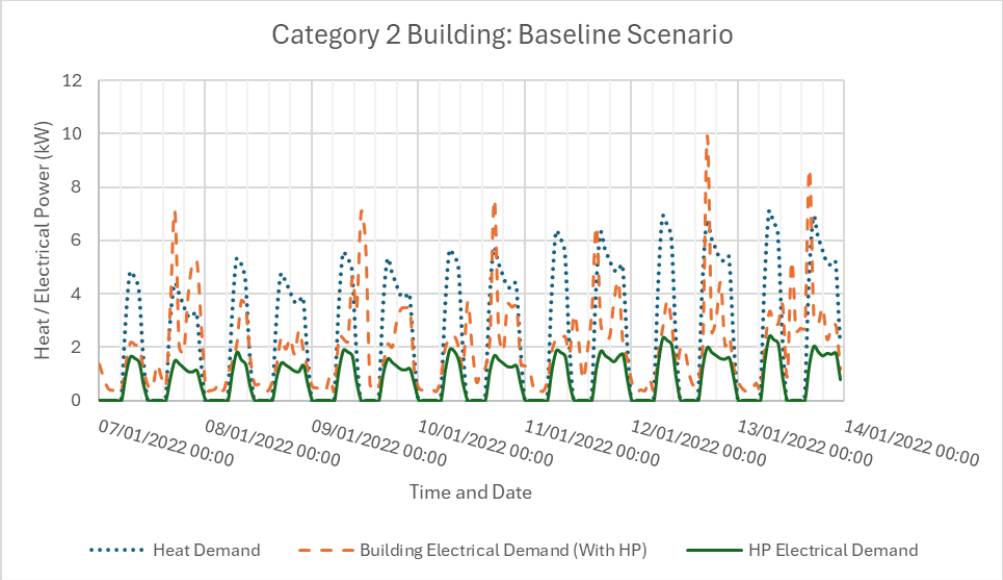


Figure 6.8: Baseline scenario energy dynamics for a Category 2 building

Under the fixed threshold and active building models, these electricity consumption patterns transform significantly through the integration of thermal storage. Figure 6.9 illustrates the energy flow for a Category 2 building under the fixed threshold model, showing the complex interaction between heat demand, electrical consumption, and storage state. The storage system charges during periods of lower electrical demand and higher heat pump efficiency, maintaining state of charge levels that enable demand shifting during peak periods. This redistribution of energy consumption creates significantly smoother electrical demand profiles while ensuring consistent heat provision.

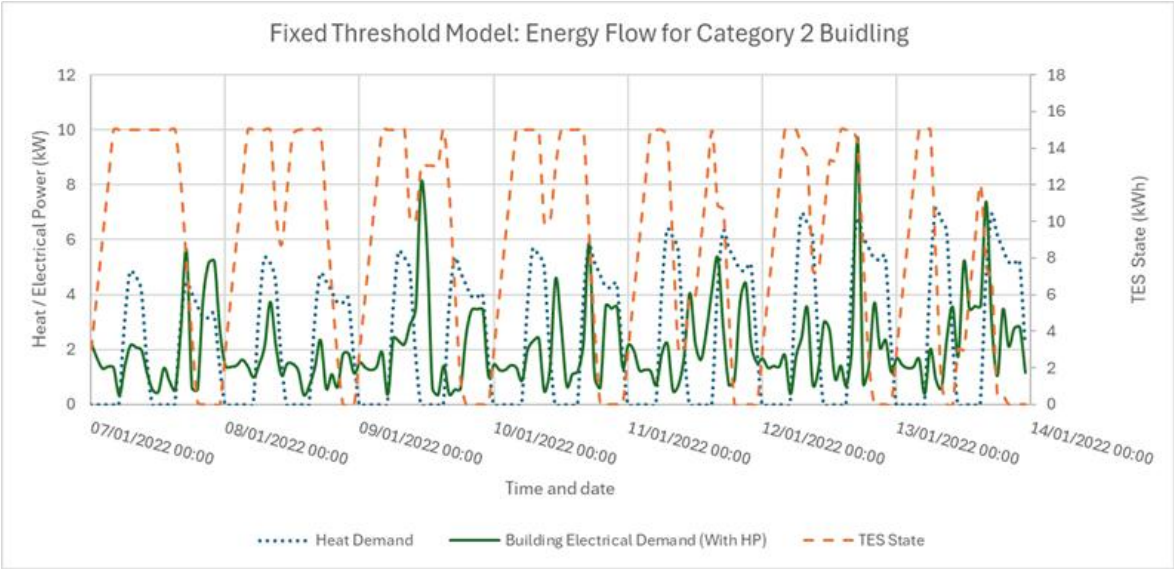


Figure 6.9: Fixed Threshold Model energy flow in a Category 2 building

Unlike the fixed threshold scenario, the active building model dynamically adjusts its thresholds daily to optimise energy usage. The following Table 6.3 illustrates the daily variations in Threshold 1 (T1) and Threshold 2 (T2) for a typical building over a week. These daily adjustments allow the system to adapt to changing conditions, potentially offering more efficient energy management than the fixed threshold approach.

Table 6.3: Summary of the LV substation operating thresholds within the active building model during the analysed week.

Day	T1 (kWe)	T2 (kWe)
1	170	40
2	110	140
3	30	160
4	140	80
5	180	40
6	110	100
7	140	90

Figure 6.10 demonstrates the intricate interplay between heat demand (blue line), building electrical power, including the HP (green line), and TES state (orange line). The dynamic nature of the system is evident in the varying patterns of TES charging and discharging, which align with the fluctuations in heat demand and electrical power consumption. The active building model's ability to adjust thresholds daily allows it to account for changing conditions, potentially leading to more optimal heat pump and thermal storage utilisation. The energy flow patterns shown in the figure reveal how the system manages to balance heat demand with electrical power consumption, using thermal energy storage as a buffer.

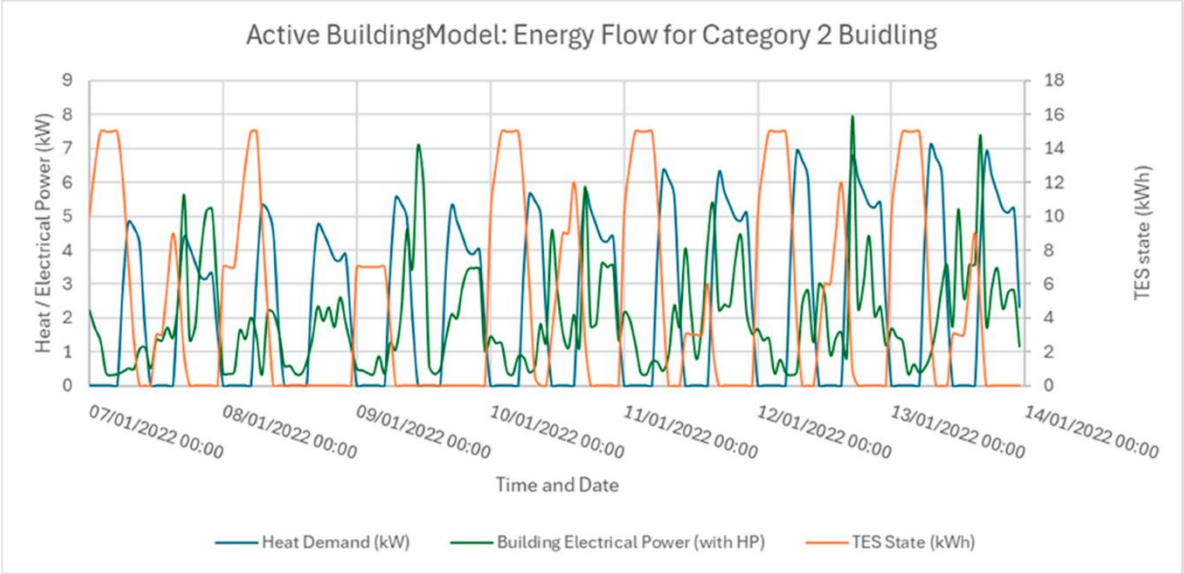


Figure 6.10: Active building model scenario energy flow in building from Category 2

These energy demand patterns establish the foundation for understanding how different control strategies impact system performance and grid integration. The observed characteristics, efficiency variations, and aggregation effects directly influence the optimization strategies explored in subsequent sections.

6.5.2 Integrated Performance Assessment

Comparative analysis of the three control scenarios reveals significant variations in system performance across multiple metrics. Figure 6.11 illustrates the hourly peak electrical power on the LV substation for all three scenarios over the coldest week of the year. The baseline scenario exhibits highly volatile demand patterns with frequent sharp peaks reaching up to 500 kW_e. The fixed threshold model demonstrates more balanced profiles with reduced peak heights, generally staying below 400 kW_e. The active building model achieves the most stable demand pattern, effectively flattening many peaks seen in baseline scenarios and rarely exceeding 350 kW_e during this critical period.

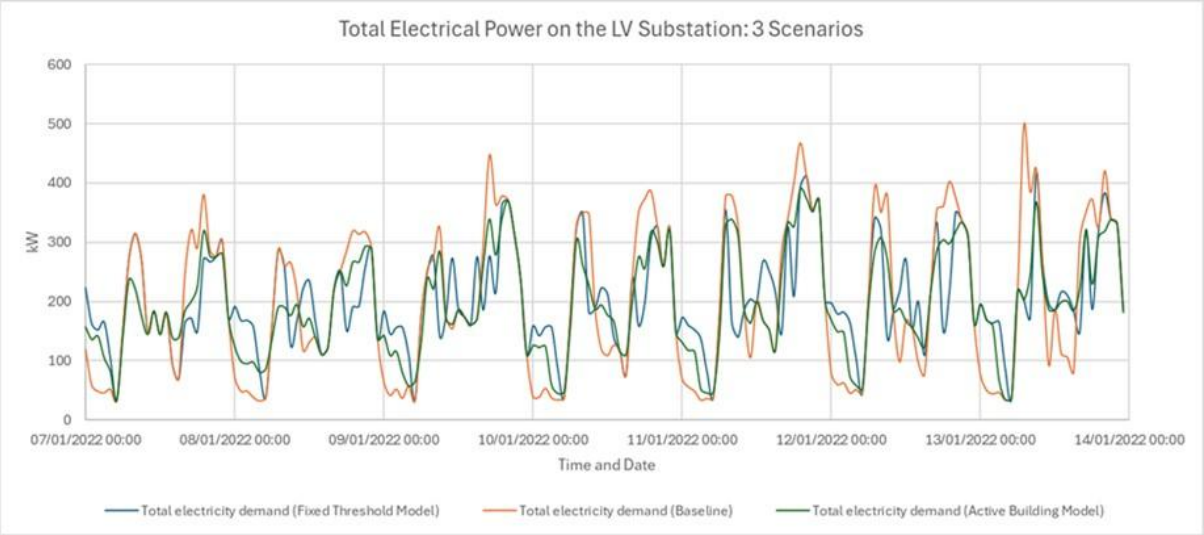


Figure 6.11: Comparison of total peak electrical power on the LV substation between the three scenarios during the coldest week of the year.

The operational dynamics of the fixed threshold model are governed by the static threshold values of T1=140kW_e and T2=180kW_e. These fixed parameters create consistent operational boundaries that govern heat pump and storage operation throughout the year. In contrast, the active building model implements dynamic

threshold optimization on a daily basis for each building. Figure 6.12 illustrates the distribution of these optimized thresholds across the simulation period.

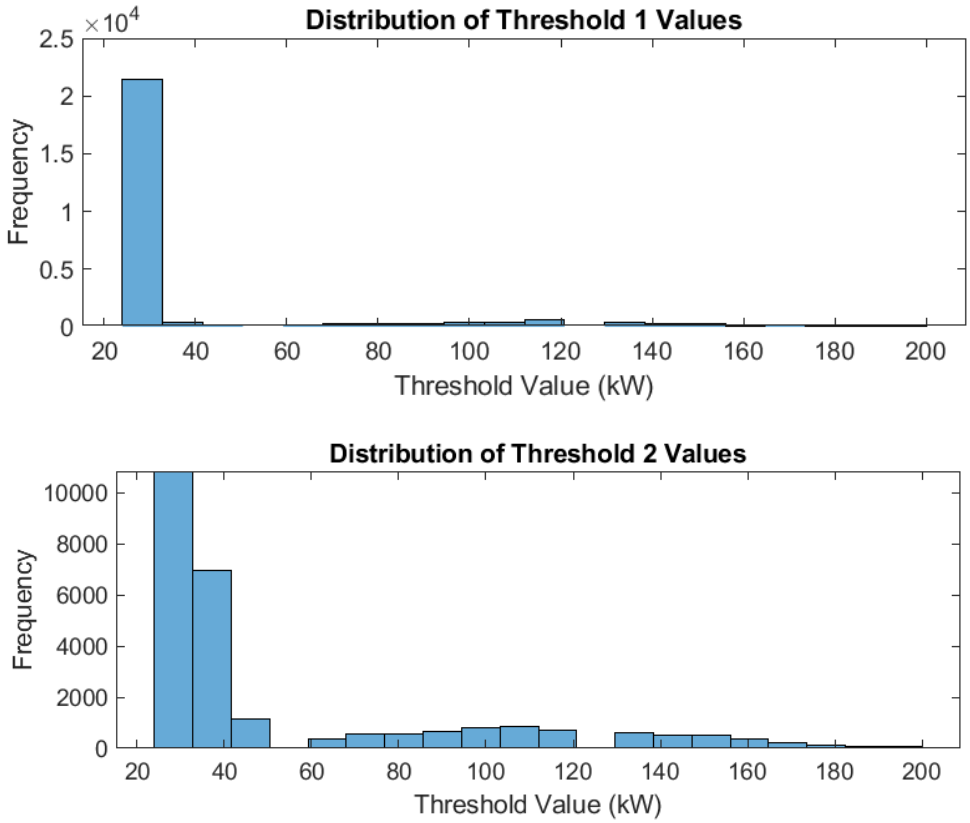


Figure 6.12: Distribution of Threshold 1 and Threshold 2 values in the active building model.

The threshold distribution reveals important insights into the optimization process. Threshold 1 values, which govern direct HP operation for heating, predominantly cluster around significantly lower values than the 140 kW_e fixed threshold, with concentrations near 30-40 kW_e. This indicates that the optimization algorithm frequently prioritizes earlier storage utilisation than the fixed threshold approach. Threshold 2 values, controlling storage charging, show greater distribution with clusters around 30-40 kW_e and 100-120 kW_e, suggesting adaptation to varying grid and environmental conditions throughout the year.

6.5.3 Environmental Performance Summary

The carbon emissions impact of the three control scenarios demonstrates important variations in environmental performance. Table 6.4 summarizes the key emissions metrics based on real-time grid carbon intensity data.

Table 6.4: Carbon emissions summary across control scenarios.

Metric	Baseline	Fixed Threshold	Active Building
Total Carbon Emissions (Kg CO_2)	47,098	48,904	44,943
Emissions Intensity (g CO_2/kWh heat)	56	58	53

The active building model achieves carbon reductions compared to the baseline scenario, with total emissions decreasing by approximately 5%. The fixed threshold model demonstrates a slight increase in emissions (+4%), despite its peak reduction capabilities, likely due to its higher overall energy consumption and occasional operation during higher carbon intensity periods.

The emissions intensity metric, measuring carbon emissions per unit of heat delivered, shows more substantial differentiation between scenarios. The active building model achieves approximately 5% lower emissions intensity than the baseline, indicating more efficient operation and better temporal alignment with lower-carbon electricity generation. More detailed analysis of these environmental performance metrics,

including seasonal patterns and temperature correlations, will be presented in Chapter 7.

6.5.4 Economic Performance Summary

Economic performance varies significantly across control scenarios and tariff structures. Table 6.5 presents a summary of annual costs under different electricity pricing schemes.

Table 6.5: Annual heat pump electricity costs by tariff structure

Tariff Structure	Baseline (£)	Fixed Threshold (£)	Active Building (£)
Standard Rate	59,675	66,160	60,807
Economy 7	66,967	68,622	58,897
Agile	49,777	45,218	41,068

The economic impact of HP operation varies considerably with tariff structure. Under the standard rate tariff (24.5p/kWh constant), the active building model shows a modest 1.90% cost increase compared to baseline, while the fixed threshold model exhibits a substantial 10.87% increase due to its higher energy consumption.

The time-of-use tariffs demonstrate more favourable outcomes for the optimized control approaches. Under the Economy 7 tariff, the active building model achieves 12.05% cost reduction compared to baseline, while the Agile tariff enables even greater savings of 17.50%. These results highlight the economic benefits of intelligent load shifting when combined with appropriate tariff structures. A comprehensive economic assessment will be presented in Chapter 7.

6.6 Conclusions

The comprehensive simulation and analysis of the Trent Basin case study demonstrates significant potential for optimized control strategies to enhance the integration of heat pumps in community-scale applications. The active building model's achievement of 19% peak demand reduction compared to baseline operation represents a crucial advancement for network integration. This substantial reduction from 497 kW_e to 403 kW_e, while maintaining effective heat provision across all properties, suggests that sophisticated control strategies could enable higher heat pump penetration within existing network constraints than conventional analysis might predict.

The fixed threshold model, while achieving 15 % peak reduction, while increased the annual energy consumption from HP operation by 10% compared to the baseline scenario. This finding highlights important limitations in static control approaches, where theoretical benefits in peak management can be undermined by suboptimal operational timing. In contrast, the active building managed to similar energy consumption of the baseline while delivering substantially improved peak management, demonstrating the potential for well-designed dynamic control strategies to address multiple objectives without significant performance compromises.

The threshold distribution analysis revealed important insights into the active building model's optimization approach. The predominance of lower threshold values than used in the fixed model demonstrates how dynamic optimization identifies different operational boundaries than static analysis might suggest. This adaptive capability enables the system to respond effectively to varying grid conditions, environmental factors, and demand patterns throughout the year.

From an environmental perspective, the active building model demonstrated carbon reductions, with emissions intensity decreasing by approximately 5% compared to the baseline scenario. Economic assessment revealed potential cost benefits under time-varying tariff structures, with the active building model achieving 12% savings under Economy 7 and 17% under Agile tariffs compared to baseline operation.

These findings provide a foundation for the more detailed performance evaluation in Chapter 7, which will further examine broader implications for energy system transformation. The demonstrated effectiveness of the active building model, particularly its ability to simultaneously improve multiple performance metrics, suggests promising potential for sophisticated control strategies in enabling rapid heat decarbonization while maintaining grid stability.

Chapter 7

7. Performance Evaluation and Impact Assessment

7.1 Introduction

Building upon the simulation results presented in Chapter 6, this chapter provides a comprehensive assessment of integrated HP and TES systems at community scale. While the previous chapter established the fundamental performance characteristics of different control strategies, this chapter examines their broader implications across multiple dimensions of system performance.

The evaluation framework addresses several interconnected aspects of system operation and impact. Energy performance analysis examines how system efficiency varies under different operational conditions, with particular focus on dynamic efficiency variations and seasonal performance. Grid integration assessment considers the implications for electrical infrastructure, examining how different control strategies influence network stability, demand volatility, and coincidence factors. Environmental impact analysis quantifies the carbon reduction potential of optimized system operation, while operational economic assessment examines the implications of different electricity tariff structures.

This multi-dimensional approach enables identification of potential synergies and trade-offs between different performance objectives. By examining system behaviour across varying temporal scales and operational conditions, the analysis provides insight into how community-scale heat decarbonization strategies might be effectively implemented while maintaining both grid stability and end-user satisfaction.

7.2 Energy Performance Evaluation

7.2.1 Dynamic Efficiency Analysis

The dynamic efficiency of HP systems varies across the three control scenarios. Seasonal analysis reveals important relationships between environmental conditions and system performance that directly influence total energy consumption and operational effectiveness.

Heat pump COP demonstrates seasonal variation, with average values ranging from approximately 2.9 during winter months to 4.0 during summer. This variation correlates directly with ambient temperature patterns and has significant implications for control strategy effectiveness. During winter periods when heating demand peaks, the coincidence of lower COP values and higher demand creates challenges for system optimisation.

The baseline scenario, implementing uncontrolled heat pump operation, demonstrates average COP values of 3.2 during winter operation. This performance level fluctuates considerably with ambient temperature, showing the fundamental relationship between environmental conditions and system efficiency. During the coldest periods when ambient temperatures approach 0°C, COP values decrease to approximately 2.9, significantly increasing electrical demand during periods of highest heating requirement.

The fixed threshold model shows minimal improvement in average COP values despite its more sophisticated control approach. The static threshold values prove insufficient to consistently prioritize operation during periods of higher efficiency. In fact, the model's emphasis on peak reduction occasionally shifts HP operation to overnight periods with lower ambient temperatures, reducing average system

efficiency and contributing to the 10% increase in total energy consumption observed in this scenario.

While, the active building model demonstrates consistent improvement in operational efficiency across the year. By optimising daily thresholds for each building based on predicted demand, this approach maintains average winter COP values of 3.4—approximately 6% higher than the baseline scenario. This improvement stems from the model's predictive optimisation capability and effective TES utilisation, enabling more strategic timing of HP operation.

The temporal distribution of efficiency improvements proves particularly significant. During spring and autumn, when greater flexibility exists in operational timing, the active building model achieves COP improvements of 8-10% compared to baseline operation.

However, this operational efficiency improvement does not translate to reduced total energy consumption. The active building model consumes 248.2 MWh compared to 245 MWh for baseline (+1.3% increase), reflecting the trade-off between peak demand management and energy minimization. The higher consumption results from increased storage charging activity and thermal losses associated with the TES systems, which experience 5% daily thermal losses as specified in the methodology.

Figure 7.1 illustrates the seasonal analysis showing average COP values by season across the three control scenarios. The bar chart clearly demonstrates the performance advantage of the active building model, particularly during spring and autumn periods where operational flexibility enables more significant efficiency improvements. The winter period shows smaller but still meaningful differences between the scenarios,

reflecting the constraints of cold weather operation when heating demands are highest and flexibility more limited.

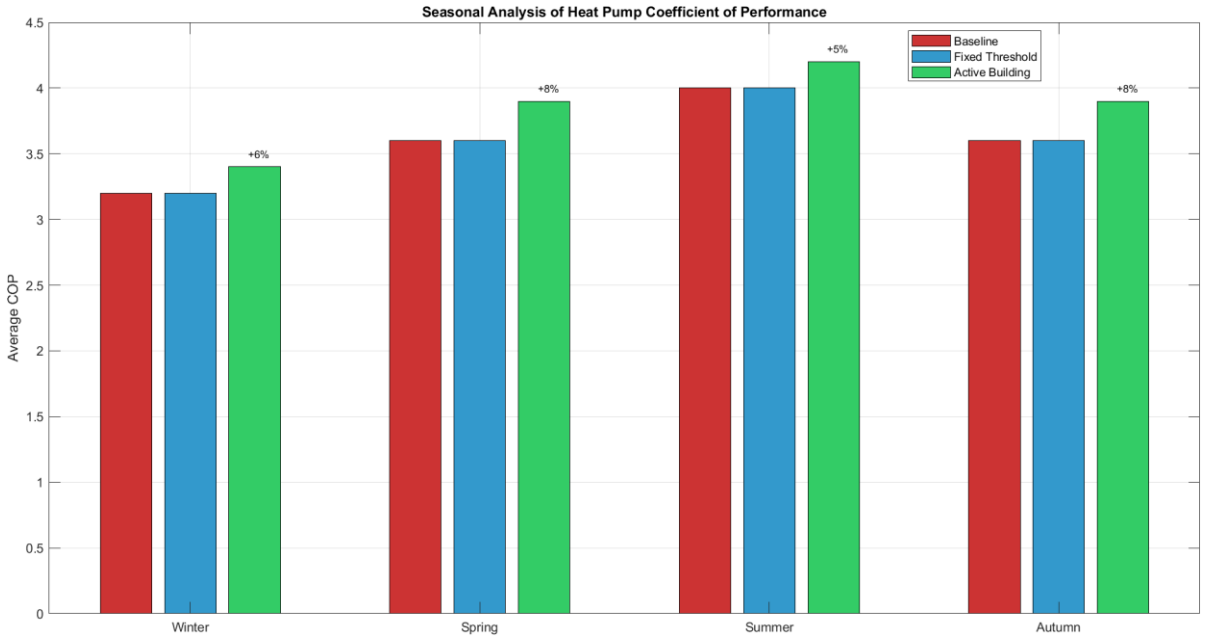


Figure 7.1: Seasonal analysis of HP's COP under three control strategies

7.2.2 Load Profile Characterization

The transformation of electrical load profiles under different control strategies reveals fundamental shifts in energy consumption patterns and their implications for system efficiency. Detailed analysis of hourly demand data demonstrates distinct characteristics across the three scenarios.

The baseline scenario exhibits highly volatile load profiles with sharp demand peaks closely following heating requirements. Morning pickup periods (06:00-09:00) show particularly pronounced demand spikes, with electrical consumption increasing by 150-200% within 1-2 hour periods. Evening demand patterns exhibit similar volatility, though somewhat moderated by the natural diversity in occupant behaviour. This

operational pattern results in low load factors (average/peak demand ratio) of approximately 0.35, indicating inefficient infrastructure utilisation.

The fixed threshold model produces more balanced load profiles with significantly reduced volatility. Peak demand periods are moderated through basic load shifting and storage utilization, improving the load factor to approximately 0.41. However, the model's static thresholds create distinctive operational patterns with clear transitions between normal operation, managed operation, and grid protection modes. These transition boundaries occasionally produce secondary demand peaks at threshold transition points, creating "stacking" effects as multiple systems respond simultaneously to threshold changes.

The active building model demonstrates the most significant transformation in load profiles, characterized by smoother demand transitions and more consistent utilization patterns. The building-specific threshold optimization eliminates the transition boundaries observed in the fixed threshold model, preventing secondary demand peaks. This approach achieves a load factor of 0.48, representing a 37% improvement over the baseline scenario. The smoother load profile directly contributes to improved operational efficiency.

Statistical analysis of demand variability further highlights differences between control approaches. The coefficient of variation in hourly demand reduced from 0.68 in the baseline scenario to 0.41 in the active building model, representing a 40% improvement in demand stability. This more consistent demand pattern supports both improved system efficiency and enhanced grid stability.

Figure 7.2 presents annual load-duration curves for the baseline (red), fixed-threshold (green) and active-building (blue) control strategies. The baseline exhibits the steepest

initial segment, with instantaneous demand exceeding 450 kW_e for the top 1 % of hours. Fixed thresholds cut the absolute peak by ≈ 15 %, but secondary 'shoulder' peaks appear around the 5–15 % percentile where devices simultaneously switch regime. The active strategy achieves the flattest curve: peaks fall by ≈ 25 % relative to baseline, and demand between the 60th and 90th percentiles rises by 10–25 kW_e, evidencing deliberate valley-filling. Overall, the slight differences in area under the curves reflect the 1.3% increase in total energy consumption for the active building model compared to baseline, while achieving 19% peak demand reduction.

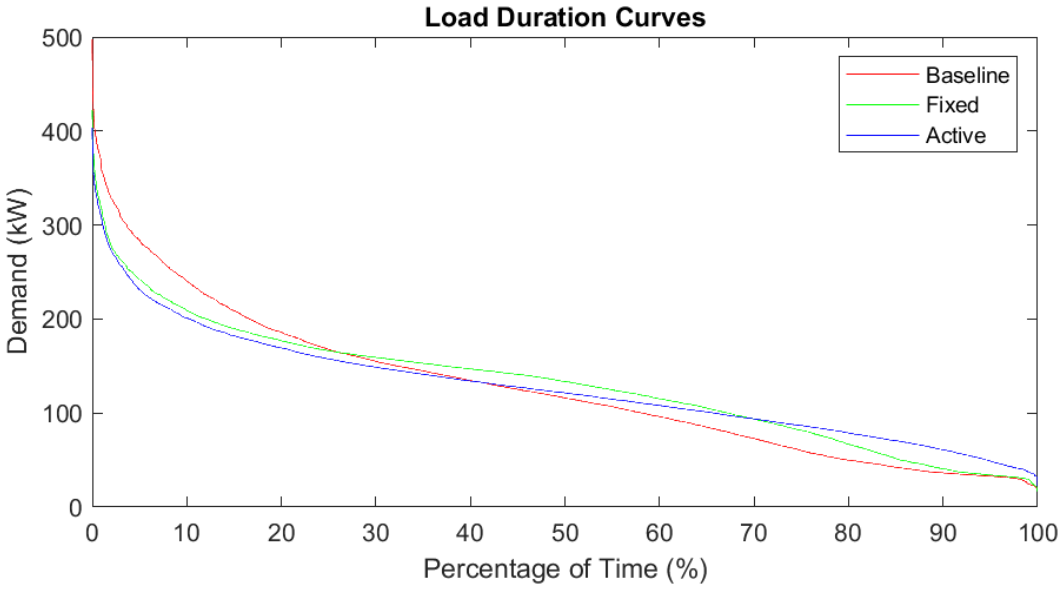


Figure 7.2: Load duration curves comparing baseline, fixed threshold, and active control strategies.

7.2.3 Storage Utilisation Patterns

TES utilization patterns vary significantly between control approaches, with distinct implications for system performance and flexibility. Detailed examination of storage cycling, temperature maintenance, and charging efficiency reveals important operational differences across the scenarios.

In the baseline scenario, TES remained effectively unused, as the system operated HPs directly in response to heating demand without consideration of storage potential. This approach resulted in increased cycling of HPs and higher instantaneous electrical demands during peak heating periods.

The fixed threshold model implemented basic storage utilisation, achieving approximately 1.2 storage cycles per day during winter operation. Storage charging occurred primarily during overnight periods when network demand fell below the lower threshold (T1=140 kW_e). This approach successfully shifted some demand away from peak periods but demonstrated limited responsiveness to efficiency opportunities. TES charge showed gradual decline during peak demand periods.

The active building model demonstrated significantly more sophisticated TES utilisation, achieving 1.8 daily storage cycles during winter operation, a 50% increase over the fixed threshold approach. The improved performance stemmed from more intelligent charging strategies that considered both immediate needs and predicted future demands.

Seasonal analysis shows storage utilization varying from over 30% during winter months to approximately 23% during summer. This pattern reflects both higher heating demands during winter and the greater flexibility requirements to manage peak demand periods. The effective integration of storage with optimized heat pump control demonstrates significant potential for enhancing system flexibility while maintaining effective heat provision.

Figure 7.3 displays storage state over time for different building categories, illustrating the utilisation patterns across the monitored period. The graph shows the cyclical nature of storage operation, with distinct charging and discharging periods visible

throughout the day. Different building categories display varying storage patterns based on their demand characteristics and thermal properties, with larger buildings (Category 3 and 4) demonstrating more pronounced storage cycles due to their greater thermal mass and storage capacity. This visualization effectively captures the operational dynamics of thermal storage and its response to both building demands and control strategies.

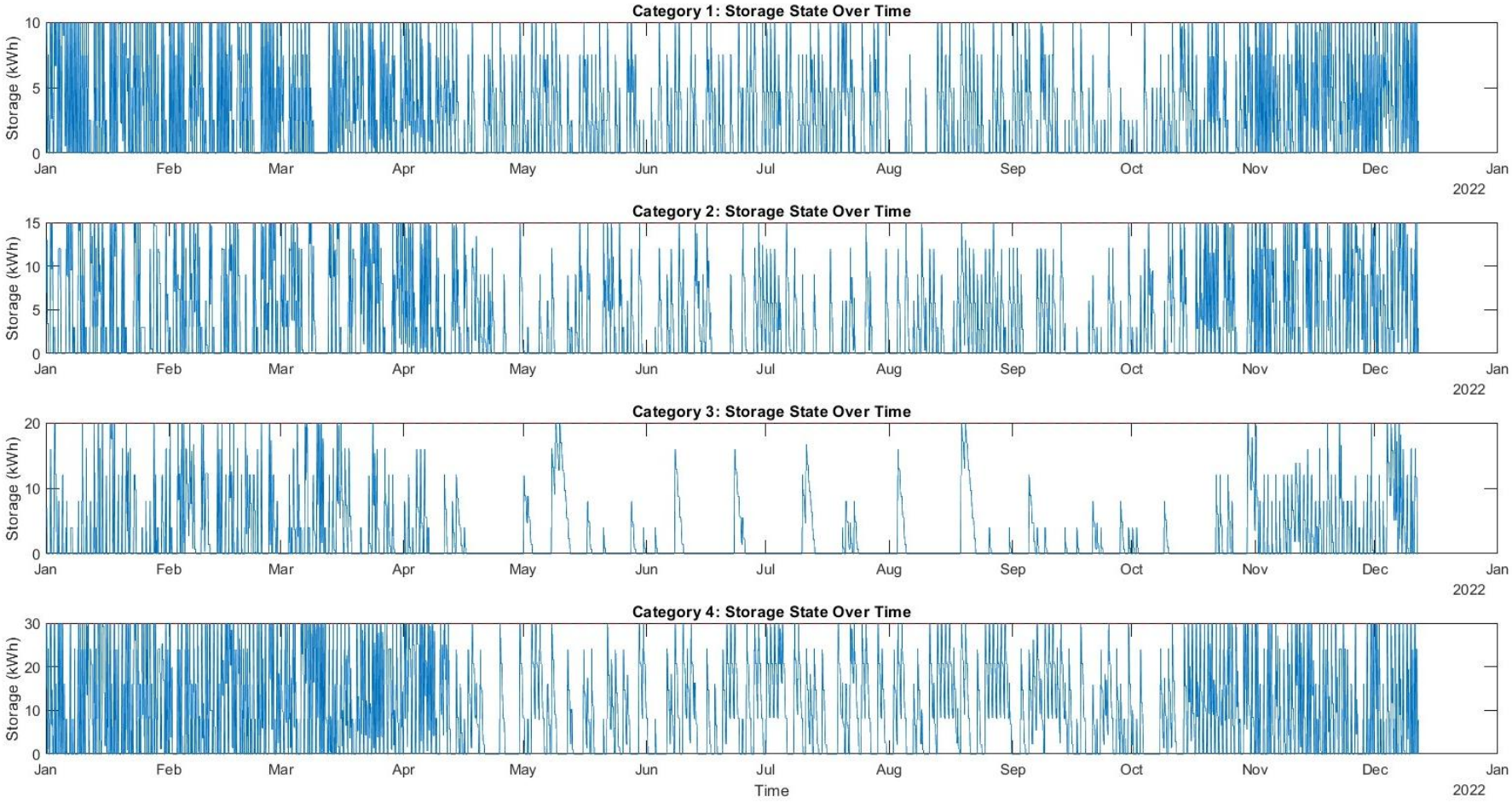


Figure 7.3: State of charge profiles for four dwelling categories over a full year.

7.3 Grid Integration Assessment

7.3.1 Network Loading Analysis

The integration of HPs at community scale introduces significant changes to electrical network loading patterns. Analysis of the Trent Basin LV substation reveals substantial variations in loading characteristics across the three control scenarios, with important implications for network capacity requirements and system stability.

Prior to heat pump integration, the LV substation experienced peak demands of approximately 300 kW_e during winter evenings, primarily driven by domestic electrical consumption. These peaks typically occurred between 17:00 and 20:00, aligning with periods of high occupancy and activity. Base load remained relatively stable at 45-50 kW_e, representing background appliance loads and standby consumption.

The baseline scenario substantially transformed these loading patterns, increasing peak demands to 500 kW_e—a 67% increase over pre-HP conditions. These peaks shifted primarily to morning periods (06:00-09:00), when simultaneous HP activation for morning heating pickup coincided with increasing domestic electricity consumption. This scenario demonstrated clear potential for network capacity exceedance during extended cold weather periods, particularly as HP efficiency decreases with lower ambient temperatures.

The fixed threshold model moderated these loading impacts, reducing maximum demands to approximately 420 kW_e. This 16% improvement over baseline operation stemmed from basic load shifting and TES utilization governed by the fixed thresholds. However, the system demonstrated limited adaptability to extreme conditions, maintaining similar thresholds regardless of ambient temperature or

demand patterns. During extended cold periods, this limitation resulted in gradual increases in peak demand as storage capacity became fully utilized.

The active building model achieved the most significant improvement in network loading patterns, limiting maximum demands to 400 kW_e—a 20% reduction from baseline operation. This improvement stemmed from sophisticated coordination of HP operation and storage utilization across the community. The model's dynamic threshold optimization enabled adaptation to varying weather conditions and demand patterns, preventing the demand clustering observed in simpler control approaches.

Analysis of substation loading duration curves reveals further distinctions between control approaches. The percentage of time that substation loading exceeded 300 kW_e dropped from 16% in the baseline scenario to 9.6% in the fixed threshold model and 7.1% in the active building model. This reduction in high-load duration has significant implications for network capacity planning and infrastructure utilization.

Figure 7.4 illustrates annual hours exceeding various demand thresholds across the three scenarios. The chart clearly shows the progressive reduction in high-demand events moving from baseline through fixed threshold to active building model. Also, it is notable is that active building model almost eliminate the events exceeding 400 kW_e, while these occurred 25 times in the baseline scenario. This visualization effectively captures the improved load distribution achieved through sophisticated control strategies and their potential impact on network management.

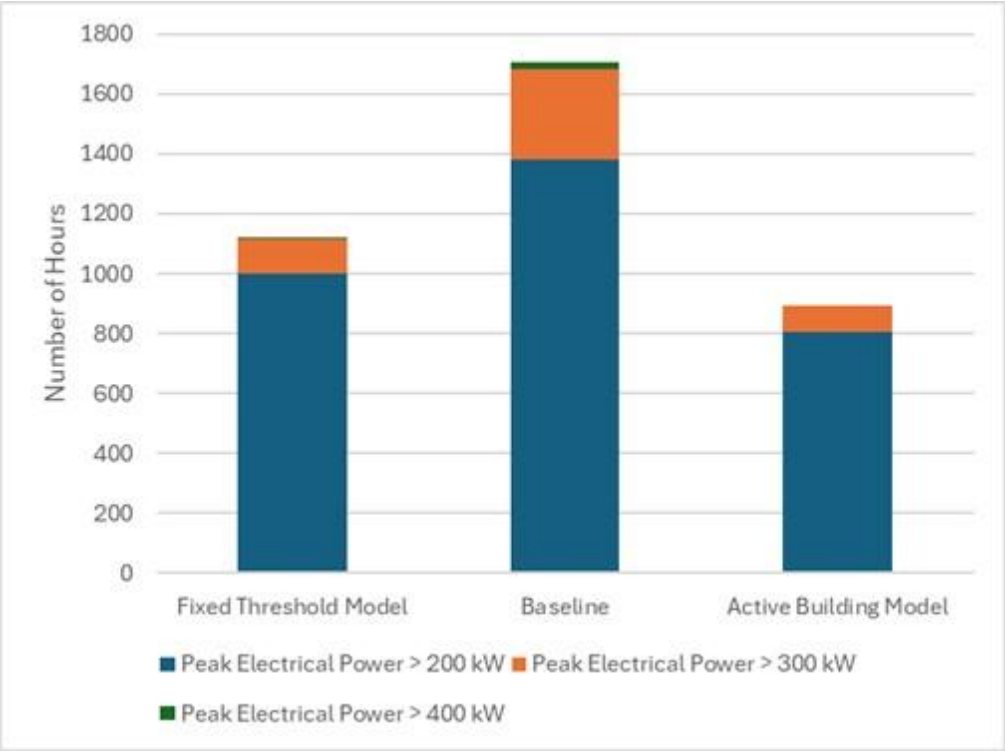


Figure 7.4: Annual number of hours exceeding 200 kW_e, 300 kW_e, and 400 kW_e peak electrical power for three scenarios.

7.3.2 Demand Rate of Change

The rate of change in electrical demand emerges as a critical factor for network stability and equipment longevity. Rapid fluctuations in loading can stress network components while creating potential power quality issues. Analysis of demand dynamics at the Trent Basin substation revealed significant variations in ramp rates across control scenarios.

The baseline scenario exhibited highly volatile demand patterns with maximum ramp rates reaching 280 kW_e per hour during winter morning periods. These rapid increases stemmed from simultaneous HP activation as heating systems recovered from night setback temperatures. The distribution of demand rate changes, as shown in Figure 7.5, demonstrates a wide spread ranging from -150 to +200 kW_e/hour, with the majority of events concentrated between -50 and +50 kW_e/hour. This broad

distribution reflects the uncoordinated nature of HP operation, creating unpredictable loading variations that challenge network management.

The fixed threshold model achieved moderate improvement in demand stability, with the distribution showing similar overall shape but reduced extreme events. Maximum ramp rates decreased to approximately 180 kW_e per hour, representing a 36% improvement over baseline operation. The distribution remains relatively wide, indicating that while the threshold-based control approach limited some rapid transitions, it could not fundamentally alter the stochastic nature of demand changes. The static thresholds occasionally created secondary effects as multiple systems responded simultaneously to threshold crossings, contributing to continued volatility.

The active building model demonstrated the most significant improvement in demand stability. The distribution of rate changes shows marked concentration around zero, with substantially reduced frequency of extreme ramp events. Maximum ramp rates were limited to approximately 100 kW_e per hour—a 64% reduction from baseline operation. This dramatic improvement stems from the model's sophisticated coordination of HP operation and storage utilisation, which effectively distributes demand changes over longer periods. The building-specific threshold optimization eliminated the synchronized transitions observed in the fixed threshold model, creating smoother aggregate demand patterns.

Statistical analysis of demand volatility further highlighted differences between control approaches. The standard deviation of hourly demand changes increased from 53.37 kW_e in the baseline scenario to 54.64 kW_e in the fixed threshold model (a slight increase due to threshold-induced clustering) and decreased to 42.55 kW_e in the active building model. This 20.27% reduction in demand volatility represents an

improvement in system behaviour, with implications extending beyond immediate operational benefits.

The narrower distribution of demand changes under active control reduces mechanical and thermal stress on network components. Transformers experience less frequent thermal cycling, potentially extending operational lifetimes and reducing maintenance requirements. Cable systems benefit from more stable current flows, minimizing insulation degradation associated with rapid thermal fluctuations. These infrastructure benefits complement the immediate operational advantages of reduced demand volatility.

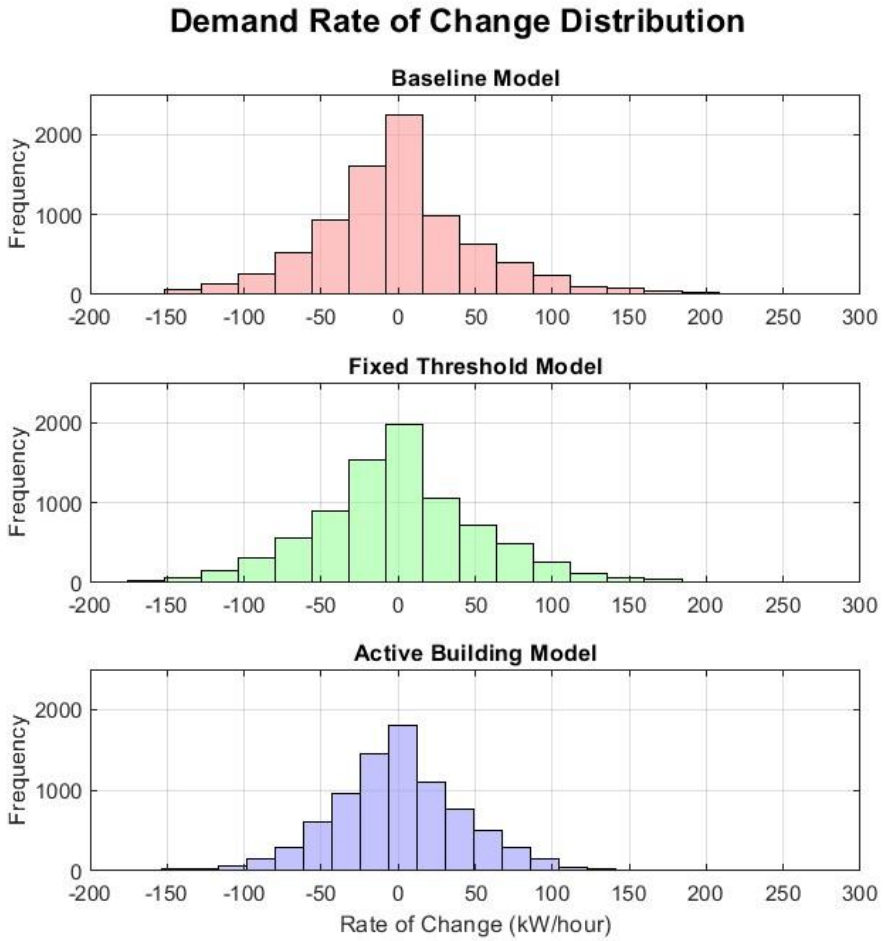


Figure 7.5: Histogram of demand rate of change under baseline, fixed threshold, and active control strategies.

Figure 7.5 presents the demand rate of change distribution across the three scenarios through separate histograms, illustrating the progressive improvement in demand stability. The baseline scenario exhibits the widest distribution with frequent occurrences of extreme ramp rates. The fixed threshold model shows moderate improvement with some reduction in extreme events. The active building model demonstrates a substantially narrower distribution concentrated around zero, indicating fundamentally more stable demand transitions. This visualization effectively captures the significant improvements in demand stability achieved through advanced control strategies and their potential benefits for network operation.

7.3.3 Coincidence Factors

HP coincidence factors, representing the proportion of systems operating simultaneously at any given time, provide crucial insight into coordination effectiveness and network impact. Analysis of coincidence patterns across the three scenarios reveals substantial differences in operational distribution and the effectiveness of different control approaches in managing collective system behaviour.

The baseline scenario exhibits a distinctive bimodal distribution of coincidence factors, as clearly shown in Figure 7.6. The distribution shows pronounced peaks at both extremes, with frequencies of approximately 3,800 hours at coincidence factor 0 (few or no systems operating) and 4,500 hours at coincidence factor 1 (most or all systems operating simultaneously). This bimodal pattern reflects the fundamental challenge of uncoordinated HP operation: systems respond independently to similar environmental triggers, creating periods of either minimal operation or near-complete synchronization. The high frequency of coincidence factors approaching unity directly

contributes to the severe peak demand challenges observed in this scenario, as the majority of HPs activate simultaneously during cold morning periods.

The fixed threshold model demonstrates moderate improvement in coincidence distribution, though the fundamental bimodal characteristic persists. The frequency of extreme coincidence factors reduces, with approximately 3,400 hours at coincidence factor 0 and 4,200 hours at coincidence factor 1. While this represents meaningful progress, the predetermined threshold values create common operational boundaries that continue to synchronize system behaviour. When network demand approaches these thresholds, multiple HPs respond similarly, maintaining clustering effects that limit the effectiveness of this approach in distributing operational patterns.

The active building model achieves a fundamental transformation in coincidence distribution, effectively eliminating the problematic bimodal pattern. The distribution becomes remarkably uniform across the middle range (0.2-0.8), with frequencies of only 1,700 hours at coincidence factor 0 and 700 hours at coincidence factor 1. This reduction in extreme coincidence events—an 84% decrease in hours with coincidence factor exceeding 0.9—stems from the building-specific threshold optimization approach. By assigning individualized operational thresholds to each building based on its characteristics and predicted demand patterns, the model creates naturally staggered operation that prevents the synchronization effects observed in simpler control approaches.

The transformation from bimodal to uniform distribution has profound implications for network operation. During peak demand periods, the average coincidence factor reduces from 0.76 in the baseline scenario to 0.68 in the fixed threshold model, and further to 0.45 in the active building model—a 41% overall improvement. This

reduced coincidence directly translates to lower instantaneous electrical demands, as the load from multiple HPs distributes more evenly across operational periods rather than concentrating during common activation times.

The mechanisms driving this improvement relate to the diversity of optimised thresholds across the buildings. Analysis of threshold distributions reveals that buildings naturally adopt different operational boundaries based on their thermal characteristics, storage capacities, and historical demand patterns. This diversity ensures that as network conditions change, buildings respond at different points rather than simultaneously, creating a cascade of responses that smooths aggregate demand rather than creating step changes.

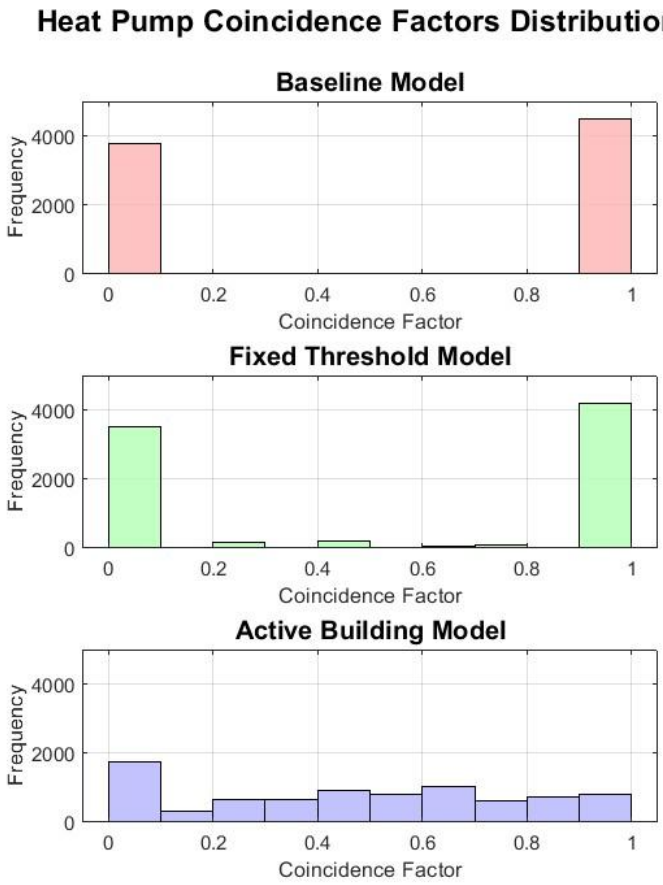


Figure 7.6: Distribution of heat pump coincidence factors under different control strategies.

Figure 7.6 illustrates these differences in operational coordination through separated visualizations of each scenario. The contrast between the baseline's bimodal distribution—indicating poor coordination with frequent synchronization—and the active model's uniform distribution—demonstrating effective load distribution—provides clear evidence of the transformative potential of sophisticated control strategies. The fixed threshold model's intermediate position highlights both the benefits and limitations of static coordination approaches, achieving some improvement while maintaining residual synchronization effects that limit ultimate performance.

These coincidence factor improvements represent one of the most significant achievements of the active building model, demonstrating that intelligent coordination can fundamentally alter the collective behaviour of distributed energy resources. The reduction in operational synchronization not only supports immediate grid stability objectives but also enables higher penetration of HP systems within existing infrastructure constraints, advancing community-scale decarbonisation goals.

7.4 Environmental Impact Assessment

7.4.1 Carbon Intensity Analysis

The carbon emissions impact of different control strategies provides insight into their environmental performance, though carbon optimization was not explicitly incorporated in the control algorithms. The analysis utilised real-time grid carbon intensity data from the National Grid ESO Data Portal to evaluate how operational patterns influenced overall environmental impact.

Figure 7.7 demonstrates total HP-related carbon emissions across the three control scenarios. The active building model achieves the most favourable environmental performance with 44.9 tons CO_2 annually, representing a 5% reduction compared to the baseline scenario (47.1 tons CO_2). Notably, the fixed threshold model shows higher emissions (48.9 tons CO_2, +3.8% increase), reflecting the environmental penalty associated with its increased energy consumption despite achieving peak demand reduction.

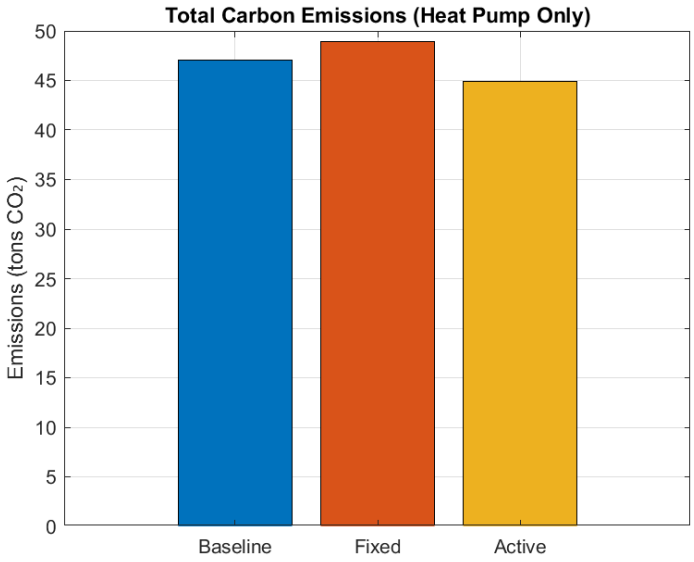


Figure 7.7: Total carbon emissions across control scenarios

Figure 7.8 illustrates emissions intensity (g CO_2 per kWh of heat delivered) across the scenarios. The active building model demonstrates the lowest emissions intensity at 53.4 g CO_2/kWh compared to 56.0 g CO_2/kWh for the baseline scenario, indicating improved operational efficiency in carbon terms. This 5% improvement appears to result from the peak demand optimization scheduling HP operation during periods that coincidentally align with lower grid carbon intensity, rather than explicit carbon-aware control.

The temporal alignment between HP operation and grid carbon intensity emerges as an important factor influencing environmental performance. The active building model's daily optimization approach enables some operational flexibility that can inadvertently coincide with periods of lower carbon intensity, particularly during off-peak hours when both electrical demand and carbon intensity tend to be reduced.

These carbon performance metrics should be considered within the context of ongoing grid decarbonisation. As the UK electricity system continues transitioning towards renewable energy sources, absolute carbon emissions from HP operation will decrease significantly, whilst maintaining the relative performance advantages demonstrated by the active building approach.

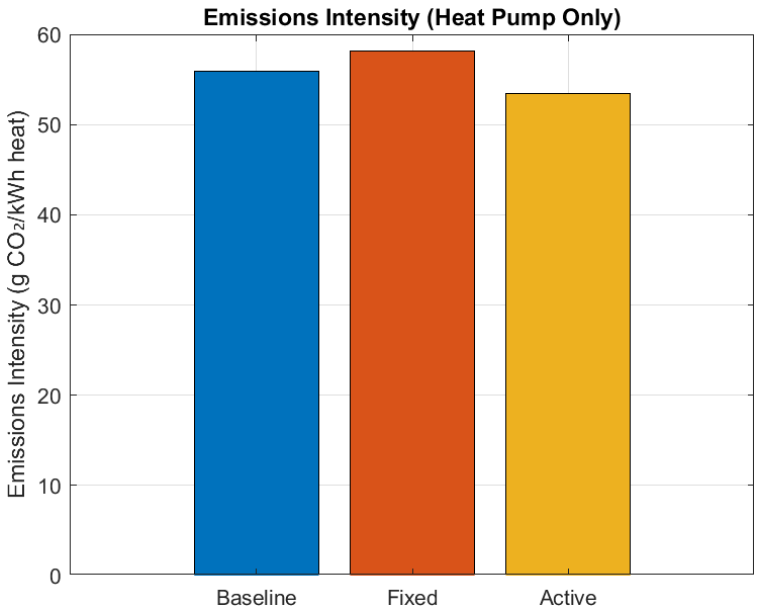


Figure 7.8: Emissions Intensity Across Control Scenarios

7.4.2 Seasonal Carbon Performance

Monthly carbon emissions patterns reveal seasonal variations in environmental impact across the control scenarios. All scenarios demonstrate highest emissions during

winter months (particularly January) when heating demand peaks, with progressive reductions through spring and minimum emissions during summer months (June-August).

The active building model achieves modest emissions improvements during most months compared to baseline operation. The largest improvements occur during January, whilst some months show minimal differences between scenarios. These variations reflect the indirect alignment between peak demand minimisation and periods of lower carbon intensity, as carbon optimisation was not explicitly incorporated in the control algorithm.

Figure 7.9 displays monthly carbon emissions across the three scenarios, illustrating seasonal patterns throughout the year. The chart shows winter peaks in emissions across all scenarios, with the active building model demonstrating marginally lower emissions in most months. Whilst the differences are modest, and statistical significance cannot be assessed with the deterministic modelling approach; these results indicate that peak demand optimisation can provide secondary environmental benefits beyond the primary grid stability objectives.

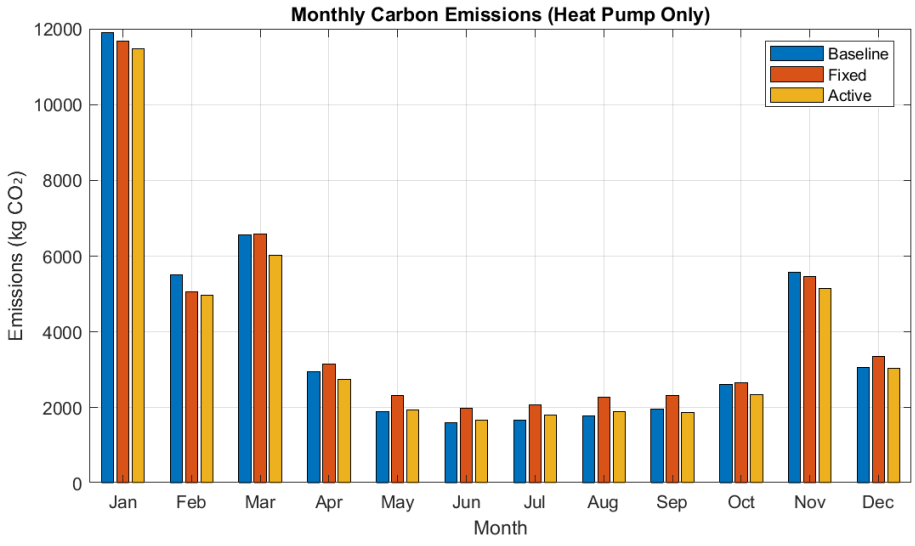


Figure 7.9: Monthly Carbon Emissions Across Control Scenarios

7.5 Operational Economic Analysis

7.5.1 Electricity Tariff Impacts

The economic performance of community-scale HP systems demonstrates significant variability across different electricity pricing structures, with important implications for decarbonisation strategies. This analysis examines three distinct electricity pricing scenarios (presented in section 5.4.4) applied to the Trent Basin implementation, revealing how tariff structures interact with control strategies to influence operational costs.

Comparative Cost Performance

Figure 7.10 presents annual HP electricity costs across the three control scenarios under each tariff structure. The visualization reveals differences in economic outcomes, with varying implications for implementation strategies.

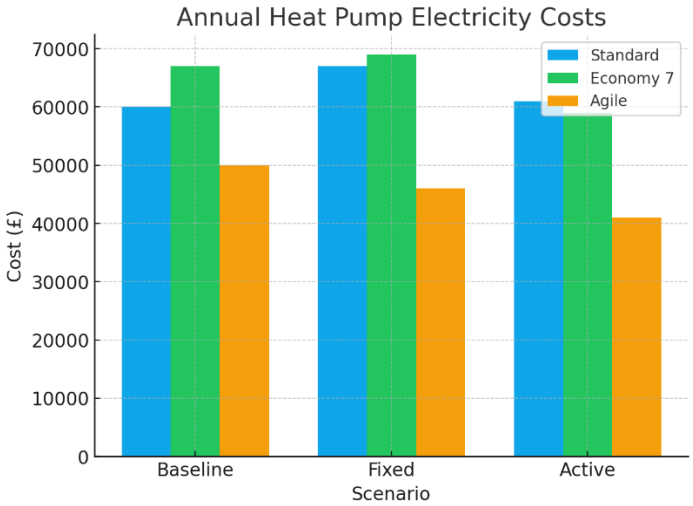


Figure 7.10: Annual electricity costs for HP operation under three tariff types (Standard, Economy 7, and Agile) across control scenarios.

Under the standard rate tariff, economic performance directly correlates with total energy consumption. The fixed threshold model demonstrates the highest costs (£66,160) due to its 10% increased energy consumption compared to baseline

(£59,675). The active building model shows marginally higher costs (£60,807) than baseline despite achieving substantial peak reduction, reflecting the limited economic value of load shifting under flat-rate pricing.

The Economy 7 tariff fundamentally alters this relationship, creating distinct incentives for overnight storage charging. While the fixed threshold model (£68,622) continues to demonstrate higher costs than baseline (£66,967) due to higher total consumption, the active building model achieves cost reduction of (£58,897) through intelligent temporal distribution of energy usage. This model effectively exploits the binary pricing differential by concentrating storage charging during the seven-hour off-peak window while maintaining effective heat provision throughout the day.

The Dynamic (Agile) tariff enables the most substantial economic benefits for both advanced control strategies. The fixed threshold model achieves modest cost reduction (£45,218) compared to baseline (£49,777), while the active building model demonstrates the most significant improvement (£41,068).

This superior economic performance stems from the model's peak demand minimization strategy, which indirectly aligns operational patterns with favourable tariff periods. While the model does not directly optimize for cost, its focus on reducing peak electrical demand and improving operational efficiency creates load shifting patterns that benefit from time-varying electricity pricing structures.

Cost Savings Analysis

Figure 7.11 quantifies these relationships by presenting percentage cost savings compared to baseline for each control strategy across tariff structures.

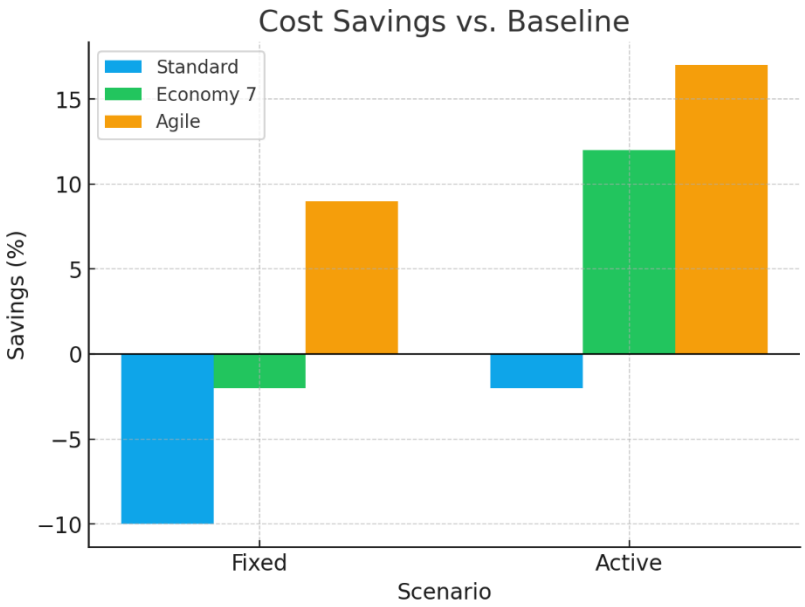


Figure 7.11: Percentage cost savings relative to the baseline scenario across different tariff types.

Under the standard rate tariff, the fixed threshold model incurs increased costs of approximately 10.9% despite achieving peak reduction, while the active building model shows a modest 1.9% cost increase. This relationship fundamentally transforms under time-varying tariffs, with the active building model achieving cost reductions of 12.1% under Economy 7 and 17.5% under Agile pricing. The fixed threshold model similarly demonstrates improved economic performance under Agile pricing (9.2% savings) but continues to underperform under Economy 7 (-2.5%).

These divergent outcomes highlight an important relationship between grid-focused optimization strategies and electricity pricing structures. While the active building model optimizes solely for peak demand reduction without considering price signals, the resulting operational patterns create economic benefits under time-varying tariffs. This demonstrates that grid stability objectives can align favourably with cost considerations, though this alignment is coincidental rather than designed.

These findings suggest that while the optimization strategy does not directly respond to price signals, electricity tariff design could potentially enhance the economic case

for grid-beneficial heat pump operation. Time-varying tariffs that align high prices with peak demand periods would strengthen the economic benefits of peak reduction strategies, creating additional incentives for deployment of sophisticated control approaches that primarily target grid stability objectives.

7.5.2 Building Type Economic Analysis

Economic performance analysis across building categories under agile pricing reveals how peak demand optimisation strategies create varying economic outcomes across different system configurations. Figure 7.12 illustrates these economic effects, showing cost reductions ranging from 11.3% to 21.3% annual savings as an indirect consequence of grid-focused optimisation.

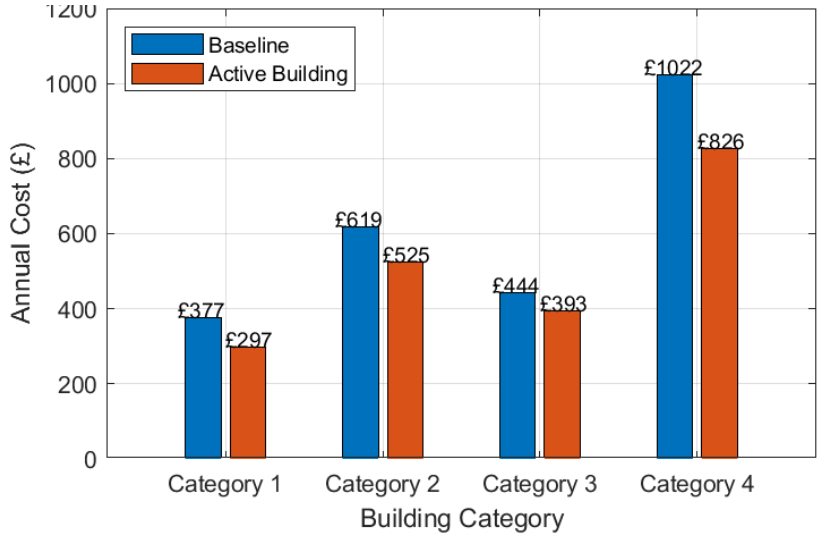


Figure 7.12: Annual HP electricity costs by building category under baseline and active control strategies.

Category 1 buildings achieve the highest economic benefit at 21.3% savings (£377 to £297 annually). Their 5kW$_e$ HPs and 10kWh TES systems, when optimised for peak demand reduction, create operational patterns that fortuitously align well with agile tariff structures, effectively avoiding high-price periods through load shifting activities.

Category 2 buildings (6kW$_e$ HPs, 15kWh TES) achieve 15.2% savings (£619 to £525), whilst Category 3 buildings (8kW$_e$ HPs, 20kWh TES) show 11.3% savings (£444 to £393). The variation in economic outcomes across these categories reflects how different equipment configurations respond to peak demand optimisation under varying demand patterns.

Category 4 buildings demonstrate strong economic performance with 19.1% savings (£1022 to £826). Their 16kW$_e$ HPs and 30kWh TES systems enable extensive load shifting for peak demand management, which coincidentally creates favourable alignment with agile pricing periods.

The non-linear pattern of economic benefits across categories illustrates that peak demand optimisation strategies do not uniformly translate to economic advantages. Categories 1 and 4 achieve the strongest economic outcomes, suggesting that their respective system configurations create load shifting patterns that better coincide with agile tariff low-price periods.

These findings demonstrate that whilst the active building model's grid-focused optimisation delivers economic co-benefits under dynamic pricing, the magnitude varies significantly with system configuration. The economic advantages emerge as beneficial side effects of peak demand reduction rather than direct optimisation targets, highlighting the potential value alignment between grid stability objectives and cost-effective operation under appropriate tariff structures.

7.6 Sensitivity Analysis and Robustness Assessment

Following the sensitivity analysis framework established in Section 4.5.3, this section evaluates the robustness of the Active Building Model under parameter uncertainties.

The analysis addresses a critical limitation of the primary simulations—the assumption of perfect parameter values and forecasting—by systematically examining performance degradation under realistic variations. The assessment focused on the coldest week of the year as a worst-case scenario, when system stress is highest and control strategy effectiveness most critical.

7.6.1 Impact of Forecast Error on Performance

The impact of forecast uncertainty on model performance represents a crucial real-world consideration, as the primary simulations assumed last year data as proxy for the forecast of the 24-hour ahead of weather conditions and demand patterns. Figure 7.13 demonstrates the Active Building Model's peak reduction benefits under increasing levels of forecast error.

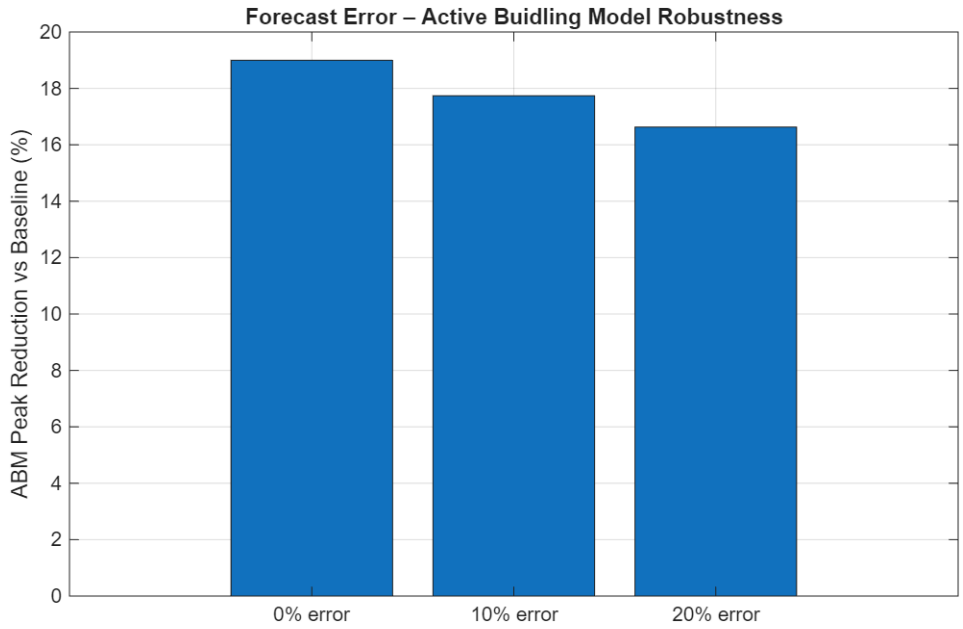


Figure 7.13: Impact of forecast error on Active Building Model peak reduction benefits relative to baseline scenario

The results reveal a gradual degradation in performance as forecast accuracy decreases. Starting from approximately 19% peak reduction with perfect forecasting,

the benefit declines to 17.7% at 10% forecast error and 16.5% at 20% forecast error. This represents a reduction of only 2.5 percentage points across the full range of tested forecast uncertainties.

Importantly, weather forecasting for 24-hour ahead predictions typically achieve accuracy within 10-15% for temperature and solar radiation in the UK climate. The demonstrated maintenance of approximately 17% peak reduction benefits at 20% forecast error therefore indicates robust performance under realistic operational conditions. This finding directly addresses concerns regarding the forecasting assumption, confirming that the Active Building Model's benefits persist under practical implementation constraints.

The relatively modest performance degradation can be attributed to the model's daily optimization approach, which provides opportunities for correction and adaptation. Even with imperfect forecasts, the building-specific threshold optimization continues to distribute control actions effectively across the community, preventing the synchronized operation that characterizes uncontrolled scenarios.

7.6.2 Comparative Parameter Sensitivity

Beyond forecast uncertainty, the sensitivity analysis examined three additional parameters critical to system performance: HP COP, heat demand levels, and thermal storage capacity. Figure 7.14 presents the comparative sensitivity of peak reduction benefits to ±20% variations in these parameters.

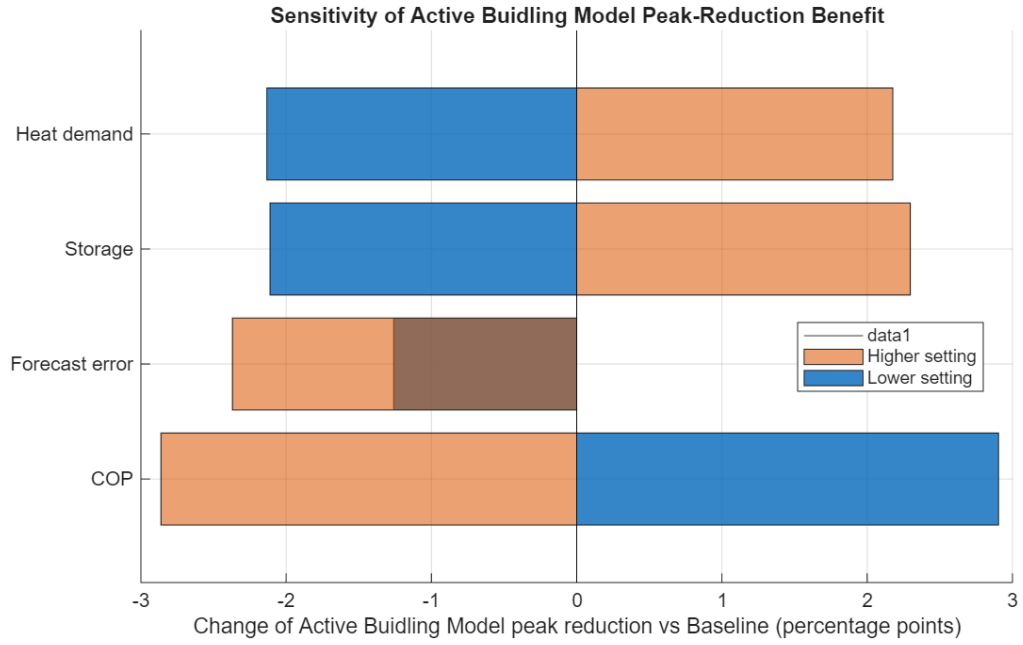


Figure 7.14:Sensitivity of Active Building Model peak reduction benefits to parameter variations

Table 7.1 summarizes the quantitative impacts of parameter variations on peak reduction performance:

Table 7.1: Quantitative sensitivity analysis results for Active Building Model performance

Parameter	Variation Tested	Model Peak Reduction (0% Variation)	Lower Setting Impact	Higher Setting Impact
Heat Pump COP	±20%	**19.0%**	**21.9%** (+2.9 pp)	**16.1%** (-2.9 pp)
Heat Demand	±20%	**19.0%**	**16.9%** (-2.1 pp)	**21.2%** (+2.2 pp)
Storage Capacity	±20%	**19.0%**	**16.9%** (-2.1 pp)	**21.3%** (+2.3 pp)
Forecast Error	0–20%	**19.0%**	**17.7%** (-1.3 pp) (10%)	**16.6%** (-2.4 pp) (20%)

pp = percentage points; positive values indicate improvement, negative values indicate degradation

The analysis reveals differential sensitivity across parameters, with important implications for system design and operation:

COP demonstrates manageable sensitivity, with ±2.9 pp. Lower COP (-20%) improves the peak reduction benefit to 21.9% (+2.9 pp), while higher COP (+20%) reduces the benefit to 16.1% (-2.9 pp). This result has important implications: when HPs operate at lower efficiency, they draw more electrical power for the same heat

output, making the peak demand problem more severe in the baseline scenario. Consequently, the Active Building Model's coordination and optimization strategies become even more valuable, delivering greater relative improvements. Conversely, when HPs operate at higher efficiency, the baseline peak demand is naturally lower, reducing the relative benefit achievable through optimization. This finding is particularly encouraging for real-world deployment, as it indicates that the control strategy delivers greatest value precisely when system efficiency is compromised whether due to extreme weather conditions, equipment degradation, or lower-specification HPs.

Heat Demand shows positive sensitivity to increased demand, with +20% variation improving peak reduction benefits to 21.2% (+2.2 pp), while -20% variation reduces benefits to 16.9% (-2.1 pp). Higher heat demand creates greater stress on the uncoordinated baseline system, amplifying the synchronized operation problems that the Active Building Model addresses. The optimization algorithm's ability to coordinate multiple buildings and utilize thermal storage becomes increasingly valuable as demand rises. This characteristic suggests the control strategy would be particularly beneficial during extreme weather events when heating demands peak.

Storage Capacity exhibits expected positive correlation with performance, with increased capacity (+20%) improving peak reduction to 21.3% (+2.3 pp) and decreased capacity (-20%) reducing benefits to 16.9% (-2.1 pp). Greater storage capacity provides additional flexibility for the optimization algorithm, enabling more effective load shifting and peak shaving. The symmetric response indicates a linear relationship between storage availability and achievable benefits within the tested range. Notably, even with reduced storage capacity, the system maintains good peak reduction benefits, confirming viability across diverse installation constraints.

Forecast Error shows progressive degradation with increasing uncertainty, from 17.7% peak reduction at 10% error (-1.3 pp) to 16.6% at 20% error (-2.4 pp). Unlike the other parameters which were tested symmetrically, forecast error represents a unidirectional degradation from the ideal case. The relatively modest impact demonstrates that the control strategy's core coordination mechanisms remain effective even with imperfect information.

7.6.3 System Robustness Under Combined Uncertainties

Across all tested parameter variations, the Active Building Model consistently delivered peak demand reductions between 16.1% and 21.9%, demonstrating robust performance under diverse conditions. The analysis reveals that the control strategy not only maintains benefits under adverse conditions but delivers greatest value when system challenges are most severe such as during low COP operation or high demand periods.

The consistency of positive benefits across all scenarios can be attributed to several factors. First, the building-specific optimization approach provides inherent adaptability, with threshold values adjusting to maintain performance under varying conditions. Second, the community-scale implementation creates diversity in system response, preventing single-point failures that might occur in centralized control approaches. Third, the daily optimization frequency enables continuous adaptation to changing conditions, compensating for parameter variations through adjusted control strategies.

7.6.4 Implications for Real-World Implementation

The sensitivity analysis provides crucial insights for practical deployment of the Active Building Model. The demonstrated robustness to forecast errors indicates that the control strategy can be implemented with standard weather forecasting services, maintaining approximately 17% peak reduction at realistic forecast error levels. This would still deliver substantial infrastructure benefits, potentially deferring network reinforcement requirements.

The inverse relationship between COP and peak reduction benefits has profound implications for deployment prioritization. Rather than requiring high-efficiency heat pumps to achieve benefits, the Active Building Model delivers greatest value with standard or even degraded equipment. This finding suggests that the control strategy could be particularly beneficial for social housing or retrofit projects where premium equipment may not be economically feasible.

The positive sensitivity to both heat demand and storage capacity provides clear guidance for system sizing. While the model maintains acceptable performance even with 20% reduced storage capacity (16.9% peak reduction), the improved performance with increased storage (21.3%) suggests that generous sizing would maximize benefits where feasible. The enhanced benefits under high demand conditions also indicate that the control strategy would be particularly valuable for buildings with variable occupancy or those in extreme climates.

These findings collectively demonstrate that the Active Building Model offers a robust approach to community-scale heat pump optimization, not only maintaining benefits across parameter uncertainties but delivering greatest value under challenging operational conditions.

7.7 Conclusions

The comprehensive multi-dimensional analysis of integrated HP-TES systems at Trent Basin demonstrates that sophisticated control strategies can effectively address several critical challenges in community-scale heat decarbonisation while maintaining practical implementation feasibility.

The energy performance evaluation revealed transformations in temporal distribution patterns while maintaining comparable energy consumption levels. The active building model achieved similar total electrical consumption to baseline operation (with only a 1.3% increase), while simultaneously implementing more efficient operational patterns. The achievement of 1.8 daily TES cycles with improved charging efficiency represents a significant advancement beyond the fixed threshold model's 1.2 cycles. This operational transformation demonstrates that coordinated TES utilization substantially enhances system performance beyond what could be achieved through simple technology deployment without advanced control.

The grid integration analysis revealed particularly significant infrastructure benefits. The 20% peak demand reduction fundamentally transforms the network impact profile of community-scale heat electrification. The improvement in demand volatility metrics—with demand rate of change decreasing from 45 kW_e/hour to 15 kW_e/hour—combined with improved coincidence factors (reduced from 0.76 to 0.45 during peak periods) suggests that sophisticated control strategies could enable higher HP penetration within existing network constraints than conventional analysis might predict. These findings have significant implications for network planning and infrastructure investment requirements.

Environmental assessment demonstrated that operational optimization provides modest carbon reduction benefits as a secondary outcome of peak demand management. The active building model improved emissions intensity from 56g CO_2/kWh to 53g CO_2/kWh heat delivered, with total HP-related emissions reduction of 5%. The observed seasonal variation in environmental performance reflects the coincidental alignment between peak demand avoidance and grid carbon intensity patterns, with the largest absolute improvements occurring during winter months when heating demands and potential optimization benefits are greatest. These carbon benefits emerge as an indirect consequence of peak demand optimization rather than explicit carbon-aware control, highlighting potential for future control strategies that incorporate both grid stability and environmental objectives.

The operational economic analysis revealed complex relationships between control strategies and tariff structures. While economic benefits remained modest under standard rate tariffs (1.9% improvement), they increased substantially under time-varying pricing regimes—reaching 12.1% under Economy 7 and 17.5% under Agile tariffs. This tariff sensitivity underscores the importance of appropriate market mechanisms to align economic incentives with grid stability objectives. The building-specific analysis demonstrated economic benefits across all property categories, though with variations corresponding to thermal characteristics and demand patterns.

The intersection of these performance dimensions reveals important synergies between optimization objectives. The active building model's ability to simultaneously improve energy efficiency, grid stability, environmental performance, and economic viability through coordinated control demonstrates that community-scale management of HP-TES systems offers advantages beyond the simple aggregation of individual building benefits. The emergence of collective system benefits through coordinated

operation suggests that heat decarbonization strategies should prioritize community-scale approaches over individual building optimization.

The sensitivity analysis confirms the Active Building Model's robustness, maintaining 16.1-21.9% peak reduction across all parameter variations. Notably, the control strategy delivers greatest benefits under adverse conditions achieving 21.9% reduction at degraded COP versus 16.1% at enhanced COP suggesting highest value for challenging retrofits and extreme weather scenarios. With only 2.4 pp degradation at 20% forecast error, the model demonstrates that its benefits persist under realistic operational uncertainties, validating its practical feasibility beyond idealized simulation conditions.

These findings collectively demonstrate that intelligent management of integrated HP-TES systems can effectively support heat decarbonisation while mitigating potential grid impacts. The improvement in multiple performance metrics achieved by the active building model, compared to both baseline and fixed threshold approaches, highlights the critical importance of sophisticated control strategies in maximizing the benefits of low-carbon heating technologies. These results provide compelling evidence that community-scale optimization represents a crucial element in achieving cost-effective, environmentally beneficial heat decarbonisation while maintaining robust grid operation.

Chapter 8

8. Discussion and Conclusions

8.1 Introduction

This research investigated the optimization of integrated HP and TES systems at community scale, focusing on reducing peak electrical demand, enhancing energy efficiency, and facilitating renewable energy integration. The Trent Basin development in Nottingham provided a practical case study comprising 76 residential properties of varying types connected to a single 800kW$_e$ low-voltage (LV) substation. This chapter summarizes the key findings, evaluates the completion of research objectives, and identifies directions for future work.

8.2 Summary of Key Findings

The development and evaluation of three distinct control approaches – baseline scenario, fixed threshold model, and active building model – revealed significant insights into community-scale heat decarbonization strategies.

The baseline scenario implemented conventional uncoordinated HP operation, where each system responded independently to building thermostats without consideration of grid conditions or storage optimization. This approach created peak electrical demands of 500kW$_e$ during winter periods, demonstrating potential for network capacity issues without sophisticated management. Load factors remained low at approximately 0.35, indicating inefficient infrastructure utilization.

The fixed threshold model introduced basic grid-aware control through static operational thresholds (T1=140 kW_e, T2=180 kW_e). This approach reduced maximum demands to 420 kW_e, representing a 16% improvement over baseline operation. However, the model unexpectedly increased total energy consumption by approximately 10%, as the static thresholds occasionally shifted operation to periods of lower efficiency, particularly during overnight storage charging. The fixed boundaries created distinctive operational patterns with clear transition points, occasionally producing secondary demand peaks when multiple systems responded simultaneously to threshold crossings.

The active building model implemented daily optimization of thresholds for each building based on predicted demand patterns and environmental conditions. This sophisticated approach achieved multiple performance improvements simultaneously:

- Peak electrical demand reduced to 400 kW_e (20% below baseline)
- Total energy consumption remained comparable with baseline (+1.3%)
- Carbon emissions reduced by 5%
- Load factor improved to 0.48 (37% above baseline)
- Demand rate of change reduced from 45kW_e/hour to 15kW_e/hour

The active building model effectively eliminated the transition boundaries observed in the fixed threshold model, preventing secondary demand peaks while maintaining smoother overall demand patterns. Building-specific optimization created naturally staggered operation as different buildings responded to individualized thresholds rather than common transition points, reducing coincidence factors from 0.76 to 0.45 during peak periods.

TES utilization proved particularly influential in system performance. The active building model achieved 1.8 storage cycles daily compared to 1.2 under the fixed threshold approach, while maintaining higher average storage temperatures with reduced electrical input.

Carbon emissions analysis, incorporating real-time grid carbon intensity data, demonstrated that operational optimization can enhance the environmental benefits of electrified heating. The active building model improved emissions intensity of heat delivery from 56g CO_2/kWh to 53g CO_2/kWh.

Economic performance varied significantly across tariff structures. Under standard rates, the active building model showed modest cost increase of 1.9% compared to baseline operation. However, under Economy 7 tariffs, it improved to 12.1%, and under Agile pricing, benefits reached 17.5%. Larger properties with greater thermal mass and storage capacity demonstrated more substantial benefits, with cost reductions exceeding 15% under time-varying tariffs.

Sensitivity analysis validated the robustness of these findings under parameter uncertainties. The Active Building Model maintained peak reduction benefits (16.1-21.9%) across ±20% variations in COP, heat demand, and storage capacity, as well as forecast errors up to 20%. Particularly the model's consistent performance under forecast uncertainty maintaining approximately 17% peak reduction at realistic error levels. These results confirm that the identified benefits represent achievable real-world improvements rather than theoretical optimums dependent on idealized conditions.

8.3 Completion of Research Objectives

This section evaluates how the research has addressed each of the 7 objectives outlined in Chapter 1, demonstrating the systematic completion of the research aims.

Objective 1: To collect and analyse comprehensive data from the Trent Basin case study

Comprehensive data collection was successfully implemented across multiple dimensions, including electricity consumption, environmental parameters, and building characteristics. The approach incorporated both directly measured variables through installed monitoring systems and derived parameters through modelling and simulation.

The data collection methodology faced challenges regarding heat demand measurement, as direct measurements of space heating and domestic hot water consumption were not consistently available across all properties. This limitation was addressed through development of validated heat demand models based on building characteristics and occupancy patterns, though this introduces some uncertainty in absolute demand values.

The granularity of electrical consumption data (hourly maximum, average, and cumulative values) provided sufficient temporal resolution for most analysis, though sub-hourly patterns could not be examined. This temporal limitation restricts understanding of very short-duration dynamics that might influence certain aspects of system operation.

Despite these constraints, the collected dataset provided a robust foundation for subsequent analysis, with sufficient coverage across building types, operational

periods, and environmental conditions to support valid conclusions regarding system performance.

Objective 2: To develop and validate heat demand models for residential buildings

Heat demand modelling was successfully implemented using the IES Intelligent Community Design (iCD) tool, with models developed for all 76 houses in the Trent Basin development. The modelling approach incorporated detailed building characteristics including construction properties, occupancy patterns, temperature setpoints, and internal gain profiles.

The validation process involved comparison against established benchmarks for UK residential buildings, including typical annual consumption values and characteristic demand patterns. While this approach confirmed broad consistency with expected performance, it could not validate absolute accuracy of hourly demand profiles due to limited availability of directly measured heat consumption data.

The modelling process involved several simplifications, including standardized occupancy profiles across building categories and consistent temperature setpoints. These simplifications likely reduced the diversity of demand patterns compared to real-world variation, potentially affecting the magnitude of coincidence effects observed in the simulation.

Despite these limitations, the validated demand models established credible baseline requirements for system sizing and control strategy development, with temporal patterns that align with established understanding of residential heating behaviour.

Objective 3: To design an advanced simulation model integrating HPs and TES

The development of an advanced simulation model progressed through multiple implementation phases, starting with commercial digital twin software and culminating in a custom MATLAB framework capable of implementing sophisticated control algorithms. This progression addressed limitations identified in the commercial tools while enabling more detailed control strategy evaluation.

The model implementation incorporated several innovative elements, including temperature-dependent heat pump performance based on manufacturer specifications, flexible thermal storage representation, and building-specific control optimization capabilities. These components were integrated within a framework that maintained computational feasibility while enabling detailed analysis of community-scale interactions.

Certain simplifications were necessary to maintain model tractability, including simplified representation of thermal dynamics within storage systems, abstracted building thermal response characteristics, and idealized control implementation without communication delays or sensing errors. These simplifications represent valid modelling compromises given the community-scale focus of the research.

The resulting simulation framework successfully supported detailed investigation of different control strategies while maintaining realistic representation of system components and constraints, fulfilling the core requirements of this research objective.

Objective 4: To conduct scenario analysis comparing performance of different control strategies

Comprehensive scenario analysis was conducted across three distinct control approaches, examining performance across multiple metrics including energy

consumption, peak demand, carbon emissions, and economic outcomes. The structured comparison methodology enabled systematic evaluation of performance differences while maintaining consistent boundary conditions across scenarios.

The analysis revealed unexpected findings regarding the fixed threshold model, where peak demand reduction was achieved at the cost of increased energy consumption. This outcome highlights the value of multi-dimensional performance assessment beyond single objectives, demonstrating the research methodology's capacity to reveal complex system behaviors and potential trade-offs.

The scenario implementation incorporated realistic operational constraints, including heat pump cycling limitations, storage charging restrictions, and effective heat provision requirements. This approach ensured that performance differences reflected practically achievable outcomes rather than theoretical ideals.

The comparative analysis conclusively demonstrated the significant advantages of sophisticated control strategies while highlighting important limitations of simplified approaches, effectively fulfilling this research objective.

Objective 5: To evaluate model performance under various operational conditions

The research systematically evaluated control strategy performance across varying operational conditions, including seasonal changes, different building types, and varying demand patterns. This comprehensive assessment confirmed the robustness of the active building model across diverse contexts, supporting potential for widespread implementation.

The analysis examined performance during critical extreme periods, including the coldest week of January 2022, confirming reliable operation when heating demands

peaked. This stress-testing approach validated the control strategy's capability to maintain effective performance under challenging conditions when grid impacts would be most pronounced.

The evaluation across different building categories revealed consistent benefits across all property types, though with varying magnitudes depending on thermal characteristics and demand patterns. This finding demonstrates the adaptability of the control approach across heterogeneous housing stock, an important consideration for practical implementation.

While the evaluation covered a wide range of conditions, it was necessarily limited to the specific climate characteristics of the Trent Basin location during the 2022 operational period. More extreme weather events or different regional contexts might present additional challenges not fully captured in this analysis.

Objective 6: To assess impact on LV networks and grid stability

The research provided detailed assessment of grid integration impacts across multiple network stability metrics, revealing significant benefits for infrastructure operation under optimized control. The analysis extended beyond simple peak reduction to examine critical grid stability factors including demand volatility, coincidence factors, and load duration characteristics.

The identified improvements in demand rate of change (from 45 kW_e/hour to 15 kW_e/hour) and coincidence factors (from 0.76 to 0.45) demonstrate the potential for fundamental transformation of network impact profiles beyond what might be achieved through simple capacity management approaches.

The analysis was conducted at the substation level rather than incorporating detailed power flow modelling of the distribution network. While this approach effectively

captured aggregate loading impacts, it could not evaluate potential location-specific issues such as voltage variations or phase imbalances that might occur at different points within the distribution network.

Despite this limitation, the assessment provided robust evidence of significant potential for enhanced network stability and higher heat pump penetration within existing infrastructure constraints, substantively fulfilling this research objective.

Objective 7: To evaluate techno-economic feasibility and environmental benefits

Comprehensive techno-economic and environmental assessment was conducted across the three control scenarios, incorporating multiple economic frameworks and real-time carbon intensity data. This multi-dimensional approach revealed important relationships between tariff structures, control strategies, and performance outcomes that would not be apparent from simplified analysis.

The economic evaluation identified significant tariff sensitivity, with benefits ranging from modest improvements under standard rates to substantial advantages under time-varying structures. This finding highlights the crucial role of market mechanisms in aligning economic incentives with system optimization objectives.

The environmental assessment incorporated real-time grid carbon intensity data, enabling more sophisticated evaluation of emission impacts than fixed emission factor approaches. This methodology revealed important temporal relationships between system operation and grid carbon intensity that significantly influenced overall environmental performance.

While the assessment focused primarily on operational aspects, it did not incorporate full lifecycle analysis of system components or detailed capital cost optimization. These additional dimensions would provide further insight into comprehensive

sustainability and economic performance beyond the operational focus of this research.

Despite these constraints, the evaluation provided substantive evidence regarding techno-economic feasibility and environmental benefits, demonstrating that the active building approach offers meaningful advantages across multiple performance dimensions.

8.4 Future Work

Several promising directions for future research emerge from this work:

1. **Enhanced forecast integration**: While the sensitivity analysis demonstrated acceptable performance with up to 20% forecast error, future work could explore adaptive or stochastic optimization approaches that explicitly account for forecast uncertainty. Machine learning techniques could potentially reduce forecast errors below the 10-15% typical of current weather services, further improving performance.

2. **Integration with additional energy vectors**: The research could be extended to examine coordination with EV charging, local renewable generation, and electrical storage systems. This multi-vector approach could reveal additional flexibility opportunities while enabling more comprehensive energy system optimization.

3. **Hardware implementation and real-world testing**: While the simulation demonstrates substantial potential benefits, hardware implementation and field testing would provide valuable validation under real-world conditions. This

could include development of practical communication protocols and control hardware suitable for residential deployment.

4. **Scalability analysis**: Future work should examine how the approach scales to larger communities with more diverse building types and demand patterns. This could include hierarchical control approaches to manage computational requirements while maintaining coordination benefits.

5. **Policy and regulatory frameworks**: Research into enabling policy frameworks would support practical implementation of community-scale heat decarbonization. This could include investigation of appropriate market mechanisms, regulatory structures, and business models to support coordinated approaches.

8.5 Conclusion

This research has demonstrated the significant potential for community-scale optimization of heat pump and thermal storage systems to support residential heat decarbonization. The Trent Basin case study revealed that sophisticated control strategies can effectively manage the challenges of widespread heat pump deployment while maintaining network stability and improving system efficiency.

The active building model's achievement of 20% peak demand reduction while maintaining comparable energy consumption (+1.3%) and achieving carbon emissions reduction of approximately 5% demonstrates that peak demand optimisation can create benefits across multiple performance dimensions without compromising system effectiveness.

The research demonstrates that community-scale implementation offers advantages beyond the aggregation of individual building benefits. The emergence of collective benefits through coordinated operation suggests that heat decarbonisation strategies should prioritize community-scale approaches over individual building optimisation.

While certain limitations and areas for future investigation remain, this research provides a robust framework for developing effective heat decarbonisation strategies. The demonstrated success of the active building model, combined with clear understanding of implementation requirements and constraints, offers practical guidance for community-scale heat pump deployment in support of net-zero carbon targets.

Bibliography

2020 UK Greenhouse Gas Emissions, Final Figures. (n.d.). Retrieved April 21, 2025, from https://www.ipcc-nggip.iges.or.jp/public/wetlands/index.html;

Active Building Centre (ABC) - Energy Systems Catapult. (n.d.). Retrieved April 17, 2025, from https://es.catapult.org.uk/about/active-building-centre/?utm_source=chatgpt.com

Agile Portal. (n.d.). Retrieved June 1, 2025, from https://agile.octopushome.net/historical-data

Alpizar-Castillo, J., Ramirez-Elizondo, L., & Bauer, P. (2023). The Effect of Non-Coordinated Heating Electrification Alternatives on a Low-Voltage Distribution Network with High PV Penetration. *CPE-POWERENG 2023 - 17th IEEE International Conference on Compatibility, Power Electronics and Power Engineering*. https://doi.org/10.1109/CPE-POWERENG58103.2023.10227394

Arpagaus, C., Bless, F., Uhlmann, M., Schiffmann, J., & Bertsch, S. S. (2018). High temperature heat pumps: Market overview, state of the art, research status, refrigerants, and application potentials. *Energy*, *152*, 985–1010. https://doi.org/10.1016/J.ENERGY.2018.03.166

Aschidamini, G. L., Holzbach, M., Reinholz, B. A., Metcalfe, M. S., & Resener, M. (2024). Impact of the Electrification of Vehicles and Integration of Solar Photovoltaic Systems on Low-voltage Distribution Networks. *Canadian Conference on Electrical and Computer Engineering*, 590–596. https://doi.org/10.1109/CCECE59415.2024.10667099

Baeten, B., Rogiers, F., & Helsen, L. (2017). Reduction of heat pump induced peak electricity use and required generation capacity through thermal energy storage and demand response. *Applied Energy*, *195*, 184–195. https://doi.org/10.1016/J.APENERGY.2017.03.055

Bauwens, T., Schraven, D., Drewing, E., Radtke, J., Holstenkamp, L., Gotchev, B., & Yildiz, Ö. (2022). Conceptualizing community in energy systems: A systematic review of 183 definitions. *Renewable and Sustainable Energy Reviews*, *156*, 111999. https://doi.org/10.1016/J.RSER.2021.111999

Beis. (n.d.). *Energy consumption in new domestic buildings 2015 – 2017 (England and Wales)*.

Bellos, E., Tsimpoukis, D., Lykas, P., Kitsopoulou, A., Korres, D. N., Vrachopoulos, M. G., & Tzivanidis, C. (2023). Investigation of a High-Temperature Heat Pump for Heating Purposes. *Applied Sciences 2023, Vol. 13, Page 2072*, *13*(4), 2072. https://doi.org/10.3390/APP13042072

Berry, O., Kiley, D., King, K., Marsden, A., Regan, A., Jacob, M., Jenkinson, R., Lopez Garcia, D., Yu, L., & Schein, A. (2023). *Automating heat pump flexibility: results from a pilot "HeatFlex UK project."* https://media.nesta.org.uk/documents/Automating_heat_pump_flexibility__results_from_a_pilot_-_final.pdf

Bland, A., Khzouz, M., Statheros, T., & Gkanas, E. I. (2017). PCMs for Residential Building Applications: A Short Review Focused on Disadvantages and Proposals for Future

Development. *Buildings 2017, Vol. 7, Page 78*, *7*(3), 78. https://doi.org/10.3390/BUILDINGS7030078

Blonsky, M., Nagarajan, A., Ghosh, S., McKenna, K., Veda, S., & Kroposki, B. (2019). Potential Impacts of Transportation and Building Electrification on the Grid: A Review of Electrification Projections and Their Effects on Grid Infrastructure, Operation, and Planning. *Current Sustainable/Renewable Energy Reports*, *6*(4), 169–176. https://doi.org/10.1007/S40518-019-00140-5/FIGURES/1

Bourne, S., & Novoselac, A. (2015). Compact PCM-based thermal stores for shifting peak cooling loads. *Building Simulation*, *8*(6), 673–688. https://doi.org/10.1007/S12273-015-0243-6/METRICS

Bouzaher, M. T., Bouchahm, N., Guerira, B., Bensaci, C. E., & Lebbi, M. (2019). On the thermal stratification inside a spherical water storage tank during dynamic mode. *Applied Thermal Engineering*, *159*, 113821. https://doi.org/10.1016/J.APPLTHERMALENG.2019.113821

Brendel, L. P. M., Bernal, S. N., Arpagaus, C., Roskosch, D., Bardow, A., & Bertsch, S. S. (2024). Experimental Performance Comparison of High-Glide Hydrocarbon and Synthetic Refrigerant Mixtures in a High-Temperature Heat Pump. *Energies 2024, Vol. 17, Page 1981*, *17*(8), 1981. https://doi.org/10.3390/EN17081981

Brunelli, L., Borri, E., Pisello, A. L., Nicolini, A., Mateu, C., & Cabeza, L. F. (2024). Thermal Energy Storage in Energy Communities: A Perspective Overview through a Bibliometric Analysis. *Sustainability 2024, Vol. 16, Page 5895*, *16*(14), 5895. https://doi.org/10.3390/SU16145895

Burkhardt, A., Billerbeck, A., Bernath, C., Manz, P., Deac, G., & Held, A. (2024). The Role of Thermal Energy Storage in Market Integration of Variable Renewable Electricity - A German Case Study. *International Conference on the European Energy Market, EEM*. https://doi.org/10.1109/EEM60825.2024.10608961

Cabeza, L. F., Bai, Q., & Bertoldi, P. (2023). Buildings. In *Climate Change 2022 - Mitigation of Climate Change* (pp. 953–1048). Cambridge University Press. https://doi.org/10.1017/9781009157926.011

Caron-Soupart, A., Fourmigué, J. F., Marty, P., & Couturier, R. (2016). Performance analysis of thermal energy storage systems using phase change material. *Applied Thermal Engineering*, *98*, 1286–1296. https://doi.org/10.1016/J.APPLTHERMALENG.2016.01.016

Carroll, P., Chesser, M., & Lyons, P. (2020). Air Source Heat Pumps field studies: A systematic literature review. In *Renewable and Sustainable Energy Reviews* (Vol. 134). Elsevier Ltd. https://doi.org/10.1016/j.rser.2020.110275

Chen, X., Zhang, Z., Qi, C., Ling, X., & Peng, H. (2018). State of the art on the high-temperature thermochemical energy storage systems. *Energy Conversion and Management*, *177*, 792–815. https://doi.org/10.1016/J.ENCONMAN.2018.10.011

Chesser, M., Lyons, P., O'Reilly, P., & Carroll, P. (2021). Air source heat pump in-situ performance. *Energy and Buildings*, *251*, 111365. https://doi.org/10.1016/J.ENBUILD.2021.111365

Childs, L., Bennett, G., Watson, S., & Wilson, G. (2025). Predicting the heat pump readiness of existing heating systems in the UK using diagnostic boiler data. *Building Services*

Engineering Research and Technology. https://doi.org/10.1177/01436244241306591/ASSET/02C4A141-5634-45FB-ABF1-6798BE4F2C5E/ASSETS/IMAGES/LARGE/10.1177_01436244241306591-FIG11.JPG

Clarke, J., Searle, J., & Lewis, R. (2020). *Active Building Design Guide* (Vol. 163).

Community Energy - GOV.UK. (n.d.). Retrieved June 17, 2022, from https://www.gov.uk/guidance/community-energy

Desguers, T., Lyden, A., & Friedrich, D. (2024). Integration of curtailed wind into flexible electrified heating networks with demand-side response and thermal storage: Practicalities and need for market mechanisms. *Energy Conversion and Management*, *304*, 118203. https://doi.org/10.1016/J.ENCONMAN.2024.118203

Digital Twins for the Built Environment | IES. (n.d.). Retrieved July 20, 2023, from https://www.iesve.com/digital-twins

Dong, J., Deng, S., Jiang, Y., Xia, L., & Yao, Y. (2012). An experimental study on defrosting heat supplies and energy consumptions during a reverse cycle defrost operation for an air source heat pump. *Applied Thermal Engineering*, *37*, 380–387. https://doi.org/10.1016/J.APPLTHERMALENG.2011.11.052

Dongellini, M., & Morini, G. L. (2019). On-off cycling losses of reversible air-to-water heat pump systems as a function of the unit power modulation capacity. *Energy Conversion and Management*, *196*, 966–978. https://doi.org/10.1016/J.ENCONMAN.2019.06.022

Dou, Y., Jiang, P., Li, Q., Jiang, P., & Xu, B. (2023). Model predictive control strategy of heat pump heating systems for demand response. *Building Simulation Conference Proceedings*, *18*, 3195–3202. https://doi.org/10.26868/25222708.2023.1263

El Feghali, J., Sandou, G., Guéguen, H., Haessig, P., Faille, D., Bouia, H., & Croteau, D. (2022). Electrical Grid Flexibility via Heat Pump and Thermal Storage Control. *IFAC-PapersOnLine*, *55*(11), 84–89. https://doi.org/10.1016/J.IFACOL.2022.08.053

ELECTRIFICATION OF HEAT DEMONSTRATION PROJECT SUMMARY REPORT. (2024).

Ellerbrok, C. (2014). Potentials of Demand Side Management Using Heat Pumps with Building Mass as a Thermal Storage. *Energy Procedia*, *46*, 214–219. https://doi.org/10.1016/J.EGYPRO.2014.01.175

Energy price cap | Ofgem. (n.d.). Retrieved June 1, 2025, from https://www.ofgem.gov.uk/information-consumers/energy-advice-households/energy-price-cap

Enescu, D., Chicco, G., Porumb, R., & Seritan, G. (2020). Thermal Energy Storage for Grid Applications: Current Status and Emerging Trends. *Energies 2020, Vol. 13, Page 340*, *13*(2), 340. https://doi.org/10.3390/EN13020340

ERA: The Trent Basin Community Energy Project - Midlands Innovation. (n.d.). Retrieved April 21, 2025, from https://midlandsinnovation.org.uk/latest/case-studies/era-the-trent-basin-community-energy-project/

Eyre, N., & Baruah, P. (2015). Uncertainties in future energy demand in UK residential heating. *Energy Policy*, *87*, 641–653. https://doi.org/10.1016/J.ENPOL.2014.12.030

Fan, G., Liu, Z., Liu, X., Shi, Y., Wu, D., Guo, J., Zhang, S., Yang, X., & Zhang, Y. (2022). Energy management strategies and multi-objective optimization of a near-zero energy community energy supply system combined with hybrid energy storage. *Sustainable Cities and Society*, *83*, 103970. https://doi.org/10.1016/J.SCS.2022.103970

Farulla, G. A., Cellura, M., Guarino, F., & Ferraro, M. (2020). A Review of Thermochemical Energy Storage Systems for Power Grid Support. *Applied Sciences 2020, Vol. 10, Page 3142*, *10*(9), 3142. https://doi.org/10.3390/APP10093142

Felten, B., & Weber, C. (2018). The value(s) of flexible heat pumps – Assessment of technical and economic conditions. *Applied Energy*, *228*, 1292–1319. https://doi.org/10.1016/J.APENERGY.2018.06.031

Foggia, G. Di, Beccarello, M., & Jammeh, B. (2024). A Global Perspective on Renewable Energy Implementation: Commitment Requires Action. *Energies 2024, Vol. 17, Page 5058*, *17*(20), 5058. https://doi.org/10.3390/EN17205058

Fosas, D., Nikolaidou, E., Roberts, M., Allen, S., Walker, I., & Coley, D. (2021). Towards active buildings: Rating grid-servicing buildings. *Building Services Engineering Research and Technology*, *42*(2), 129–155. https://doi.org/10.1177/0143624420974647/ASSET/IMAGES/10.1177_0143624420974647-IMG2.PNG

Gao, W., Masum, S., & Jiang, L. (2023). Technical Performance Comparison of Horizontal and Vertical Ground-Source Heat Pump Systems. *Journal of GeoEnergy*, *2023*(1), 6106360. https://doi.org/10.1155/2023/6106360

Gaur, A. S., Fitiwi, D. Z., & Curtis, J. (2021). Heat pumps and our low-carbon future: A comprehensive review. *Energy Research and Social Science*, *71*. https://doi.org/10.1016/J.ERSS.2020.101764

Georges, E., Cornélusse, B., Ernst, D., Lemort, V., & Mathieu, S. (2017). Residential heat pump as flexible load for direct control service with parametrized duration and rebound effect. *Applied Energy*, *187*, 140–153. https://doi.org/10.1016/J.APENERGY.2016.11.012

Glembin, J., Büttner, C., Steinweg, J., & Rockendorf, G. (2015). Thermal Storage Tanks in High Efficiency Heat Pump Systems – Optimized Installation and Operation Parameters. *Energy Procedia*, *73*, 331–340. https://doi.org/10.1016/J.EGYPRO.2015.07.700

Gonzato, S., Chimento, J., O'Dwyer, E., Bustos-Turu, G., Acha, S., & Shah, N. (2019). Hierarchical price coordination of heat pumps in a building network controlled using model predictive control. *Energy and Buildings*, *202*, 109421. https://doi.org/10.1016/J.ENBUILD.2019.109421

Groulx, D., Castell, A., & Solé, C. (2021). Design of latent heat energy storage systems using phase change materials. *Advances in Thermal Energy Storage Systems: Methods and Applications*, 331–357. https://doi.org/10.1016/B978-0-12-819885-8.00011-5

Gupta, R., & Gregg, M. (2023). A new local area energy mapping approach for targeting high-density deployment of heat pumps in the UK. *Building Simulation Conference Proceedings*, *18*, 306–313. https://doi.org/10.26868/25222708.2023.1383

Gupta, R., & Zahiri, S. (2020). Meta-study of smart and local energy system demonstrators in the UK: technologies, leadership and user engagement. *IOP Conference Series:*

Earth and Environmental Science, *588*(2), 022049. https://doi.org/10.1088/1755-1315/588/2/022049

Haller, M. Y., Haberl, R., & Reber, A. (2019a). Stratification efficiency of thermal energy storage systems – A new KPI based on dynamic hardware in the loop testing - Part II: Test results. *Energy and Buildings*, *202*, 109366. https://doi.org/10.1016/J.ENBUILD.2019.109366

Haller, M. Y., Haberl, R., & Reber, A. (2019b). Stratification efficiency of thermal energy storage systems – A new KPI based on dynamic hardware in the loop testing - Part II: Test results. *Energy and Buildings*, *202*, 109366. https://doi.org/10.1016/J.ENBUILD.2019.109366

Han, M. E., Alston, M., & Gillott, M. (2022). A multi-vector community energy system integrating a heating network, electricity grid and PV production to manage an electrified community. *Energy and Buildings*, *266*, 112105. https://doi.org/10.1016/J.ENBUILD.2022.112105

Haque, A. N. M. M., Nguyen, P. H., Vo, T. H., & Bliek, F. W. (2017). Agent-based unified approach for thermal and voltage constraint management in LV distribution network. *Electric Power Systems Research*, *143*, 462–473. https://doi.org/10.1016/J.EPSR.2016.11.007

Harkin, S., & Turton, A. (2017). Managing the future network impact of the electrification of heat. *CIRED - Open Access Proceedings Journal*, *2017*(1), 1888–1891. https://doi.org/10.1049/OAP-CIRED.2017.1123/ASSET/6E4F2003-107E-41FC-98D4-A0E4766577F2/ASSETS/IMAGES/LARGE/OAP-CIRED.2017.1123.06.JPG

Henni, S., Staudt, P., Kandiah, B., & Weinhardt, C. (2021). Infrastructural coupling of the electricity and gas distribution grid to reduce renewable energy curtailment. *Applied Energy*, *288*, 116597. https://doi.org/10.1016/J.APENERGY.2021.116597

Hirschey, J., Li, Z., Gluesenkamp, K. R., LaClair, T. J., & Graham, S. (2023). Demand reduction and energy saving potential of thermal energy storage integrated heat pumps. *International Journal of Refrigeration*, *148*, 179–192. https://doi.org/10.1016/J.IJREFRIG.2023.01.026

Historic generation mix and carbon intensity | ESO. (n.d.). Retrieved March 19, 2024, from https://www.nationalgrideso.com/data-portal/historic-generation-mix

Home - Trent Basin. (n.d.). Retrieved June 17, 2022, from https://www.trentbasin.co.uk/

homemicro.co.uk. (2016). *THERMAL STORAGE VESSEL SIZING*. http://www.homemicro.co.uk/lzc_vessel.html

Hu, B., Wang, R. Z., Xiao, B., He, L., Zhang, W., & Zhang, S. (2019). Performance evaluation of different heating terminals used in air source heat pump system. *International Journal of Refrigeration*, *98*, 274–282. https://doi.org/10.1016/J.IJREFRIG.2018.10.014

Huang, P., Fan, C., Zhang, X., & Wang, J. (2019). A hierarchical coordinated demand response control for buildings with improved performances at building group. *Applied Energy*, *242*, 684–694. https://doi.org/10.1016/J.APENERGY.2019.03.148

Hutty, T. D., Patel, N., Dong, S., & Brown, S. (2020). Can thermal storage assist with the electrification of heat through peak shaving? *Energy Reports*, *6*, 124–131. https://doi.org/10.1016/J.EGYR.2020.03.006

Innovate UK. (2016). *Building Performance Evaluation Programme: Findings from domestic projects At a glance*.

Ireneo C. Plando, Jr. (2023). Performance Evaluation of Heat Pump Systems for Cold Climate Regions. *International Journal of Advanced Research in Science, Communication and Technology*, 872–876. https://doi.org/10.48175/ijarsct-12386

Janakarajan, R., Prakash, D., Sundar, S., & Kasthurirangan, L. (2019). Analysis and optimisation of an insulated water tank for the domestic purpose. *Australian Journal of Mechanical Engineering*, *17*(1), 14–23. https://doi.org/10.1080/14484846.2018.1461732

Johnson, R. C., & Mayfield, M. (2022). The effectiveness of decentralised electro-thermal load shifting strategies in low voltage network violation management. *International Journal of Electrical Power & Energy Systems*, *142*, 108317. https://doi.org/10.1016/J.IJEPES.2022.108317

Jouhara, H., Żabnieńska-Góra, A., Delpech, B., Olabi, V., El Samad, T., & Sayma, A. (2024). High-temperature heat pumps: Fundamentals, modelling approaches and applications. *Energy*, *303*, 131882. https://doi.org/10.1016/J.ENERGY.2024.131882

Jung, W., Kim, D., Kang, B. H., & Chang, Y. S. (2017). Investigation of Heat Pump Operation Strategies with Thermal Storage in Heating Conditions. *Energies 2017, Vol. 10, Page 2020*, *10*(12), 2020. https://doi.org/10.3390/EN10122020

Kargar, S. M., & Bahamin, M. (2025). Advanced model predictive control strategy for thermal management in multi-zone buildings with energy storage and dynamic pricing. *Energy Exploration and Exploitation*. https://doi.org/10.1177/01445987241298534/ASSET/64C47222-C91D-4951-BC5A-69AD6907D035/ASSETS/IMAGES/LARGE/10.1177_01445987241298534-FIG7.JPG

Knobloch, F., Pollitt, H., Chewpreecha, U., Daioglou, V., & Mercure, J. F. (2019). Simulating the deep decarbonisation of residential heating for limiting global warming to 1.5 °C. *Energy Efficiency*, *12*(2), 521–550. https://doi.org/10.1007/S12053-018-9710-0/FIGURES/10

Konrad, M. E., & MacDonald, B. D. (2023). Cold climate air source heat pumps: Industry progress and thermodynamic analysis of market-available residential units. *Renewable and Sustainable Energy Reviews*, *188*, 113739. https://doi.org/10.1016/J.RSER.2023.113739

Kropp, M., Lämmle, M., Herkel, S., Henning, H. M., & Velte-Schäfer, A. (2025). Enhancing heat pump performance for domestic hot water preparation: A comparative analysis in existing multi-family houses. *Energy and Buildings*, *328*, 115155. https://doi.org/10.1016/J.ENBUILD.2024.115155

Lämmle, M., Bongs, C., Wapler, J., Günther, D., Hess, S., Kropp, M., & Herkel, S. (2022). Performance of air and ground source heat pumps retrofitted to radiator heating systems and measures to reduce space heating temperatures in existing buildings. *Energy*, *242*, 122952. https://doi.org/10.1016/J.ENERGY.2021.122952

Lämmle, M., Metz, J., Kropp, M., Wapler, J., Oltersdorf, T., Günther, D., Herkel, S., & Bongs, C. (2023). Heat Pump Systems in Existing Multifamily Buildings: A Meta-Analysis of Field Measurement Data Focusing on the Relationship of Temperature and Performance of Heat Pump Systems. *Energy Technology*, *11*(12), 2300379. https://doi.org/10.1002/ENTE.202300379

Le, K. X., Huang, M. J., Shah, N. N., Wilson, C., Artain, P. Mac, Byrne, R., & Hewitt, N. J. (2019). Techno-economic assessment of cascade air-to-water heat pump retrofitted into residential buildings using experimentally validated simulations. *Applied Energy*, *250*, 633–652. https://doi.org/10.1016/J.APENERGY.2019.05.041

Lee, D., Ooka, R., Ikeda, S., Choi, W., & Kwak, Y. (2020). Model predictive control of building energy systems with thermal energy storage in response to occupancy variations and time-variant electricity prices. *Energy and Buildings*, *225*, 110291. https://doi.org/10.1016/J.ENBUILD.2020.110291

Lee, H., & Romero, J. (n.d.). *Climate Change 2023 Synthesis Report IPCC, 2023: Sections. In: Climate Change 2023: Synthesis Report. Contribution of Working Groups I, II and III to the Sixth Assessment Report of the Intergovernmental Panel on Climate Change [Core Writing Team*. 35–115. https://doi.org/10.59327/IPCC/AR6-9789291691647

Li, X., Lyu, W., Ran, S., Wang, B., Wu, W., Yang, Z., Jiang, S., Cui, M., Song, P., You, T., & Shi, W. (2020). Combination principle of hybrid sources and three typical types of hybrid source heat pumps for year-round efficient operation. *Energy*, *193*, 116772. https://doi.org/10.1016/J.ENERGY.2019.116772

Li, Y., Rosengarten, G., & Mojiri, A. (2023). Performance sensitivity of hot and cold thermal storage with onsite photovoltaics and heat pumps. *Solar Energy*, *263*, 111946. https://doi.org/10.1016/J.SOLENER.2023.111946

Ling, J. M., & Mulani, F. I. (2024). Planning and optimization of a residential microgrid utilizing renewable resources and integrated energy storage. *Journal of Energy Storage*, *97*, 112933. https://doi.org/10.1016/J.EST.2024.112933

Love, J., Smith, A. Z. P., Watson, S., Oikonomou, E., Summerfield, A., Gleeson, C., Biddulph, P., Chiu, L. F., Wingfield, J., Martin, C., Stone, A., & Lowe, R. (2017). The addition of heat pump electricity load profiles to GB electricity demand: Evidence from a heat pump field trial. *Applied Energy*, *204*, 332–342. https://doi.org/10.1016/J.APENERGY.2017.07.026

Ma, Y., Wang, J., Hu, F., Yan, E., Zhang, Y., Huang, Y., Deng, H., Gao, X., Kang, J., Shi, H., Zhang, X., Zheng, J., & Guo, J. (2024). Analysis of the Heat Transfer Performance of a Buried Pipe in the Heating Season Based on Field Testing. *Energies 2024, Vol. 17, Page 5466*, *17*(21), 5466. https://doi.org/10.3390/EN17215466

Mahmoudi, M., Dehghan, M., Haghgou, H., & Keyanpour-Rad, M. (2021). Techno-economic performance of photovoltaic-powered air-conditioning heat pumps with variable-speed and fixed-speed compression systems. *Sustainable Energy Technologies and Assessments*, *45*, 101113. https://doi.org/10.1016/J.SETA.2021.101113

McGarry, C., Dixon, J., Flower, J., Bukhsh, W., Brand, C., Bell, K., & Galloway, S. (2024). Electrified heat and transport: Energy demand futures, their impacts on power networks and what it means for system flexibility. *Applied Energy*, *360*, 122836. https://doi.org/10.1016/J.APENERGY.2024.122836

Milev, G., Al-Habaibeh, A., Fanshawe, S., & Siena, F. L. (2023). Investigating the effect of the defrost cycles of air-source heat pumps on their electricity demand in residential buildings. *Energy and Buildings*, *300*, 113656. https://doi.org/10.1016/J.ENBUILD.2023.113656

MITSUBISHI ELECTRIC. (2018). *MITSUBISHI ELECTRIC: ECODAN HEAT PUMP DATA BOOK*.

Mota-Babiloni, A., Mateu-Royo, C., Navarro-Esbrí, J., Molés, F., Amat-Albuixech, M., & Barragán-Cervera, Á. (2018). Optimisation of high-temperature heat pump cascades with internal heat exchangers using refrigerants with low global warming potential. *Energy*, *165*, 1248–1258. https://doi.org/10.1016/J.ENERGY.2018.09.188

Moulakhnif, K., Ait Ousaleh, H., Sair, S., Bouhaj, Y., El Majd, A., Ghazoui, M., Faik, A., & El Bouari, A. (2024). Renewable approaches to building heat: exploring cutting-edge innovations in thermochemical energy storage for building heating. *Energy and Buildings*, *318*, 114421. https://doi.org/10.1016/J.ENBUILD.2024.114421

Mukherjee, A., Kumar, L., Subramaniam, C., & Saha, S. K. (2021). Performance evaluation of a seasonal residential space heating system based on thermochemical energy storage. *Applied Thermal Engineering*, *194*, 117059. https://doi.org/10.1016/J.APPLTHERMALENG.2021.117059

National Grid. (2023). *Distribution Substations - Dataset - Connected Data Portal | National Grid*. Distribution Substations . https://connecteddata.nationalgrid.co.uk/dataset/distribution-substations

Navarro-Espinosa, A., & Mancarella, P. (2014). Probabilistic modeling and assessment of the impact of electric heat pumps on low voltage distribution networks. *Applied Energy*, *127*, 249–266. https://doi.org/10.1016/J.APENERGY.2014.04.026

Nazari, N., Bahramian, A. R., & Allahbakhsh, A. (2022). Thermal storage achievement of paraffin wax phase change material systems with regard to novolac aerogel/carbon monofilament/zinc borate form stabilization. *Journal of Energy Storage*, *50*, 104741. https://doi.org/10.1016/J.EST.2022.104741

Nérot, B., Lamaison, N., Mabrouk, M. T., Bavière, R., & Lacarrière, B. (2023). Optimization framework for evaluating urban thermal systems potential. *Energy*, *270*, 126851. https://doi.org/10.1016/J.ENERGY.2023.126851

Obalanlege, M. A., Xu, J., Markides, C. N., & Mahmoudi, Y. (2022). Techno-economic analysis of a hybrid photovoltaic-thermal solar-assisted heat pump system for domestic hot water and power generation. *Renewable Energy*, *196*, 720–736. https://doi.org/10.1016/J.RENENE.2022.07.044

O'Dwyer, E., Pan, I., Charlesworth, R., Butler, S., & Shah, N. (2020). Integration of an energy management tool and digital twin for coordination and control of multi-vector smart energy systems. *Sustainable Cities and Society*, *62*, 102412. https://doi.org/10.1016/J.SCS.2020.102412

Osibodu, S. J., Adeyinka, A. M., & Mbelu, O. V. (2024). Phase change material integration in concrete for thermal energy storage: techniques and applications in sustainable building. *Sustainable Energy Research 2024 11:1*, *11*(1), 1–17. https://doi.org/10.1186/S40807-024-00138-8

Passivhaus Trust. (2017). *The performance of Passivhaus in new construction: Post occupancy evaluation of certified Passivhaus dwellings in the UK: Early Results*. www.passivhaustrust.org.uk

Peacock, M., Fragaki, A., & Matuszewski, B. J. (2023). The impact of heat electrification on the seasonal and interannual electricity demand of Great Britain. *Applied Energy*, *337*, 120885. https://doi.org/10.1016/J.APENERGY.2023.120885

Peng, B., He, Z., Wang, H., & Su, F. (2021). Optimization of patterned-fins for enhancing charging performances of phase change materials-based thermal energy storage systems. *International Journal of Heat and Mass Transfer*, *164*, 120573. https://doi.org/10.1016/J.IJHEATMASSTRANSFER.2020.120573

Perelli-Rocco, S., Tekler, Z. D., & Grunewald, P. (2024). *Understanding the Impact of Building Characteristics on the Heat Pump Energy Consumption: A Case Study in the United Kingdom*. https://doi.org/10.2139/SSRN.4705991

Pudjianto, D., Djapic, P., Aunedi, M., Gan, C. K., Strbac, G., Huang, S., & Infield, D. (2013). Smart control for minimizing distribution network reinforcement cost due to electrification. *Energy Policy*, *52*, 76–84. https://doi.org/10.1016/J.ENPOL.2012.05.021

Quiggin, D., & Buswell, R. (2016). The implications of heat electrification on national electrical supply-demand balance under published 2050 energy scenarios. *Energy*, *98*, 253–270. https://doi.org/10.1016/j.energy.2015.11.060

Rabczak, S., Mateichyk, V., Smieszek, M., Nowak, K., & Kolomiiets, S. (2024). Evaluating the Energy Efficiency of Combining Heat Pumps and Photovoltaic Panels in Eco-Friendly Housing. *Applied Sciences 2024, Vol. 14, Page 5575*, *14*(13), 5575. https://doi.org/10.3390/APP14135575

Reguis, A., Vand, B., & Currie, J. (2021). *Challenges for the Transition to Low-Temperature Heat in the UK: A Review*. https://doi.org/10.3390/en14217181

Renaldi, R., Kiprakis, A., & Friedrich, D. (2017). An optimisation framework for thermal energy storage integration in a residential heat pump heating system. *Applied Energy*, *186*, 520–529. https://doi.org/10.1016/j.apenergy.2016.02.067

Rendall, J., Elatar, A., Nawaz, K., & Sun, J. (2023). Medium-temperature phase change material integration in domestic heat pump water heaters for improved thermal energy storage. *Renewable and Sustainable Energy Reviews*, *185*, 113656. https://doi.org/10.1016/J.RSER.2023.113656

Rhee, K. N., & Kim, K. W. (2015). A 50 year review of basic and applied research in radiant heating and cooling systems for the built environment. *Building and Environment*, *91*, 166–190. https://doi.org/10.1016/J.BUILDENV.2015.03.040

Rheem Hybrid Electric Heat Pump Water Heater. (2023).

Romero Rodríguez, L., Sánchez Ramos, J., Álvarez Domínguez, S., & Eicker, U. (2018). Contributions of heat pumps to demand response: A case study of a plus-energy dwelling. *Applied Energy*, *214*, 191–204. https://doi.org/10.1016/J.APENERGY.2018.01.086

Rony, R. U., & Gladen, A. (2021). Parametric study and sensitivity analysis of a PV/microchannel direct-expansion CO2 heat pump. *Solar Energy*, *218*, 282–295. https://doi.org/10.1016/J.SOLENER.2021.02.006

Sager, J., Mackintosh, T., St-Onge, G., McDonald, E., & Kegel, M. (2019). *Detailed Performance Assessment of Variable Capacity Inverter-Driven Cold Climate Air Source Heat Pumps*. 441–451. https://doi.org/10.1007/978-3-030-00662-4_37

Salite, D., Miao, Y., & Turner, E. (2024). A comparative analysis of policies and strategies supporting district heating expansion and decarbonisation in Denmark, Sweden, the Netherlands and the United Kingdom – Lessons for slow adopters of district heating. *Environmental Science & Policy*, *161*, 103897. https://doi.org/10.1016/J.ENVSCI.2024.103897

SAMSUNG. (2022). *SAMSUNG EHS High Temprature Heat Pump Technical Data Book*.

Sarbu, I., & Sebarchievici, C. (2014). General review of ground-source heat pump systems for heating and cooling of buildings. *Energy and Buildings*, *70*, 441–454. https://doi.org/10.1016/J.ENBUILD.2013.11.068

Sarbu, I., & Sebarchievici, C. (2018). A Comprehensive Review of Thermal Energy Storage. *Sustainability 2018, Vol. 10, Page 191*, *10*(1), 191. https://doi.org/10.3390/SU10010191

Shah, N., & Hewitt, N. (2016). High temperature heat pump operational experience as a retrofit technology in domestic sector. *2015 IEEE International Conference on Engineering, Technology and Innovation/ International Technology Management Conference, ICE/ITMC 2015*. https://doi.org/10.1109/ICE.2015.7438691

Shah, N. N., Wilson, C., Huang, M. J., & Hewitt, N. J. (2018). Analysis on field trial of high temperature heat pump integrated with thermal energy storage in domestic retrofit installation. *Applied Thermal Engineering*, *143*, 650–659. https://doi.org/10.1016/J.APPLTHERMALENG.2018.07.135

Shank, K. ;, Tiari, S. A., Sousa, C. M., Shank, K., & Tiari, S. (2023). A Review on Active Heat Transfer Enhancement Techniques within Latent Heat Thermal Energy Storage Systems. *Energies 2023, Vol. 16, Page 4165*, *16*(10), 4165. https://doi.org/10.3390/EN16104165

Sharif, M. K. A., Al-Abidi, A. A., Mat, S., Sopian, K., Ruslan, M. H., Sulaiman, M. Y., & Rosli, M. A. M. (2015). Review of the application of phase change material for heating and domestic hot water systems. *Renewable and Sustainable Energy Reviews*, *42*, 557–568. https://doi.org/10.1016/J.RSER.2014.09.034

Shipman, R., & Gillott, M. (2019). SCENe things: IoT-based monitoring of a community energy scheme. *Future Cities and Environment*, *5*(1). https://doi.org/10.5334/FCE.64/METRICS/

Singh, H., Muetze, A., & Eames, P. C. (2010). Factors influencing the uptake of heat pump technology by the UK domestic sector. *Renewable Energy*, *35*(4), 873–878. https://doi.org/10.1016/J.RENENE.2009.10.001

Srithapon, C., & Månsson, D. (2023). Predictive control and coordination for energy community flexibility with electric vehicles, heat pumps and thermal energy storage. *Applied Energy*, *347*, 121500. https://doi.org/10.1016/J.APENERGY.2023.121500

Stalinski, D., & Duquette, J. (2021). Development of a simplified method for optimally sizing hot water storage tanks subject to short-term intermittent charge/discharge cycles. *Journal of Energy Storage*, *37*, 102463. https://doi.org/10.1016/J.EST.2021.102463

Sultan, S., Hirschey, J., Kumar, N., Cui, B., Liu, X., LaClair, T. J., & Gluesenkamp, K. R. (2023). Techno-Economic Assessment of Residential Heat Pump Integrated with Thermal Energy Storage. *Energies 2023, Vol. 16, Page 4087*, *16*(10), 4087. https://doi.org/10.3390/EN16104087

Sweetnam, T., Fell, M., Oikonomou, E., & Oreszczyn, T. (2019). Domestic demand-side response with heat pumps: controls and tariffs. *Building Research & Information*, *47*(4), 344–361. https://doi.org/10.1080/09613218.2018.1442775

Tang, Q., Wang, H., & Guo, H. (2024). Performance analysis of a novel dual exhaust mixed refrigerant heat pump with large temperature lift. *Thermal Science and Engineering Progress*, *56*, 103034. https://doi.org/10.1016/J.TSEP.2024.103034

Tito, S. R., Walmsley, M., & Apperley, M. (2023). Impact of Thermal Energy Storage on Optimal Sizing of a Grid Connected Wind-Photovoltaic-Battery System for an Industry Edged Community. *5th IEEE International Conference on DC Microgrids, ICDCM 2023*. https://doi.org/10.1109/ICDCM54452.2023.10433591

Transitioning to a net zero energy system: Smart Systems and Flexibility Plan 2021. (2021).

Trent Basin · Project Scene (Sustainable Community Energy Networks). (n.d.). Retrieved June 17, 2022, from https://www.projectscene.uk/trentbasin/

Trinchieri, R., Pieve, M., Boccardi, G., Calabrese, N., Rovella, P., & Saraceno, L. (2020). Experimental analysis of a CO2 heat pump for instantaneous domestic hot water production. *Journal of Physics: Conference Series*, *1599*(1), 012059. https://doi.org/10.1088/1742-6596/1599/1/012059

Vahidinasab, V., Ardalan, C., Mohammadi-Ivatloo, B., Giaouris, D., & Walker, S. L. (2021). Active Building as an Energy System: Concept, Challenges, and Outlook. *IEEE Access*, *9*, 58009–58024. https://doi.org/10.1109/ACCESS.2021.3073087

Vaillant UK uniSTOR Cylinders . (n.d.). Retrieved April 21, 2025, from https://professional.vaillant.co.uk/for-installers/products/domestic-boiler-cylinders-25601.html?

van der Schoor, T., & Scholtens, B. (2015). Power to the people: Local community initiatives and the transition to sustainable energy. *Renewable and Sustainable Energy Reviews*, *43*, 666–675. https://doi.org/10.1016/J.RSER.2014.10.089

Veldman, E., Gibescu, M., Slootweg, H., & Kling, W. L. (2011). Impact of electrification of residential heating on loading of distribution networks. *2011 IEEE PES Trondheim PowerTech: The Power of Technology for a Sustainable Society, POWERTECH 2011*. https://doi.org/10.1109/PTC.2011.6019179

Wang, Y., Qu, K., Chen, X., Zhang, X., & Riffat, S. (2022). Holistic electrification vs deep energy retrofits for optimal decarbonisation pathways of UK dwellings: A case study of the 1940s' British post-war masonry house. *Energy*, *241*, 122935. https://doi.org/10.1016/J.ENERGY.2021.122935

Wang, Y., Wang, J., & He, W. (2022). Development of efficient, flexible and affordable heat pumps for supporting heat and power decarbonisation in the UK and beyond: Review and perspectives. In *Renewable and Sustainable Energy Reviews* (Vol. 154). Elsevier Ltd. https://doi.org/10.1016/j.rser.2021.111747

Watson, S. D., Crawley, J., Lomas, K. J., & Buswell, R. A. (2023). Predicting future GB heat pump electricity demand. *Energy and Buildings*, *286*, 112917. https://doi.org/10.1016/J.ENBUILD.2023.112917

Watson, S. D., Lomas, K. J., & Buswell, R. A. (2019). Decarbonising domestic heating: What is the peak GB demand? *Energy Policy*, *126*, 533–544. https://doi.org/10.1016/J.ENPOL.2018.11.001

Wu, Q., Xu, S., Zhou, W., & LaMoreaux, J. (2015). Hydrogeology and design of groundwater heat pump systems. *Environmental Earth Sciences*, *73*(7), 3683–3695. https://doi.org/10.1007/S12665-014-3654-2/FIGURES/4

Xu, Y. X., Yan, J., & Zhao, C. Y. (2022). Investigation on application temperature zone and exergy loss regulation based on MgCO3/MgO thermochemical heat storage and release process. *Energy*, *239*, 122155. https://doi.org/10.1016/J.ENERGY.2021.122155

Xu, Z., Li, H., Xu, W., Shao, S., Wang, Z., Gou, X., Zhao, M., & Li, J. (2022). Investigation on the efficiency degradation characterization of low ambient temperature air source heat pump under partial load operation. *International Journal of Refrigeration*, *133*, 99–110. https://doi.org/10.1016/J.IJREFRIG.2021.10.002

Xu, Z., Sun, X., Li, X., Wang, Z., Xu, W., Shao, S., Xu, C., Yang, Q., Li, H., & Zhao, W. (2021). On-off cycling model featured with pattern recognition of air-to-water heat pumps. *Applied Thermal Engineering*, *196*, 117317. https://doi.org/10.1016/J.APPLTHERMALENG.2021.117317

Yang, T., King, W. P., & Miljkovic, N. (2021). Phase change material-based thermal energy storage. *Cell Reports Physical Science*, *2*(8), 100540. https://doi.org/10.1016/J.XCRP.2021.100540

Zhang, L., Feng, G., Huang, K., Bi, Y., Chang, S., & Li, A. (2025). Design and optimization for photovoltaic heat pump system integrating thermal energy storage and battery energy storage. *Energy and Buildings*, *329*, 115277. https://doi.org/10.1016/J.ENBUILD.2025.115277

Zhang, N., Yuan, Y., Cao, X., Du, Y., Zhang, Z., & Gui, Y. (2018). Latent Heat Thermal Energy Storage Systems with Solid–Liquid Phase Change Materials: A Review. *Advanced Engineering Materials*, *20*(6), 1700753. https://doi.org/10.1002/ADEM.201700753

Zhao, X., Long, E., Zhang, Y., Liu, Q., Jin, Z., & Liang, F. (2017). Experimental Study on Heating Performance of Air - source Heat Pump with Water Tank for Thermal Energy Storage. *Procedia Engineering*, *205*, 2055–2062. https://doi.org/10.1016/J.PROENG.2017.10.087

Zhou, W., He, Y., Xu, Q., Wang, C., Ling, Z., Zhang, Z., & Fang, X. (2024). Numerical simulation and optimization of compact latent heat exchanger with micro-channel plate in shape-stabilized composite phase change material. *Applied Thermal Engineering*, *245*, 122740. https://doi.org/10.1016/J.APPLTHERMALENG.2024.122740

Zinsmeister, D., Tzscheutschler, P., Perić, V. S., & Goebel, C. (2023). Stratified thermal energy storage model with constant layer volume for predictive control — Formulation, comparison, and empirical validation. *Renewable Energy*, *219*, 119511. https://doi.org/10.1016/J.RENENE.2023.119511

Zuberi, M. J. S., Chambers, J., & Patel, M. K. (2021). Techno-economic comparison of technology options for deep decarbonization and electrification of residential heating. *Energy Efficiency*, *14*(7), 1–18. https://doi.org/10.1007/S12053-021-09984-7/FIGURES/4

Appendix A: Simulation Framework MATLAB Code

```
%% Community Heat Decarbonisation Simulation Model
% Author: Zaid Al-Atari
% Last Modified: April 2025
% University of Nottingham, Faculty of Engineering
%
% This simulation evaluates three control approaches for heat pump integration
% in residential communities:
%   1. Baseline: Uncoordinated heat pump operation
%   2. Fixed Threshold: Static grid-aware thresholds
%   3. Active Building: Dynamic daily optimized thresholds
%
% INPUTS:
%   - Electricity demand data (hourly)
%   - Heat demand data (modelled, hourly)
%   - Weather data (outdoor temperature)
%   - Building specifications (heat pump capacities, storage sizes)
%   - Grid carbon intensity data
%
% OUTPUTS:
%   - Energy consumption analysis
%   - Peak demand assessment
%   - Grid impact metrics
%   - Carbon emissions evaluation
%   - Economic performance comparison


clear; clc; clf;


%% CONFIGURATION SETTINGS
% User-defined scenario selection
% 1 = Baseline only, 2 = Fixed threshold, 3 = Active building model, 4 = All scenarios
```

```
scenario_to_run = 4;

% Define building categories for analysis
% Select a sample building from each Category
building_categories = struct();
building_categories.cat1 = [1];    % Category 1
building_categories.cat2 = [7];    % Category 2
building_categories.cat3 = [2];    % Category 3
building_categories.cat4 = [6];    % Category 4

% Path settings - update these paths as needed for your system
demandDataPath = 'C:\Research\TrentBasin\Total Demands.csv';
buildingSpecsPath = 'C:\Research\TrentBasin\Building_Specs_2.csv';
resultsPath = 'C:\Research\TrentBasin\Results_CombinedAnalysis.csv';

%% LOAD DATA
% Load demand data
fprintf('Loading demand data from %s\n', demandDataPath);
data = readtable(demandDataPath);

% Load building specs data
fprintf('Loading building specifications from %s\n', buildingSpecsPath);
buildingSpecs = readtable(buildingSpecsPath);

% COP Table for temperature-dependent efficiency
% Format: [Temperature (°C), COP]
% Based on manufacturer performance data for high-temperature heat pumps
copTable = 'C:\Research\TrentBasin\COPtables.csv';

%% CONSTANTS
initial_storage = 7;  % Initial storage value for all buildings (kWh)
```

```
% Tariff settings – 2024/2025 UK market rates
STANDARD_RATE = 0.245;    % 24.5p/kWh - standard flat rate

% Economy 7 settings
OFF_PEAK_RATE = 0.1332;   % 13.32p/kWh
PEAK_RATE = 0.305;        % 30.5p/kWh
OFF_PEAK_START = 0;       % Midnight
OFF_PEAK_END = 7;         % 7 AM

% Fixed threshold values (kW) - determined through iterative analysis
FIXED_T1 = 140;  % Threshold for direct HP operation
FIXED_T2 = 180;  % Threshold for TES charging

%% INITIALIZE DATA STRUCTURES
numDays = floor(height(data) / 24);
fprintf('Simulating %d days of operation\n', numDays);

% Initialize scenario datasets based on configuration
if scenario_to_run == 1 || scenario_to_run == 4
    baseline_data = data;
    fprintf('Initializing baseline scenario\n');
end

if scenario_to_run == 2 || scenario_to_run == 4
    fixed_data = data;
    fprintf('Initializing fixed threshold scenario\n');
end

if scenario_to_run == 3 || scenario_to_run == 4
    active_data = data;
    daily_thresholds = zeros(numDays, 2, 75);  % [day, threshold1/2, building]
    hourly_cop = zeros(height(data), 75);      % [hour, building]
```

```
    fprintf('Initializing active building model\n');
end

%% PROCESS EACH BUILDING
fprintf('Starting building-by-building simulation...\n');

for bldg = 1:75
    fprintf('Processing building %d of 75\n', bldg);

    % Generate field names for dynamic access
    heatDemandField = sprintf('HeatBuilding%d', bldg);
    elecDemandField = sprintf('ElectricityBuilding%d', bldg);

    % Building-specific HP capacity and storage capacity from specs file
    HP_max = buildingSpecs.HP_Capacity(bldg);
    storage_capacity = buildingSpecs.Storage_Capacity(bldg);
    charging_rate = buildingSpecs.charging_rate(bldg);

    %% BASELINE SCENARIO (Unoptimized)
    if scenario_to_run == 1 || scenario_to_run == 4
        % Initialize fields for baseline scenario
        baseline_data.([sprintf('B%d_storage_state', bldg)]) = zeros(height(data), 1);
        baseline_data.([sprintf('B%d_hp_operation', bldg)]) = zeros(height(data), 1);
        baseline_data.([sprintf('B%d_HP_elec_demand', bldg)]) = zeros(height(data), 1);
        baseline_data.([sprintf('B%d_storage_operation', bldg)]) = zeros(height(data), 1);
        baseline_data.([sprintf('B%d_electricity_demand_tot', bldg)]) = zeros(height(data), 1);
        baseline_data.([sprintf('B%d_heat_demand_met', bldg)]) = false(height(data), 1);

        % Initialize cost fields for different tariffs
        baseline_data.([sprintf('B%d_hp_cost_standard', bldg)]) = zeros(height(data), 1);
        baseline_data.([sprintf('B%d_hp_cost_economy7', bldg)]) = zeros(height(data), 1);
        baseline_data.([sprintf('B%d_hp_cost_agile', bldg)]) = zeros(height(data), 1);
```

```
% Calculate baseline (unoptimized) demand - HP responds directly to heat demand
for hour = 1:height(data)
    % Get COP based on ambient temperature
    ambientTemp = data.OutdoorTemperature(hour);
    [~, idx] = min(abs(copTable(:, 1) - ambientTemp));
    copForThisHour = copTable(idx, 2);

    % Simple direct heating with heat pump, no storage
    if data.(heatDemandField)(hour) > 0
        baseline_data.([sprintf('B%d_hp_operation', bldg)])(hour) = 1;
        baseline_data.([sprintf('B%d_HP_elec_demand', bldg)])(hour) =
data.(heatDemandField)(hour) / copForThisHour;
        baseline_data.([sprintf('B%d_electricity_demand_tot', bldg)])(hour) =
data.(elecDemandField)(hour) + baseline_data.([sprintf('B%d_HP_elec_demand',
bldg)])(hour);
        baseline_data.([sprintf('B%d_heat_demand_met', bldg)])(hour) = true;

        % Calculate costs for each tariff
        % Standard rate
        baseline_data.([sprintf('B%d_hp_cost_standard', bldg)])(hour) =
baseline_data.([sprintf('B%d_HP_elec_demand', bldg)])(hour) * STANDARD_RATE;

        % Economy 7
        current_hour = mod(hour-1, 24);
        if current_hour >= OFF_PEAK_START && current_hour < OFF_PEAK_END
            rate = OFF_PEAK_RATE;
        else
            rate = PEAK_RATE;
        end
        baseline_data.([sprintf('B%d_hp_cost_economy7', bldg)])(hour) =
baseline_data.([sprintf('B%d_HP_elec_demand', bldg)])(hour) * rate;

        % Agile pricing (using data from file)
```

```
            baseline_data.([sprintf('B%d_hp_cost_agile', bldg)])(hour) =
baseline_data.([sprintf('B%d_HP_elec_demand', bldg)])(hour) * data.ElectricityPrice(hour);
        else
            baseline_data.([sprintf('B%d_electricity_demand_tot', bldg)])(hour) =
data.(elecDemandField)(hour);
        end
    end
end

%% FIXED THRESHOLD SCENARIO
if scenario_to_run == 2 || scenario_to_run == 4
    % Initialize fields for fixed threshold model
    fixed_data.([sprintf('B%d_storage_state', bldg)]) = zeros(height(data), 1);
    fixed_data.([sprintf('B%d_hp_operation', bldg)]) = zeros(height(data), 1);
    fixed_data.([sprintf('B%d_HP_elec_demand', bldg)]) = zeros(height(data), 1);
    fixed_data.([sprintf('B%d_storage_operation', bldg)]) = zeros(height(data), 1);
    fixed_data.([sprintf('B%d_electricity_demand_tot', bldg)]) = zeros(height(data), 1);
    fixed_data.([sprintf('B%d_heat_demand_met', bldg)]) = false(height(data), 1);

    % Initialize cost fields for different tariffs
    fixed_data.([sprintf('B%d_hp_cost_standard', bldg)]) = zeros(height(data), 1);
    fixed_data.([sprintf('B%d_hp_cost_economy7', bldg)]) = zeros(height(data), 1);
    fixed_data.([sprintf('B%d_hp_cost_agile', bldg)]) = zeros(height(data), 1);

    prev_storage = initial_storage;

    % Main simulation loop for fixed threshold approach
    for hour = 1:height(data)
        % Get COP based on ambient temperature
        ambientTemp = data.OutdoorTemperature(hour);
        [~, idx] = min(abs(copTable(:, 1) - ambientTemp));
        copForThisHour = copTable(idx, 2);
```

```
        % Fixed threshold control logic
        % Case 1: Direct heating when LV demand below T1
        if data.(heatDemandField)(hour) > 0 && data.LV_demand(hour) < FIXED_T1
            if data.(heatDemandField)(hour) <= HP_max
                % Heat demand can be met directly by HP
                fixed_data.([sprintf('B%d_hp_operation', bldg)])(hour) = 1;
                fixed_data.([sprintf('B%d_HP_elec_demand', bldg)])(hour) = 
data.(heatDemandField)(hour) / copForThisHour;
                fixed_data.([sprintf('B%d_storage_state', bldg)])(hour) = prev_storage;
                fixed_data.([sprintf('B%d_electricity_demand_tot', bldg)])(hour) = 
data.(elecDemandField)(hour) + fixed_data.([sprintf('B%d_HP_elec_demand', bldg)])(hour);
            else
                % Heat demand exceeds HP capacity, use storage to supplement
                fixed_data.([sprintf('B%d_hp_operation', bldg)])(hour) = 1;
                fixed_data.([sprintf('B%d_HP_elec_demand', bldg)])(hour) = HP_max / 
copForThisHour;
                storage_needed = data.(heatDemandField)(hour) - HP_max;
                fixed_data.([sprintf('B%d_storage_state', bldg)])(hour) = max(prev_storage - 
storage_needed, 0);
                fixed_data.([sprintf('B%d_electricity_demand_tot', bldg)])(hour) = 
data.(elecDemandField)(hour) + fixed_data.([sprintf('B%d_HP_elec_demand', bldg)])(hour);
            end

% Case 2: Storage charging when LV demand below T2 and no immediate heat demand
        elseif data.LV_demand(hour) < FIXED_T2 && data.(heatDemandField)(hour) == 0
            if prev_storage < storage_capacity
                fixed_data.([sprintf('B%d_hp_operation', bldg)])(hour) = 1;
                charge_amount = min(storage_capacity - prev_storage, charging_rate);
                fixed_data.([sprintf('B%d_storage_state', bldg)])(hour) = prev_storage + 
charge_amount;
                fixed_data.([sprintf('B%d_HP_elec_demand', bldg)])(hour) = HP_max / 
(copForThisHour * 2); % Run at half capacity for charging
                fixed_data.([sprintf('B%d_electricity_demand_tot', bldg)])(hour) = 
data.(elecDemandField)(hour) + fixed_data.([sprintf('B%d_HP_elec_demand', bldg)])(hour);
            else
```

```
            fixed_data.([sprintf('B%d_hp_operation', bldg)])(hour) = 0;
            fixed_data.([sprintf('B%d_storage_state', bldg)])(hour) = prev_storage;
            fixed_data.([sprintf('B%d_electricity_demand_tot', bldg)])(hour) =
data.(elecDemandField)(hour);
        end

    % Case 3: Use storage when LV demand above T1 and heat demand exists
    elseif data.(heatDemandField)(hour) > 0 && data.LV_demand(hour) > FIXED_T1
        if prev_storage >= data.(heatDemandField)(hour)
            % Sufficient storage to meet demand
            fixed_data.([sprintf('B%d_storage_state', bldg)])(hour) = prev_storage -
data.(heatDemandField)(hour);
            fixed_data.([sprintf('B%d_HP_elec_demand', bldg)])(hour) = 0;
            fixed_data.([sprintf('B%d_hp_operation', bldg)])(hour) = 0;
            fixed_data.([sprintf('B%d_storage_operation', bldg)])(hour) = 1;
            fixed_data.([sprintf('B%d_electricity_demand_tot', bldg)])(hour) =
data.(elecDemandField)(hour);
        else
            % Insufficient storage, use HP to supplement
            fixed_data.([sprintf('B%d_storage_state', bldg)])(hour) = 0;
            fixed_data.([sprintf('B%d_HP_elec_demand', bldg)])(hour) =
(data.(heatDemandField)(hour) - prev_storage) / copForThisHour;
            fixed_data.([sprintf('B%d_hp_operation', bldg)])(hour) = 1;
            fixed_data.([sprintf('B%d_storage_operation', bldg)])(hour) = (prev_storage >
0);
            fixed_data.([sprintf('B%d_electricity_demand_tot', bldg)])(hour) =
data.(elecDemandField)(hour) + fixed_data.([sprintf('B%d_HP_elec_demand', bldg)])(hour);
        end

    % Case 4: No action needed
    else
        fixed_data.([sprintf('B%d_storage_state', bldg)])(hour) = prev_storage;
        fixed_data.([sprintf('B%d_electricity_demand_tot', bldg)])(hour) =
data.(elecDemandField)(hour);
    end
```

```
        % Calculate costs for each tariff if heat pump was used
        if fixed_data.([sprintf('B%d_HP_elec_demand', bldg)])(hour) > 0
            % Standard rate
            fixed_data.([sprintf('B%d_hp_cost_standard', bldg)])(hour) =
fixed_data.([sprintf('B%d_HP_elec_demand', bldg)])(hour) * STANDARD_RATE;

            % Economy 7
            current_hour = mod(hour-1, 24);
            if current_hour >= OFF_PEAK_START && current_hour < OFF_PEAK_END
                rate = OFF_PEAK_RATE;
            else
                rate = PEAK_RATE;
            end
            fixed_data.([sprintf('B%d_hp_cost_economy7', bldg)])(hour) =
fixed_data.([sprintf('B%d_HP_elec_demand', bldg)])(hour) * rate;

            % Agile pricing
            fixed_data.([sprintf('B%d_hp_cost_agile', bldg)])(hour) =
fixed_data.([sprintf('B%d_HP_elec_demand', bldg)])(hour) * data.ElectricityPrice(hour);
        end

        % Check if heat demand is met
        heat_from_hp = fixed_data.([sprintf('B%d_HP_elec_demand', bldg)])(hour) *
copForThisHour;
        storage_change = 0;
        if hour > 1
            storage_change = fixed_data.([sprintf('B%d_storage_state', bldg)])(hour-1) -
fixed_data.([sprintf('B%d_storage_state', bldg)])(hour);
        else
            storage_change = initial_storage - fixed_data.([sprintf('B%d_storage_state',
bldg)])(hour);
        end
        heat_from_storage = max(0, storage_change);
```

```
        heat_provided = heat_from_hp + heat_from_storage + 0.01; % Small margin for
numerical stability

        fixed_data.([sprintf('B%d_heat_demand_met', bldg)])(hour) = (heat_provided >=
data.(heatDemandField)(hour));

        % Update previous storage for next iteration
        prev_storage = fixed_data.([sprintf('B%d_storage_state', bldg)])(hour);
    end
end

%% ACTIVE BUILDING MODEL WITH DAILY OPTIMIZATION
if scenario_to_run == 3 || scenario_to_run == 4
    % Initialize fields for active building model
    active_data.([sprintf('B%d_storage_state', bldg)]) = zeros(height(data), 1);
    active_data.([sprintf('B%d_hp_operation', bldg)]) = zeros(height(data), 1);
    active_data.([sprintf('B%d_HP_elec_demand', bldg)]) = zeros(height(data), 1);
    active_data.([sprintf('B%d_storage_operation', bldg)]) = zeros(height(data), 1);
    active_data.([sprintf('B%d_electricity_demand_tot', bldg)]) = zeros(height(data), 1);
    active_data.([sprintf('B%d_heat_demand_met', bldg)]) = false(height(data), 1);

    % Initialize cost fields for different tariffs
    active_data.([sprintf('B%d_hp_cost_standard', bldg)]) = zeros(height(data), 1);
    active_data.([sprintf('B%d_hp_cost_economy7', bldg)]) = zeros(height(data), 1);
    active_data.([sprintf('B%d_hp_cost_agile', bldg)]) = zeros(height(data), 1);

    % Process data day by day for active building model
    for day = 1:numDays
        dayStart = (day-1)*24 + 1;
        dayEnd = day*24;

        % Skip incomplete days at the end of dataset
        if dayEnd > height(data)
```

```
            continue;
        end

        dayData = data(dayStart:dayEnd, :);

        % Optimize thresholds for the day based on predicted conditions

        [threshold1, threshold2] = optimizeThresholds(dayData, bldg, HP_max,
storage_capacity, charging_rate, copTable);

        % Store the optimized thresholds
        daily_thresholds(day, 1, bldg) = threshold1;
        daily_thresholds(day, 2, bldg) = threshold2;

        % Apply optimized thresholds for each hour of the day
        prev_storage = initial_storage;
        if day > 1
            prev_storage = active_data.([sprintf('B%d_storage_state', bldg)])(dayStart-1);
        end

        for hour = dayStart:dayEnd
            ambientTemp = data.OutdoorTemprature(hour);
            [~, idx] = min(abs(copTable(:, 1) - ambientTemp));
            copForThisHour = copTable(idx, 2);

            hourly_cop(hour, bldg) = copForThisHour;

            % Active building model control logic with optimized thresholds
            if data.(heatDemandField)(hour) > 0 && data.LV_demand(hour) < threshold1
                if data.(heatDemandField)(hour) <= HP_max
                    active_data.([sprintf('B%d_hp_operation', bldg)])(hour) = 1;
                    active_data.([sprintf('B%d_HP_elec_demand', bldg)])(hour) =
data.(heatDemandField)(hour) / copForThisHour;
```

```
                active_data.([sprintf('B%d_storage_state', bldg)])(hour) = prev_storage;

                active_data.([sprintf('B%d_electricity_demand_tot', bldg)])(hour) =
data.(elecDemandField)(hour) + active_data.([sprintf('B%d_HP_elec_demand',
bldg)])(hour);

            else

                active_data.([sprintf('B%d_hp_operation', bldg)])(hour) = 1;

                active_data.([sprintf('B%d_HP_elec_demand', bldg)])(hour) = HP_max /
copForThisHour;

                storage_needed = data.(heatDemandField)(hour) - HP_max;

                active_data.([sprintf('B%d_storage_state', bldg)])(hour) = max(prev_storage -
storage_needed, 0);

                active_data.([sprintf('B%d_electricity_demand_tot', bldg)])(hour) =
data.(elecDemandField)(hour) + active_data.([sprintf('B%d_HP_elec_demand',
bldg)])(hour);

            end

        elseif data.LV_demand(hour) < threshold2 && data.(heatDemandField)(hour) ==
0

            if prev_storage < storage_capacity

                active_data.([sprintf('B%d_hp_operation', bldg)])(hour) = 1;

                charge_amount = min(storage_capacity - prev_storage, charging_rate);

                active_data.([sprintf('B%d_storage_state', bldg)])(hour) = prev_storage +
charge_amount;

                active_data.([sprintf('B%d_HP_elec_demand', bldg)])(hour) = HP_max /
(copForThisHour * 2);

                active_data.([sprintf('B%d_electricity_demand_tot', bldg)])(hour) =
data.(elecDemandField)(hour) + active_data.([sprintf('B%d_HP_elec_demand',
bldg)])(hour);

            else

                active_data.([sprintf('B%d_hp_operation', bldg)])(hour) = 0;

                active_data.([sprintf('B%d_storage_state', bldg)])(hour) = prev_storage;

                active_data.([sprintf('B%d_electricity_demand_tot', bldg)])(hour) =
data.(elecDemandField)(hour);

            end

        elseif data.(heatDemandField)(hour) > 0 && data.LV_demand(hour) > threshold1

            if prev_storage >= data.(heatDemandField)(hour)

                active_data.([sprintf('B%d_storage_state', bldg)])(hour) = prev_storage -
data.(heatDemandField)(hour);
```

```
                active_data.([sprintf('B%d_HP_elec_demand', bldg)])(hour) = 0;
                active_data.([sprintf('B%d_hp_operation', bldg)])(hour) = 0;
                active_data.([sprintf('B%d_storage_operation', bldg)])(hour) = 1;
                active_data.([sprintf('B%d_electricity_demand_tot', bldg)])(hour) =
data.(elecDemandField)(hour);
            else
                active_data.([sprintf('B%d_storage_state', bldg)])(hour) = prev_storage -
min(prev_storage, data.(heatDemandField)(hour));
                active_data.([sprintf('B%d_HP_elec_demand', bldg)])(hour) =
(data.(heatDemandField)(hour) - prev_storage) / copForThisHour;
                active_data.([sprintf('B%d_hp_operation', bldg)])(hour) = 1;
                active_data.([sprintf('B%d_storage_operation', bldg)])(hour) = prev_storage >
0;
                active_data.([sprintf('B%d_electricity_demand_tot', bldg)])(hour) =
data.(elecDemandField)(hour) + active_data.([sprintf('B%d_HP_elec_demand',
bldg)])(hour);
            end
        else
            active_data.([sprintf('B%d_electricity_demand_tot', bldg)])(hour) =
data.(elecDemandField)(hour);
            active_data.([sprintf('B%d_storage_state', bldg)])(hour) = prev_storage;
        end

        % Calculate costs for each tariff if heat pump was used
        if active_data.([sprintf('B%d_HP_elec_demand', bldg)])(hour) > 0
            % Standard rate
            active_data.([sprintf('B%d_hp_cost_standard', bldg)])(hour) =
active_data.([sprintf('B%d_HP_elec_demand', bldg)])(hour) * STANDARD_RATE;

            % Economy 7
            current_hour = mod(hour-1, 24);
            if current_hour >= OFF_PEAK_START && current_hour < OFF_PEAK_END
                rate = OFF_PEAK_RATE;
            else
                rate = PEAK_RATE;
```

```
            end

            active_data.([sprintf('B%d_hp_cost_economy7', bldg)])(hour) =
active_data.([sprintf('B%d_HP_elec_demand', bldg)])(hour) * rate;


            % Agile pricing

            active_data.([sprintf('B%d_hp_cost_agile', bldg)])(hour) =
active_data.([sprintf('B%d_HP_elec_demand', bldg)])(hour) * data.ElectricityPrice(hour);

        end


        % Check if heat demand is met

        heat_from_hp = active_data.([sprintf('B%d_HP_elec_demand', bldg)])(hour) *
copForThisHour;

        storage_change = max(0, prev_storage - active_data.([sprintf('B%d_storage_state',
bldg)])(hour));

        heat_provided = heat_from_hp + storage_change + 0.01;


        active_data.([sprintf('B%d_heat_demand_met', bldg)])(hour) = (heat_provided >=
data.(heatDemandField)(hour));


        % Update previous storage for next iteration

        prev_storage = active_data.([sprintf('B%d_storage_state', bldg)])(hour);

      end

    end

  end

end


%% CALCULATE AGGREGATE METRICS

fprintf('Calculating aggregate performance metrics...\n');


% Calculate total electricity demand and costs across all buildings

if scenario_to_run == 1 || scenario_to_run == 4

  baseline_data.total_electricity_demand = sum(baseline_data{:,
contains(baseline_data.Properties.VariableNames, 'electricity_demand_tot')}, 2);
```

```
    % Sum costs for each tariff type
    baseline_data.total_hp_cost_standard = sum(baseline_data{:,
contains(baseline_data.Properties.VariableNames, 'hp_cost_standard')}, 2);
    baseline_data.total_hp_cost_economy7 = sum(baseline_data{:,
contains(baseline_data.Properties.VariableNames, 'hp_cost_economy7')}, 2);
    baseline_data.total_hp_cost_agile = sum(baseline_data{:,
contains(baseline_data.Properties.VariableNames, 'hp_cost_agile')}, 2);
end

if scenario_to_run == 2 || scenario_to_run == 4
    fixed_data.total_electricity_demand = sum(fixed_data{:,
contains(fixed_data.Properties.VariableNames, 'electricity_demand_tot')}, 2);

    % Sum costs for each tariff type
    fixed_data.total_hp_cost_standard = sum(fixed_data{:,
contains(fixed_data.Properties.VariableNames, 'hp_cost_standard')}, 2);
    fixed_data.total_hp_cost_economy7 = sum(fixed_data{:,
contains(fixed_data.Properties.VariableNames, 'hp_cost_economy7')}, 2);
    fixed_data.total_hp_cost_agile = sum(fixed_data{:,
contains(fixed_data.Properties.VariableNames, 'hp_cost_agile')}, 2);
end

if scenario_to_run == 3 || scenario_to_run == 4
    active_data.total_electricity_demand = sum(active_data{:,
contains(active_data.Properties.VariableNames, 'electricity_demand_tot')}, 2);

    % Sum costs for each tariff type
    active_data.total_hp_cost_standard = sum(active_data{:,
contains(active_data.Properties.VariableNames, 'hp_cost_standard')}, 2);
    active_data.total_hp_cost_economy7 = sum(active_data{:,
contains(active_data.Properties.VariableNames, 'hp_cost_economy7')}, 2);
    active_data.total_hp_cost_agile = sum(active_data{:,
contains(active_data.Properties.VariableNames, 'hp_cost_agile')}, 2);
end

%% PRINT SUMMARY STATISTICS
```

```
fprintf('\n----- PERFORMANCE SUMMARY -----\n');

if scenario_to_run == 1 || scenario_to_run == 4
    fprintf('\nBASELINE SCENARIO:\n');
    fprintf('Peak Demand: %.2f kW\n', max(baseline_data.total_electricity_demand));
    fprintf('Total Energy Consumption: %.2f kWh\n',
sum(baseline_data.total_electricity_demand));
    fprintf('Total Cost (Standard Rate): £%.2f\n', sum(baseline_data.total_hp_cost_standard));
    fprintf('Total Cost (Economy 7): £%.2f\n', sum(baseline_data.total_hp_cost_economy7));
    fprintf('Total Cost (Agile): £%.2f\n', sum(baseline_data.total_hp_cost_agile));
end

if scenario_to_run == 2 || scenario_to_run == 4
    fprintf('\nFIXED THRESHOLD MODEL:\n');
    fprintf('Peak Demand: %.2f kW\n', max(fixed_data.total_electricity_demand));
    fprintf('Total Energy Consumption: %.2f kWh\n',
sum(fixed_data.total_electricity_demand));
    fprintf('Total Cost (Standard Rate): £%.2f\n', sum(fixed_data.total_hp_cost_standard));
    fprintf('Total Cost (Economy 7): £%.2f\n', sum(fixed_data.total_hp_cost_economy7));
    fprintf('Total Cost (Agile): £%.2f\n', sum(fixed_data.total_hp_cost_agile));

    if scenario_to_run == 4
        baseline_peak = max(baseline_data.total_electricity_demand);
        baseline_energy = sum(baseline_data.total_electricity_demand);

        fprintf('Peak Reduction vs Baseline: %.2f%% \n', (baseline_peak -
max(fixed_data.total_electricity_demand)) / baseline_peak * 100);
        fprintf('Energy Change vs Baseline: %.2f%% \n',
(sum(fixed_data.total_electricity_demand) - baseline_energy) / baseline_energy * 100);
    end
end

if scenario_to_run == 3 || scenario_to_run == 4
    fprintf('\nACTIVE BUILDING MODEL:\n');
```

```
    fprintf('Peak Demand: %.2f kW\n', max(active_data.total_electricity_demand));
    fprintf('Total Energy Consumption: %.2f kWh\n',
sum(active_data.total_electricity_demand));
    fprintf('Total Cost (Standard Rate): £%.2f\n', sum(active_data.total_hp_cost_standard));
    fprintf('Total Cost (Economy 7): £%.2f\n', sum(active_data.total_hp_cost_economy7));
    fprintf('Total Cost (Agile): £%.2f\n', sum(active_data.total_hp_cost_agile));

    if scenario_to_run == 4
        baseline_peak = max(baseline_data.total_electricity_demand);
        baseline_energy = sum(baseline_data.total_electricity_demand);

        fprintf('Peak Reduction vs Baseline: %.2f%% \n', (baseline_peak -
max(active_data.total_electricity_demand)) / baseline_peak * 100);
        fprintf('Energy Change vs Baseline: %.2f%% \n',
(sum(active_data.total_electricity_demand) - baseline_energy) / baseline_energy * 100);
    end
end

% Export results if running all scenarios
if scenario_to_run == 4
    % Create combined results table
    fprintf('\nExporting combined results to %s\n', resultsPath);

    results = table();
    results.Time = data.Time;
    results.OutdoorTemperature = data.OutdoorTemperature;
    results.ElectricityPrice = data.ElectricityPrice;
    results.Baseline_Total_Demand = baseline_data.total_electricity_demand;
    results.Fixed_Total_Demand = fixed_data.total_electricity_demand;
    results.Active_Total_Demand = active_data.total_electricity_demand;

    % Export to CSV
    writetable(results, resultsPath);
```

```
    % Create a summary table with key metrics
    summary = table();
    summary.Scenario = {'Baseline'; 'Fixed Threshold'; 'Active Building'};
    summary.PeakDemand_kW = [max(baseline_data.total_electricity_demand);
                             max(fixed_data.total_electricity_demand);
                             max(active_data.total_electricity_demand)];
    summary.TotalEnergy_kWh = [sum(baseline_data.total_electricity_demand);
                               sum(fixed_data.total_electricity_demand);
                               sum(active_data.total_electricity_demand)];

    % Calculate reductions
    baseline_peak = max(baseline_data.total_electricity_demand);
    baseline_energy = sum(baseline_data.total_electricity_demand);

    summary.PeakReduction_pct = [0;
                                 (baseline_peak -
max(fixed_data.total_electricity_demand))/baseline_peak*100;
                                 (baseline_peak -
max(active_data.total_electricity_demand))/baseline_peak*100];

    summary.EnergyChange_pct = [0;
                                (sum(fixed_data.total_electricity_demand) -
baseline_energy)/baseline_energy*100;
                                (sum(active_data.total_electricity_demand) -
baseline_energy)/baseline_energy*100];

    % Export summary
    writetable(summary, 'performance_summary.csv');
    fprintf('Summary metrics exported to performance_summary.csv\n');
end

fprintf('Simulation complete.\n');
```

```
%% HELPER FUNCTIONS
function [threshold1, threshold2] = optimizeThresholds(dayData, bldg, HP_max, storage_capacity, charging_rate, copTable)
    % Optimizes operational thresholds for a specific building and day
    %
    % INPUTS:
    %   dayData - Table with 24 hours of data for the day being optimized
    %   bldg - Building ID
    %   HP_max - Maximum heat pump capacity (kW)
    %   storage_capacity - Maximum thermal storage capacity (kWh)
    %   charging_rate - Maximum TES charging rate (kW)
    %   copTable - Temperature-COP lookup table
    %
    % OUTPUTS:
    %   threshold1 - Optimized threshold for direct HP operation (kW)
    %   threshold2 - Optimized threshold for TES charging (kW)

    % optimization: test a range of thresholds and choose the best
    best_peak_demand = inf;
    best_threshold1 = 140;  % Default values
    best_threshold2 = 180;  % Similar to fixed threshold model

    % Threshold search ranges
    t1_range = 30:10:200;  % Range with 10kW step size
    t2_range = 30:10:200;

    % Test all combinations

    for t1 = t1_range
        for t2 = t2_range
            % Simulate day with these threshold values
            [peak_demand, demand_met] = simulateDayWithThresholds(dayData, bldg, HP_max, storage_capacity, charging_rate, copTable, t1, t2);
```

```
            % Check if this is better than current best
            if peak_demand < best_peak_demand && demand_met > 0.99  % Ensure heat demand is satisfied
                best_peak_demand = peak_demand;
                best_threshold1 = t1;
                best_threshold2 = t2;
            end
        end
    end

    threshold1 = best_threshold1;
    threshold2 = best_threshold2;
end

function [peak_demand, demand_met] = simulateDayWithThresholds(dayData, bldg, HP_max, storage_capacity, charging_rate, copTable, threshold1, threshold2)
    % Simulates a day of operation with specified thresholds
    %
    % INPUTS:
    %   dayData - Table with 24 hours of data
    %   bldg - Building ID
    %   HP_max - Maximum heat pump capacity (kW)
    %   storage_capacity - Maximum thermal storage capacity (kWh)
    %   charging_rate - Maximum TES charging rate (kW)
    %   copTable - Temperature-COP lookup table
    %   threshold1 - Threshold for direct HP operation (kW)
    %   threshold2 - Threshold for TES charging (kW)
    %
    % OUTPUTS:
    %   peak_demand - Maximum electricity demand during simulation (kW)
    %   demand_met - Ratio of satisfied heat demand (0-1)
```

```
% Initialize variables
numHours = height(dayData);
storage_state = zeros(numHours, 1);
hp_operation = zeros(numHours, 1);
hp_elec_demand = zeros(numHours, 1);
storage_operation = zeros(numHours, 1);
elec_demand_tot = zeros(numHours, 1);
heat_demand_met = zeros(numHours, 1);

% Initial storage state (assumed known from previous day)
initial_storage = 7;  % kWh
prev_storage = initial_storage;

% Generate field names for dynamic access
heatDemandField = sprintf('HeatBuilding%d', bldg);
elecDemandField = sprintf('ElectricityBuilding%d', bldg);

% Simulation variables
total_heat_demand = 0;
total_heat_met = 0;

% Run hour-by-hour simulation
for hour = 1:numHours
    % Get COP based on ambient temperature
    ambientTemp = dayData.OutdoorTemperature(hour);
    [~, idx] = min(abs(copTable(:, 1) - ambientTemp));
    copForThisHour = copTable(idx, 2);

    % Hourly values from data
    hourly_heat_demand = dayData.(heatDemandField)(hour);
    hourly_elec_demand = dayData.(elecDemandField)(hour);
    hourly_LV_demand = dayData.LV_demand(hour);
```

```
total_heat_demand = total_heat_demand + hourly_heat_demand;

% Control logic - follows same structure as main simulation
if hourly_heat_demand > 0 && hourly_LV_demand < threshold1
    if hourly_heat_demand <= HP_max
        hp_operation(hour) = 1;
        hp_elec_demand(hour) = hourly_heat_demand / copForThisHour;
        storage_state(hour) = prev_storage;
        elec_demand_tot(hour) = hourly_elec_demand + hp_elec_demand(hour);
        total_heat_met = total_heat_met + hourly_heat_demand;
    else
        hp_operation(hour) = 1;
        hp_elec_demand(hour) = HP_max / copForThisHour;
        storage_needed = hourly_heat_demand - HP_max;
        storage_state(hour) = max(prev_storage - storage_needed, 0);
        elec_demand_tot(hour) = hourly_elec_demand + hp_elec_demand(hour);
        total_heat_met = total_heat_met + HP_max + (prev_storage - storage_state(hour));
    end
elseif hourly_LV_demand < threshold2 && hourly_heat_demand == 0
    if prev_storage < storage_capacity
        hp_operation(hour) = 1;
        charge_amount = min(storage_capacity - prev_storage, charging_rate);
        storage_state(hour) = prev_storage + charge_amount;
        hp_elec_demand(hour) = HP_max / (copForThisHour * 2);
        elec_demand_tot(hour) = hourly_elec_demand + hp_elec_demand(hour);
    else
        hp_operation(hour) = 0;
        storage_state(hour) = prev_storage;
        elec_demand_tot(hour) = hourly_elec_demand;
    end
elseif hourly_heat_demand > 0 && hourly_LV_demand > threshold1
```

```
            if prev_storage >= hourly_heat_demand
                storage_state(hour) = prev_storage - hourly_heat_demand;
                hp_elec_demand(hour) = 0;
                hp_operation(hour) = 0;
                storage_operation(hour) = 1;
                elec_demand_tot(hour) = hourly_elec_demand;
                total_heat_met = total_heat_met + hourly_heat_demand;
            else
                storage_state(hour) = 0;
                hp_elec_demand(hour) = (hourly_heat_demand - prev_storage) / copForThisHour;
                hp_operation(hour) = 1;
                storage_operation(hour) = (prev_storage > 0);
                elec_demand_tot(hour) = hourly_elec_demand + hp_elec_demand(hour);
                total_heat_met = total_heat_met + hourly_heat_demand;
            end
        else
            elec_demand_tot(hour) = hourly_elec_demand;
            storage_state(hour) = prev_storage;
        end

        % Update previous storage for next iteration
        prev_storage = storage_state(hour);
    end

    % Calculate peak demand and demand satisfaction metrics
    peak_demand = max(elec_demand_tot);
    if total_heat_demand > 0
        demand_met = total_heat_met / total_heat_demand;
    else
        demand_met = 1;  % No heat demand to meet
    end
end
```

Appendix B: HP Manufacturers' Data

Table 0.1: Mitsubishi HTHP Performance Datasheet (MITSUBISHI ELECTRIC, 2018)

Water outlet temperature [°C]		25		35		40		45		50		55		60	
Ambient temperature [°C]		Capacity	COP	Capacity	COP	Capacity	COP	Capacity	COP	Capacity	COP	Capacity	COP	Capacity	COP
Max	-20	-	-	4.9	1.89	4.9	1.70	4.9	1.52	-	-	-	-	-	-
	-15	-	-	6.1	2.15	6.1	1.95	6.1	1.74	-	-	-	-	-	-
	-10	7.3	2.94	7.3	2.41	7.3	2.19	7.3	1.97	7.6	1.79	7.9	1.62	-	-
	-7	8.0	3.42	8.0	2.57	8.0	2.34	8.0	2.10	8.0	1.92	8.0	1.73	-	-
	2	8.5	3.61	8.5	3.17	8.5	2.89	8.5	2.61	8.5	2.34	8.4	2.06	8.4	1.82
	7	9.0	5.33	9.0	4.19	9.0	3.72	9.0	3.24	9.0	2.88	9.0	2.51	9.0	2.23
	12	9.0	5.69	9.1	4.74	9.2	4.17	9.4	3.59	9.2	3.17	9.1	2.76	9.1	2.37
	15	9.1	6.12	9.1	5.08	9.3	4.44	9.6	3.80	9.4	3.35	9.2	2.90	9.2	2.46
	20	9.1	6.86	9.2	5.63	9.5	4.89	9.9	4.15	9.6	3.65	9.4	3.15	9.4	2.60
Nominal	-20	-	-	4.9	1.89	4.9	1.70	4.9	1.52	-	-	-	-	-	-
	-15	-	-	6.1	2.15	6.1	1.95	6.1	1.74	-	-	-	-	-	-
	-10	7.3	2.94	7.3	2.41	7.3	2.19	7.3	1.97	7.6	1.79	7.9	1.62	-	-
	-7	8.0	3.42	8.0	2.57	8.0	2.34	8.0	2.10	8.0	1.92	8.0	1.73	-	-
	2	8.5	3.61	8.5	3.17	8.5	2.89	8.5	2.61	8.5	2.34	8.4	2.06	8.4	1.82
	7	9.0	5.33	9.0	4.19	9.0	3.72	9.0	3.24	9.0	2.88	9.0	2.51	9.0	2.23
	12	9.0	5.69	9.1	4.74	9.2	4.17	9.4	3.59	9.2	3.17	9.1	2.76	9.1	2.37
	15	9.1	6.12	9.1	5.08	9.3	4.44	9.6	3.80	9.4	3.35	9.2	2.90	9.2	2.46
	20	9.1	6.86	9.2	5.63	9.5	4.89	9.9	4.15	9.6	3.65	9.4	3.15	9.4	2.60
Mid	-20	-	-	5.3	2.29	5.1	2.03	4.9	1.78	-	-	-	-	-	-
	-15	-	-	5.7	2.55	5.5	2.30	5.4	2.04	-	-	-	-	-	-
	-10	6.2	3.15	6.0	2.81	6.0	2.56	5.9	2.30	6.2	2.12	6.5	1.94	-	-
	-7	6.3	3.54	6.2	2.97	6.2	2.72	6.2	2.46	6.2	2.25	6.3	2.04	-	-
	2	5.6	4.27	5.6	3.90	5.6	3.50	5.6	3.10	5.5	2.72	5.4	2.34	5.4	2.09
	7	6.3	5.58	5.8	4.66	5.6	4.11	5.4	3.56	5.5	3.12	5.5	2.68	5.6	2.34
	12	6.3	6.58	6.0	5.39	5.9	4.70	5.8	4.00	5.8	3.49	5.9	2.99	5.9	2.63
	15	6.4	7.26	6.1	5.84	6.1	5.05	6.0	4.26	6.0	3.72	6.1	3.17	6.1	2.81
	20	6.4	8.01	6.3	6.57	6.4	5.64	6.4	4.70	6.4	4.09	6.4	3.48	6.4	3.10
Min	-20	-	-	5.3	2.29	5.1	2.03	4.9	1.78	-	-	-	-	-	-
	-15	-	-	5.7	2.55	5.5	2.30	5.4	2.04	-	-	-	-	-	-
	-10	6.2	3.15	6.0	2.81	6.0	2.56	5.9	2.30	6.2	2.12	6.5	1.94	-	-
	-7	3.4	3.51	3.3	3.00	3.5	2.75	3.7	2.49	3.8	2.26	3.8	2.02	-	-
	2	3.4	4.69	3.3	4.01	3.3	3.44	3.2	2.86	3.2	2.52	3.2	2.18	-	-
	7	4.1	5.76	3.9	4.80	3.9	4.17	3.8	3.53	3.8	3.06	3.8	2.58	-	-
	12	4.7	7.02	4.5	5.65	4.5	4.85	4.4	4.06	4.4	3.50	4.5	2.94	-	-
	15	5.0	7.70	4.9	6.16	4.8	5.27	4.8	4.37	4.8	3.77	4.9	3.16	-	-
	20	5.6	8.66	5.5	7.01	5.4	5.96	5.3	4.90	5.5	4.21	5.6	3.52	-	-

Table 0.2: Samsung HTHP Performance Datasheet for multiple available capacities (SAMSUNG, 2022)

Model	LWT (°C)	25		30		35		40		45		50		55		60		65		70	
	Tamb (°C)	HC(kW)	PI(kW)	HC(kW)	PI(kW)	HC(kW)	PI(kW)	HC(kW)	PI(kW)	HC(kW)	PI(kW)	HC(kW)	PI(kW)	HC(kW)	PI(kW)	HC(kW)	PI(kW)	HC(kW)	PI(kW)	HC(kW)	PI(kW)
AE080BXYDGG/EU	-30	5.82	2.53	5.89	2.80	5.96	3.14	6.22	3.48	6.48	3.88	6.74	4.19	6.92	4.43	6.94	4.69				
	-25	8.00	3.47	8.00	3.63	8.00	3.79	8.00	4.03	8.00	4.28	8.00	4.49	8.00	4.85	8.40	5.17	8.80	5.85		
	-20	8.00	3.05	8.00	3.20	8.00	3.39	8.00	3.59	8.00	3.84	8.00	4.09	8.00	4.31	9.11	5.13	9.12	5.48		
	-15	8.00	2.61	8.00	2.86	8.00	3.14	8.00	3.36	8.00	3.61	8.00	3.84	8.00	4.01	9.35	4.87	9.54	5.24	8.00	4.85
	-10	8.00	2.28	8.00	2.47	8.00	2.72	8.00	2.88	8.00	3.06	8.00	3.33	8.00	3.56	9.65	4.48	10.01	4.96	10.46	5.40
	-7	8.00	2.10	8.00	2.34	8.00	2.46	8.00	2.64	8.00	2.87	8.00	3.10	8.00	3.26	10.19	4.39	10.43	4.81	10.79	5.18
	-2	8.00	1.95	8.00	2.05	8.00	2.10	8.00	2.32	8.00	2.57	8.00	2.69	8.00	2.79	10.36	3.92	10.80	4.62	11.04	4.86
	2	8.00	1.62	8.00	1.72	8.00	1.82	8.00	2.01	8.00	2.26	8.00	2.44	8.00	2.58	10.11	3.57	10.63	4.21	11.01	4.75
	7	8.00	1.29	8.00	1.43	8.00	1.60	8.00	1.80	8.00	2.05	8.00	2.23	8.00	2.50	9.11	3.16	9.66	3.79	10.03	4.29
	12	8.92	1.18	8.95	1.35	8.98	1.57	9.02	1.80	9.05	2.11	9.08	2.38	9.11	2.71	9.57	3.11	10.08	3.72	10.43	4.25
	15	9.10	1.09	9.14	1.26	9.20	1.49	9.26	1.71	9.30	2.01	9.36	2.29	9.42	2.62	9.85	3.01	10.33	3.59	10.67	4.10
	20	9.39	0.99	9.48	1.14	9.57	1.34	9.66	1.50	9.74	1.77	9.83	2.08	9.91	2.46	10.31	2.82	10.76	3.38	11.08	4.04
	25	9.69	0.93	9.82	1.07	9.93	1.24	10.06	1.42	10.17	1.66	10.30	1.96	10.41	2.32	10.78	2.67	11.18	3.20	11.48	3.99
	30	9.99	0.93	10.15	1.06	10.30	1.23	10.45	1.37	10.60	1.55	10.76	1.83	10.91	2.17	11.24	2.49	11.59	3.01	11.88	3.79
	35	10.29	0.92	10.48	1.03	10.66	1.17	10.75	1.29	10.99	1.46	11.22	1.73	11.41	2.04	11.70	2.35	12.02	2.85	12.28	3.62
	43	10.77	0.92	11.01	1.01	11.25	1.11	11.49	1.24	11.73	1.41	11.97	1.65	12.21	1.93	12.45	2.23	12.69	2.72	12.92	3.33
Model	LWT (°C)	25		30		35		40		45		50		55		60		65		70	
	Tamb (°C)	HC(kW)	PI(kW)	HC(kW)	PI(kW)	HC(kW)	PI(kW)	HC(kW)	PI(kW)	HC(kW)	PI(kW)	HC(kW)	PI(kW)	HC(kW)	PI(kW)	HC(kW)	PI(kW)	HC(kW)	PI(kW)	HC(kW)	PI(kW)
AE120BXYDGG/EU	-30	7.76	3.45	7.85	3.83	7.95	4.30	8.29	4.78	8.64	5.30	8.99	5.74	9.23	6.07	9.26	6.41				
	-25	11.23	5.00	11.62	5.43	12.00	5.83	12.00	6.20	12.00	6.58	12.00	6.90	12.00	7.27	12.00	7.59	12.00	8.19		
	-20	11.88	4.62	11.95	4.90	12.00	5.23	12.00	5.55	12.00	5.90	12.00	6.29	12.00	6.61	12.00	6.98	12.00	7.43		
	-15	12.00	4.02	12.00	4.38	12.00	4.53	12.00	5.16	12.00	5.55	12.00	5.89	12.00	6.17	12.00	6.42	12.00	6.77	12.00	7.27
	-10	12.00	3.82	12.00	4.04	12.00	4.29	12.00	4.54	12.00	4.81	12.00	5.25	12.00	5.58	12.86	6.28	13.34	6.92	13.95	7.57
	-7	12.00	3.42	12.00	3.60	12.00	3.81	12.00	4.14	12.00	4.51	12.00	4.87	12.00	5.16	13.59	6.13	13.90	6.73	14.38	7.21
	-2	12.00	3.01	12.00	3.11	12.00	3.29	12.00	3.64	12.00	4.03	12.00	4.23	12.00	4.38	13.81	5.47	14.40	6.46	14.72	6.78
	2	12.00	2.45	12.00	2.62	12.00	2.79	12.00	3.15	12.00	3.55	12.00	3.83	12.00	4.06	13.48	4.98	14.18	5.87	14.68	6.27
	7	12.00	1.90	12.00	2.10	12.00	2.35	12.00	2.64	12.00	3.00	12.00	3.26	12.00	3.53	13.66	4.46	14.49	5.35	15.05	6.17
	12	13.38	1.73	13.42	1.98	13.47	2.30	13.52	2.64	13.57	3.08	13.62	3.48	13.67	3.83	14.35	4.40	15.12	5.25	15.65	6.01
	15	13.64	1.61	13.72	1.85	13.80	2.18	13.88	2.51	13.96	2.94	14.04	3.35	14.12	3.70	14.78	4.25	15.50	5.07	16.01	5.78
	20	14.09	1.45	14.22	1.67	14.35	1.96	14.48	2.21	14.61	2.59	14.74	3.04	14.87	3.47	15.47	3.98	16.14	4.77	16.62	5.71
	25	14.54	1.37	14.72	1.56	14.90	1.82	15.08	2.08	15.26	2.43	15.44	2.87	15.62	3.28	16.17	3.76	16.76	4.52	17.22	5.63
	30	14.99	1.36	15.22	1.55	15.44	1.80	15.67	2.01	15.90	2.27	16.14	2.68	16.37	3.06	16.86	3.52	17.39	4.24	17.82	5.35
	35	15.43	1.35	15.72	1.51	16.00	1.71	16.27	1.91	16.53	2.14	16.84	2.53	17.11	2.89	17.56	3.32	18.03	4.02	18.42	5.11
	43	16.15	1.35	16.51	1.48	16.87	1.63	17.23	1.83	17.59	2.06	17.95	2.41	18.31	2.72	18.67	3.14	19.03	3.83	19.38	4.70
Model	LWT (°C)	25		30		35		40		45		50		55		60		65		70	
	Tamb (°C)	HC(kW)	PI(kW)	HC(kW)	PI(kW)	HC(kW)	PI(kW)	HC(kW)	PI(kW)	HC(kW)	PI(kW)	HC(kW)	PI(kW)	HC(kW)	PI(kW)	HC(kW)	PI(kW)	HC(kW)	PI(kW)	HC(kW)	PI(kW)
AE140BXYDGG/EU	-30	8.46	3.82	8.57	4.24	8.67	4.75	9.05	5.27	9.42	5.87	9.80	6.35	10.07	6.71	10.10	7.09				
	-25	12.25	5.53	12.68	5.99	13.11	6.48	13.26	6.94	13.41	7.47	13.75	8.05	14.00	8.48	13.68	8.78	13.29	9.20		
	-20	12.96	5.13	13.42	5.59	13.87	6.11	13.94	6.52	14.00	6.98	14.00	7.46	14.00	7.84	14.00	8.23	14.00	8.77		
	-15	13.86	4.72	13.78	5.12	13.70	5.59	13.85	6.05	14.00	6.58	14.00	6.98	14.00	7.30	14.00	7.60	14.00	8.01	14.00	8.48
	-10	13.91	4.49	13.94	4.75	13.97	5.05	13.99	5.35	14.00	5.69	14.00	6.20	14.00	6.61	14.00	6.93	14.00	7.37	14.65	8.05
	-7	13.93	4.15	13.97	4.32	14.00	4.52	14.00	4.90	14.00	5.35	14.00	5.76	14.00	6.09	14.27	6.54	14.60	7.19	15.10	7.70
	-2	13.95	3.54	13.98	3.74	14.00	3.90	14.00	4.30	14.00	4.78	14.00	5.00	14.00	5.17	14.50	5.84	15.12	6.87	15.46	7.22
	2	13.96	2.73	13.98	3.00	14.00	3.33	14.00	3.72	14.00	4.20	14.00	4.54	14.00	4.81	14.60	5.45	15.36	6.44	15.90	6.88
	7	14.00	2.24	14.00	2.48	14.00	2.77	14.00	3.11	14.00	3.54	14.00	3.85	14.00	4.18	14.00	4.90	15.70	5.88	16.30	6.78
	12	14.49	1.89	14.54	2.17	14.59	2.52	14.65	2.89	14.70	3.38	14.76	3.82	14.81	4.21	15.55	4.83	16.38	5.77	16.95	6.61
	15	14.78	1.76	14.86	2.03	14.95	2.39	15.04	2.75	15.12	3.23	15.21	3.67	15.30	4.07	16.01	4.67	16.79	5.58	17.34	6.36
	20	15.26	1.59	15.40	1.83	15.55	2.15	15.69	2.42	15.83	2.84	15.97	3.34	16.11	3.81	16.76	4.38	17.48	5.24	18.00	6.27
	25	15.75	1.50	15.95	1.71	16.14	1.99	16.34	2.29	16.53	2.67	16.73	3.15	16.92	3.61	17.52	4.14	18.16	4.97	18.65	6.19
	30	16.24	1.49	16.49	1.70	16.73	1.98	16.98	2.21	17.23	2.49	17.48	2.94	17.73	3.37	18.27	3.87	18.84	4.66	19.30	5.88
	35	16.72	1.48	17.03	1.66	17.33	1.88	17.63	2.09	17.91	2.35	18.24	2.77	18.54	3.17	19.02	3.65	19.53	4.42	19.96	5.62
	43	17.50	1.48	17.89	1.62	18.28	1.79	18.67	2.00	19.06	2.26	19.45	2.64	19.84	3.00	20.23	3.46	20.62	4.21	21.00	5.16

Appendix C: Optimisation Tool: Sample of Inputs and Outputs

Table 0.3: Sample of the Input Data into the Optimisation tool for Category 1 Building

Time	LV Peak demand kW	Electricity Price (Dynamic £/kWh)	Carbon Intensity gCO_2/kWh	Outdoor Temperature (°C)	Heat Demand kW	Electricity Demand kW
01/01/2022 01:00	86.48	0.0925	72.5	13.00	0	0.312
01/01/2022 02:00	98.83	0.1101	68.5	13.10	0	0.158
01/01/2022 03:00	58.99	0.0538	70	13.27	0	0.162
01/01/2022 04:00	82.67	0.0378	60.5	13.39	0	0.168
01/01/2022 05:00	44.85	-0.0006	58	13.34	0	0.152
01/01/2022 06:00	38.33	0.0116	53	13.30	1.785	0.159
01/01/2022 07:00	34.17	0.0105	50	13.06	3.109	0.16
01/01/2022 08:00	80.81	0.0565	47	13.04	3.134	0.149
01/01/2022 09:00	123.72	0.0840	50	13.13	2.769	3.169
01/01/2022 10:00	154.62	0.1218	50	13.32	1.062	0.244
01/01/2022 11:00	115.10	0.1134	48.5	14.05	0	0.404
01/01/2022 12:00	157.43	0.1493	44	13.83	0	0.362
01/01/2022 13:00	163.76	0.1229	54	14.00	0	3.471
01/01/2022 14:00	140.33	0.1631	53.5	14.20	0	0.458
01/01/2022 15:00	127.76	0.1499	57	14.45	0	3.454
01/01/2022 16:00	168.47	0.1470	64	14.51	1.839	0.461
01/01/2022 17:00	178.34	0.3368	75.5	13.93	2.723	3.35
01/01/2022 18:00	286.71	0.3381	78.5	13.32	2.614	5.644
01/01/2022 19:00	139.18	0.3039	82	12.97	2.309	4.277
01/01/2022 20:00	178.84	0.1251	69.5	12.78	1.904	0.552
01/01/2022 21:00	149.39	0.1176	74	12.75	1.873	0.506
01/01/2022 22:00	148.08	0.1237	65	12.31	1.954	3.639
01/01/2022 23:00	66.099	0.0638	56.5	11.78	0.875	0.276

Table 0.4: Sample of the output Data from the Optimisation tool for Category 1 Building (Active Building Model)

Time	Storage State	HP Operation	HP Electrical Demand	TES Operation	Total Electrical Demand (kW)	Heat Demand Satisfaction (1= yes, 0= No)
01/01/2022 01:00	9.5	1	0.70	0	1.01	1
01/01/2022 02:00	10	1	0.70	0	0.85	1
01/01/2022 03:00	10	0	0	0	0.16	1
01/01/2022 04:00	10	0	0	0	0.16	1
01/01/2022 05:00	10	0	0	0	0.15	1
01/01/2022 06:00	8.21	0	0	1	0.15	1
01/01/2022 07:00	5.10	0	0	1	0.1	1
01/01/2022 08:00	1.97	0	0	1	0.14	1
01/01/2022 09:00	0	1	0.22	1	3.39	1
01/01/2022 10:00	0	1	0.29	0	0.54	1
01/01/2022 11:00	2.50	1	0.65	0	1.0	1
01/01/2022 12:00	2.50	0	0	0	0.36	1
01/01/2022 13:00	2.50	0	0	0	3.47	1
01/01/2022 14:00	5.00	1	0.65	0	1.11	1
01/01/2022 15:00	7.50	1	0.65	0	4.10	1
01/01/2022 16:00	5.66	0	0	1	0.46	1
01/01/2022 17:00	2.93	0	0	1	3.35	1
01/01/2022 18:00	0.32	0	0	1	5.64	1
01/01/2022 19:00	0	1	0.55	1	4.83	1
01/01/2022 20:00	0	1	0.53	0	1.08	1
01/01/2022 21:00	0	1	0.52	0	1.03	1
01/01/2022 22:00	0	1	0.54	0	4.18	1
01/01/2022 23:00	0	1	0.24	0	0.52	1

Table 0.5: Sample of the summary of performance metrics from the optimisation tool

Scenario	Peak Demand (kW)	Total Cost Standard Tariff	Total Cost E7 Tariff	Total Cost Dynamic Tariff	Peak Reduction %	Cost Change Standard %	Cost Change E7 %	Cost Change Dynamic %
Baseline	497.44	59675	66967	49777	0	0	0	0
Fixed Threshold	421.93	66159	68622	45218	15.17	10.86	2.47	-9.15
Active Building	403.47	60806	58897	41068	18.89	1.89	-12.05	-17.49

Appendix D: The UK electricity grid

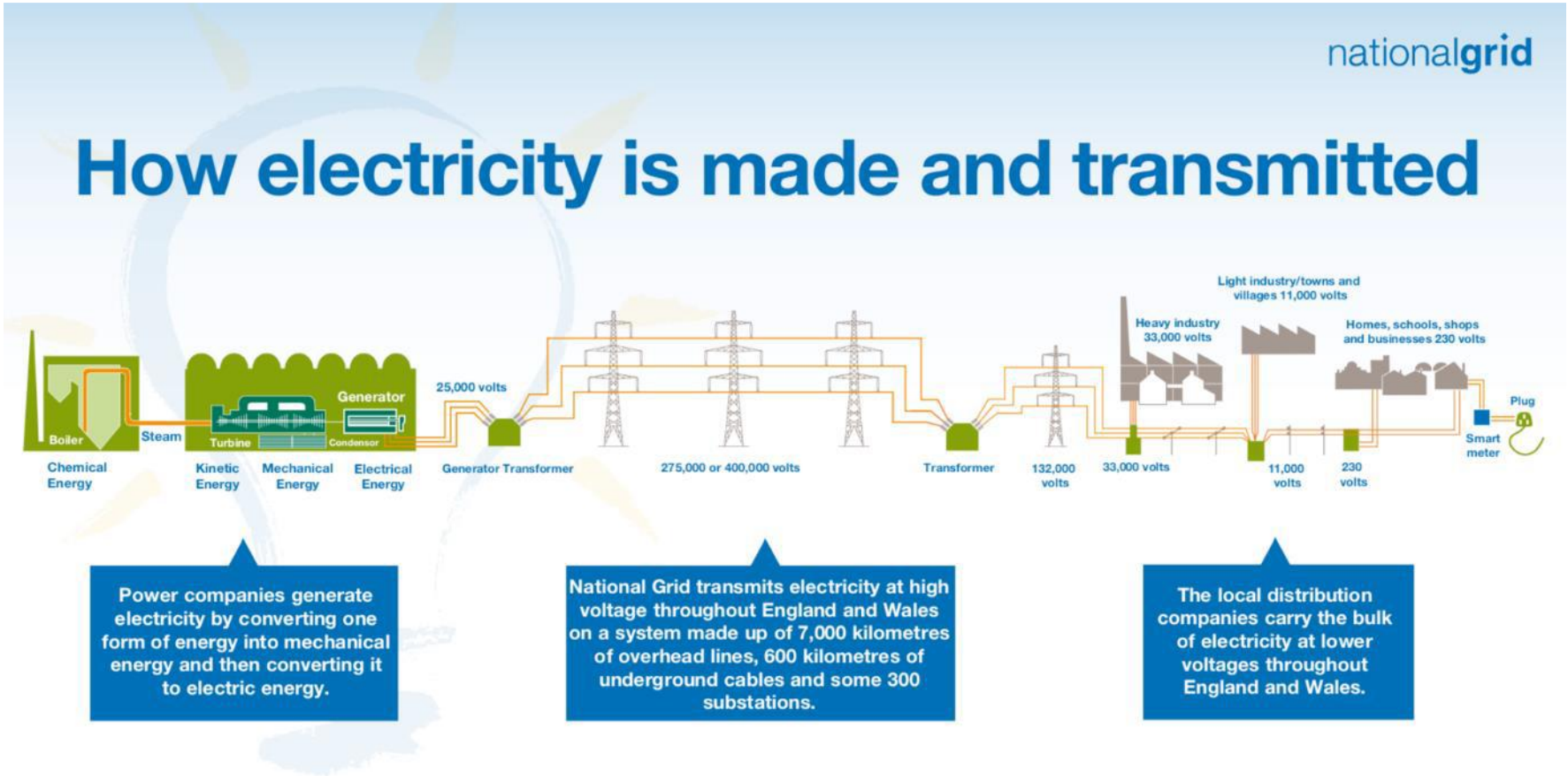


Figure 0.1: An illustration of UK electricity grid generation, transmission and distribution (National Grid, 2023)